The role of Munc-18c in GLUT4 vesicle fusion

A thesis submitted to the
COLLEGE OF MEDICAL, VETERINARY AND LIFE SCIENCES

For the degree of
DOCTOR OF PHILOSOPHY

By Kimberley Boney

Institute of Molecular, Cell and Systems Biology
College of Medical, Veterinary and Life Sciences
University of Glasgow

May 2013

Abstract

Under normal physiological conditions, insulin is released from the pancreas in response to an increase in blood-sugar concentration. The insulin signalling pathway culminates with the presentation of the glucose transporter GLUT4 on the plasma membrane of muscle and adipose tissue, leading to the uptake of glucose into these tissues and the subsequent lowering of blood-glucose concentration to basal levels. This system is faulty in patients with Type 2 diabetes.

SNARE proteins have been identified as important regulators of membrane fusion *in vivo*. Formation of SNARE complexes has been shown to provide the energy required for two opposing membranes to fuse. The SNARE complex consisting of Syntaxin 4, SNAP-23 and VAMP 2 has been implicated in the fusion of GLUT4 Storage Vesicles (GSVs) with the plasma membrane of adipocytes in response to insulin, and thus unravelling the interactions involved in complex formation will allow a greater understanding into the translocation of GLUT4 in response to insulin.

In this thesis I developed an *in vitro* fusion assay, which confirmed that the SNARE complex consisting of Syntaxin 4, SNAP-23 and VAMP 2 is able to sustain fusion of two vesicle populations. This assay was utilised further to investigate the role of the SM protein Munc-18c on SNARE-mediated membrane fusion. Using this method, Munc-18c was shown to have both positive and negative regulatory roles, depending on experimental conditions. Site-directed mutagenesis of the SM protein was also used in an attempt to dissect the interactions involved in binding of the SM protein to the assembled SNARE complex.

Finally, I developed a second *in vitro* fusion assay which utilised isolated plasma membrane fractions from 3T3-L1 adipocytes. This assay was used to investigate the effect of insulin on the plasma membrane proteins found in these cells. Analysis of the fractions showed that insulin increased the rate of SNARE-mediated membrane fusion; however the levels of the t-SNAREs were unaltered in response to insulin, indicating that the hormone functions to alter protein structure or function, but not amount.

Table of Contents

List of Figures

Acknowledgements

Firstly, I would like to thank my supervisor Professor Gwyn Gould for his support and guidance throughout my time in his lab, and for helpful comments on this thesis. I would also like to thank Diabetes UK for funding this project.

Huge thanks also go to past and present members of Lab 241, all of whom have contributed to this project in a variety of ways – even if it was just heading out for a drink (Pub Wednesday!). Particular thanks go to Dr Chris MacDonald and Andy Fuller for their help with protein work and *in vitro* fusion assays. I also have to thank Sarah Mancini for letting me use her Ponceau, PBS, TBS, Bradford reagent, and everything else that I stole/borrowed, and for helping to maintain my sanity in the lab over the last couple of years.

I would like to thank my family (Mum, Adam and Gran) for their support during my PhD.

And finally, thanks to Siobhan for her love and support (and generally just putting up with my grumps) during my time in the lab.

Declaration

I declare that the work presented in this thesis has been carried out by myself, unless otherwise stated. It is entirely of my own composition and has not been submitted, in whole or in part, for any other degree.

Kimberley Boney

May 2013

Abbreviations

(v/v)	Volume to Volume Ratio
(w/v)	Weight to Volume Ratio
~	Approximately
°C	Degrees Celsius
Å	Angstroms
APS	Ammonium Persulphate
ATP	Adenosine Triphosphate
bp	Base Pair
BSA	Bovine Serum Albumin
CAPS	Ca^{2+}-dependent Activator Protein for Secretion
cDNA	Complementary DNA
C. elegans	*Caenorhabditis elegans*
CMC	Critical Micelle Concentration
D. melanogaster	*Drosophila melanogaster*
DMEM	Dulbecco's Modified Eagle Medium
DMSO	Dimethyl Sulphoxide
DNA	Deoxyribonucleic Acid
dNTP	Deoxynucleoside 5'-triphosphate
DOPS	1,2-dioleoyl phosphatidyl serine
DTT	Dithiothreitol
E. coli	*Escherichia coli*
ECL	Enhanced Chemiluminescence
EDTA	Ethylenediaminetetracetic Acid
EM	Electron Microscopy

ER	Endoplasmic Reticulum
EtBr	Ethidium Bromide
FBS	Foetal Bovine Serum
FCS	Fluorescence Correlation Spectroscopy
FRET	Fluorescence Resonance Energy Transfer
g	Gram
g	Gravitational Force
GDP	Guanosine Diphosphate
GLUT	Glucose Transporter
GST	Glutathione S-Transferase
GSV	Glucose Storage Vesicle
GTP	Guanosine-5'-triphosphate
h	Hour
HÁ	Haemagglutinin
HCl	Hydrochloric Acid
HDM	High Density Microsome
HEPES	2-[4-(2-hydroxyethyl)-1-piperazine] ethanesuphonic acid
His-tag	Hexa-histidine tag
HRP	Horseradish Peroxidise
IBMX	3-isobutyl-1-methylxanthine
IgG	Immunoglobulin G
IPTG	Isopropyl-β-D-thiogalactopyranoside
ITC	Isothermal Titration Calorimetry
kb	Kilo basepair

KCl	Potassium Chloride
kDa	Kilodalton
KH_2PO_4	Potassium dihydrogen orthophosphate
KO	Knockout
KOH	Potassium Hydroxide
L	Litre
LDM	Low Density Microsome
µ	Micro
m	Milli
M	Molar
mA	Milliamps
$MgCl_2$	Magnesium Chloride
$MgSO_4$	Magnesium Sulphate
min	Minute
M. musculus	*Mus musculus*
MWCO	Molecular Weight Cut-off
n	Nano
Na_2HPO_4	Disodium Hydrogen Orthophosphate
NaCl	Sodium Chloride
NBD-DPPE	(N-(7-nitro-2,1,3-benzoxadiazol-4-yl)-1,2-dipalmitoylphosphatidylethanolamine
NCS	Newborn Calf Serum
Ni-NTA	$Nickel^{2+}$- Nitriltriacetic Acid
NMR	Nuclear Magnetic Resonance
NSF	N-ethylmaleimide Sensitive Factor

Histodenz©	((5-[*N*-(2,3-dihydroxypropyl)acetamido]-2,4,6-triiodo-*N*,*N*'-bis(2,3-dihyrdoxypropyl)isophthalamide))
OD_{600}	Optical Density at 600 nm
OG	n-octyl-β-D-glucopyranoside
PBS	Phosphate Buffered Saline
PBS-T	Phosphate Buffered Saline Tween20
PCR	Polymerase Chain Reaction
Pfu	*Pyrococcus furiosus*
PI	Protease Inhibitor
PI3K	Phosphoinositide-3-Kinase
PK	Protein Kinase
PM	Plasma Membrane
PMSF	Phenylmethylsulphonyl Fluoride
POPC	1-palmitoyl-2-oleoyl phosphatidyl choline
psi	Pounds per square inch
Rhodamine-DPPE	(N-(lissamine rhodamine B sulphonyl))-1,2-dipalmitoylphosphatidylethanolamine
rpm	Rotations per minute
S. cerevisiae	*Saccharomyces cerevisiae*
SAP	Shrimp Alkaline Phosphatase
SDM	Site Directed Mutagenesis
SDS	Sodium Dodecyl Sulphate
SDS-PAGE	Sodium Dodecyl Sulphate Polyacrylamide Gel Electrophoresis
SM Protein	Sec1/Munc-18 Protein
SNAP	Soluble NSF Attachment Protein

SNAP-23/-25	Synaptosome-associated protein of 23/25kDa
SNARE	SNAP Receptor
SPR	Surface Plasmon Resonance
Stx	Syntaxin
t-SNARE	Target SNARE
TAE	Tris Acetate EDTA
TEMED	N,N,N',N'-Tetramethylethylenediamine
TfR	Transferrin Receptor
TGN	*Trans*-Golgi Network
TIRM	Total Internal Reflection Fluorescence
Tris	Tris(hydroxymethyl)aminoethane
TWEEN	Polyoxyethylene Sorbitan Monolaurate
v-SNARE	Vesicle SNARE
VAMP	Vesicle-associated Membrane Protein
WCL	Whole-cell Lysate
X-Gal	X-Gal (5-bromo-4-chloro-3-indolyl-β-D-galacto-pyranoside

1 Introduction

1.1 Membrane trafficking

The plasma membrane of eukaryotic cells serves two important functions: to provide a physical barrier between a cell and its neighbouring environment, and to carefully regulate the transport of molecules to and from the extracellular environment in order to maintain homeostasis inside the cell. Membranes are also important inside the cell: each organelle within the cell (for example, the nucleus or the endoplasmic reticulum (ER)) is encompassed by a lipid membrane which, similar to the plasma membrane, carefully regulates transport into and out of each organelle.

Early experiments into the transport of newly synthesised secretory proteins in pancreatic cells showed that before reaching the plasma membrane, the peptide chains were trafficked in vesicles through a series of organelle (Palade, 1975). This carefully controlled mechanism of vesicle trafficking highlights both the spatial and temporal regulation which is required to ensure that vesicle cargo reaches its intended destination.

One system controlled in such a fashion is the translocation of the glucose transporter GLUT4 to the plasma membrane upon stimulation by insulin. After a meal, the increase in blood sugar causes the hormone insulin to be released from the pancreas. Insulin binds its receptor, triggering a signalling cascade which ultimately results in the translocation of GLUT4 Storage Vesicles (GSVs) from intracellular pools to the cell surface, where they dock and fuse with the plasma membrane (Cushman & Wardzala, 1980; Suzuki & Kono, 1980; Bryant *et al*, 2002).

1.2 Membrane fusion

Membranes are fluid structures, which contain lipids, proteins and carbohydrates. The ratio of components varies depending on the membrane, for example, retina rods contain roughly a 50:50 protein:lipid mix; however myelin is composed predominantly of lipid (Guidotti, 1972). Both lipids and proteins are important in

the trafficking of vesicles between cellular compartments, from signalling pathways to the budding of transport vesicles.

Membrane fusion is neither spontaneous nor random. In close proximity, lipid bilayers experience strong electrostatic repulsion, which must be overcome before the two membranes can interact (Rand, 1981; Jahn *et al*, 2003). Furthermore, when the two bilayers do come together, water molecules around the hydrophilic head group of the lipid molecules create a repulsive force: the energy required to remove these water molecules from this favourable conformation is termed the hydration force (P_H) and hinders spontaneous fusion between membranes (Rand, 1981). Removal of this water allows transition states to form, where the interface between the hydrophilic head groups and the hydrophobic tails is disrupted.

Studies into membrane fusion by viral fusion proteins, such as haemagglutinin (HA), helped to define a fusion intermediate called hemifusion (Kemble *et al*, 1994). During hemifusion, the two proximal (outer) monolayers of the lipid bilayer interact, but the distal (inner) layers do not (Figure 1.1). Hemifusion is thought to help overcome the hydration force by bringing two opposing membranes together, allowing full lipid and content mixing to occur (Zimmerberg *et al*, 1993). Small molecules, such as Ca^{2+} and Mg^{2+}, have been implicated in the dehydration of lipid head groups and aggregation of vesicles with high phosphatidylserine content through formation of *trans* complexes between lipids on opposing membranes (Portis *et al*, 1979). Membranes containing lipids with lower levels of hydration, such as phosphatidylethanolamine also promote interaction between bilayers (Zimmerberg *et al*, 1993).

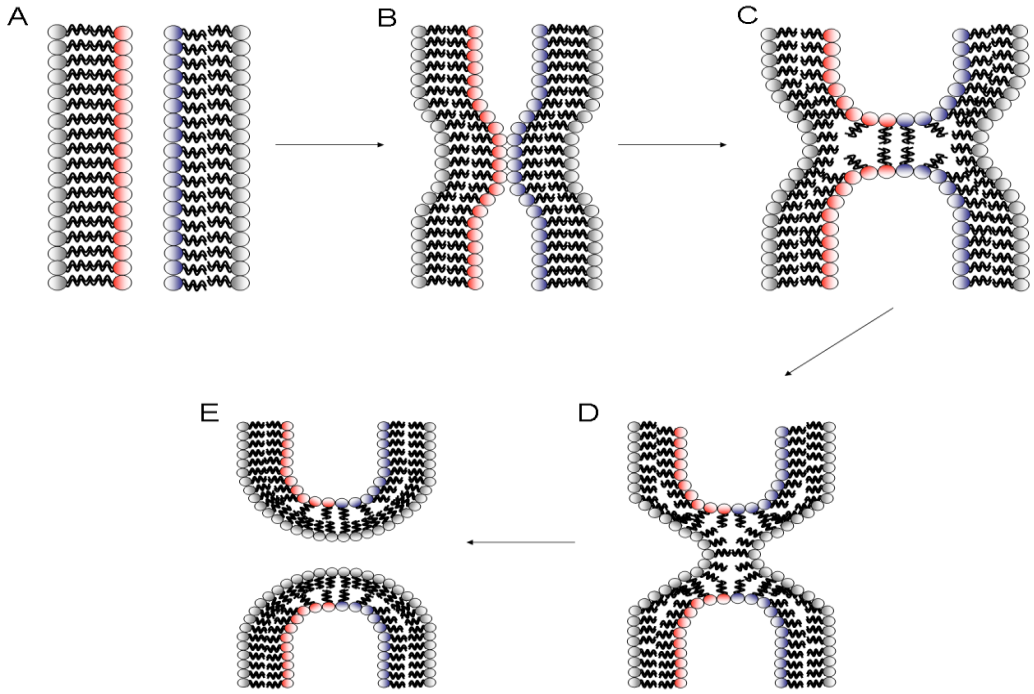

Figure 1.1 The Mechanism of Hemifusion
When two membranes come into close proximity (A and B), the proximal lipids from the two populations (shown in blue and red) mix – this is called hemifusion (C). After hemifusion, the two distal leaflets form a fusion stalk (D) which expands and allows the two membranes to merge (E).

Unlike viral systems, where one protein (such as haemagglutinin found on the influenza virus (Kemble *et al*, 1994)) is able to sustain fusion, in intracellular membrane fusion, multiple proteins were found to regulate the system. One candidate family of proteins are the Soluble N-ethylmaleimide sensitive attachment protein receptors (SNAREs), which are thought to provide the energy required to overcome the energy barrier required for two opposing bilayers to fuse, as well as contributing to the specificity of membrane fusion.

1.3 The SNARE hypothesis

The SNARE hypothesis proposes that each trafficking event within cells is regulated by specific target (t-) and vesicle (v-) SNAREs. This hypothesis was based on the discovery of SNARE proteins, which were isolated from brain extract via their ability to bind NSF (N-ethylmaleimide sensitive factor) and its adapter protein α SNAP (soluble NSF attachment protein), two proteins known to play a role in synaptic vesicle fusion (Söllner *et al*, 1993; 1993b; see also Section 1.8.1).

Following this discovery, members of the SNARE superfamily were discovered out with brain tissue, leading to the hypothesis that almost all fusion events in intracellular trafficking pathways are mediated by SNARE protein (Chen & Scheller, 2001).

Experiments utilising the neuronal SNARE proteins Syntaxin 1a, SNAP-25 and VAMP 2 in an *in vitro* fusion assay identified that four helical SNARE domains (three helixes donated by the t-SNAREs and one by the v-SNARE) interact to form a SNARE complex, the "minimal machinery" necessary for membrane fusion (Weber *et al*, 1998). This is discussed in more detail in Section 1.7.

Initially, SNARE proteins were classified according to the membrane they reside in, either the target (t-SNAREs) or vesicle (v-SNARE). However, elucidation of the 3D structure of the neuronal SNARE complex showed that the central ionic layer of the helical bundle contained three glutamine (Q) residues and one arginine (R), leading to the reclassification of SNARE proteins as either R- or Q-SNAREs depending on which residue they contribute to this polar region (Fasshauer *et al*, 1998).

1.4 Syntaxins (Qa SNARE)

Syntaxins are a family of Qa SNARE proteins which were first identified in neurons (Inoue *et al*, 1992) and characterised as α-SNAP binding proteins (Bennett *et al*, 1992). Syntaxin 1 was the first to be identified as being involved in the docking of synaptic vesicles (Bennett *et al*, 1992), but since then more family members have been identified. Syntaxins are localised to different membrane compartments, and function at different stages of trafficking pathways. For example, Syntaxin 16 is a Golgi t-SNARE which is involved in the recycling of GLUT4 from the recycling endosome to the *trans*-Golgi network (Simonsen *et al*, 1994), whilst Syntaxin 4 is found on the plasma membrane and regulates the fusion of GLUT4 Storage Vesicles (GSVs) with the plasma membrane in response to insulin signalling (Tellam *et al*, 1997).

With the exception of Syntaxin 11, all Syntaxin family members are transmembrane proteins, anchored at their C-terminus (Teng *et al*, 2001). The cytoplasmic domain of Syntaxin proteins contains a conserved coiled-coil SNARE domain, which is involved in the formation of SNARE complexes (Section 1.7) and, in some Syntaxins, a regulatory Habc domain at the N-terminus which consists of three anti-parallel helices (Fernandez *et al*, 1998). The Habc domain is able to regulate SNARE complex formation by the adoption of two distinct conformations, termed open and closed (Figure 1.2). In the open conformation the Habc is separated from the SNARE domain, allowing the Syntaxin to interact with its cognate partners and form a SNARE complex. However, in the closed conformation, the Habc domain folds back onto the SNARE domain, creating a physical barrier which prevents SNARE complex formation (Dulubova *et al*, 1999).

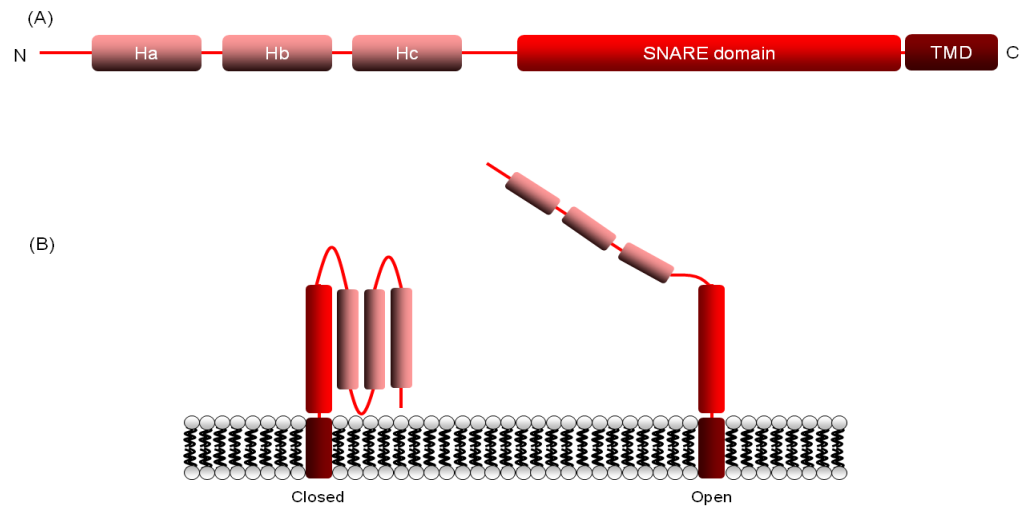

Figure 1.2 (A) Schematic structure and (B) proposed conformations of Syntaxins
Some Syntaxin proteins are able to form two distinct conformations: a closed conformation where the Habc domain autoinhibits binding to the SNARE domain, and second open conformation where the Habc domain is spatially removed from the SNARE domain, allowing SNARE complex formation.

1.5 SNAP-25 proteins (Qb and Qc SNARE)

Synaptosome-associated protein of 25 kiloDaltons (SNAP-25) was the first identified SNAP protein (Oyler *et al*, 1989), and was implicated in neurotransmitter release. In mammalian systems, three other SNAP proteins have been identified; SNAP-23 (Ravichandran *et al*, 1996), SNAP-29 (Steegmaier *et al*, 1998) and SNAP-47

(Holt *et al*, 2006). These SNAP-25 homologues are ubiquitously expressed, unlike SNAP-25 which is mainly found in neuronal tissue.

SNAP-25 family members have a unique structure amongst SNARE proteins. They contain two Q-SNARE domains which are termed Qb and Qc. These two SNARE domains are separated by a flexible linker region which contains a cluster of cysteine residues. Rather than being inserted into the membrane via a transmembrane domain (as is the case for Syntaxins and Synaptobrevins), most family members associate with the membrane by post-translational palmitoylation of these cysteine residues (Hess *et al*, 1992). Both SNARE domains of SNAP-25 family proteins are contributed to the SNARE complex, as deletion of one or both SNARE domains inhibits neurotransmitter release in neurons (Yang *et al*, 2000).

1.6 Synaptobrevins (R SNARE)

Vesicle-associated membrane proteins (VAMPs) are members of the Synaptobrevin family of R-SNAREs. VAMPs are the smallest members of the SNARE family, and consist of a C-terminal transmembrane domain followed by a SNARE domain and a non-conserved N-terminus.

Multiple VAMP isoforms have been identified, each functioning at different fusion events in different membrane compartments. VAMP 2 has been located in the membranes of both synaptic vesicles (Südhof *et al*, 1995) and GLUT4 storage vesicles (Martin *et al*, 1996), indicating a more generic role in the mechanism of exocytosis. Other VAMP isoforms have a more specialised role, including VAMP 7 which transports GLUT4 to the plasma membrane in response to osmotic shock, and VAMP 8 which is involved in retrograde transport of GLUT4 from the plasma membrane to the recycling endosome (Williams & Pessin, 2008).

1.7 SNARE complex formation and membrane fusion

In 1993, the publication of two studies laid the foundation for what later became known as the SNARE hypothesis. The first study identified that the proteins Syntaxin 1, SNAP-25 and VAMP 2 formed a complex with NSF and α SNAP, two

proteins known to play a role in membrane fusion (Glick & Rothman, 1987; Clary *et al*, 1990). As Syntaxin 1 is localised to the plasma membrane, and VAMP 2 to the synaptic vesicle membrane, it was postulated that this complex may contribute to the fusion of synaptic vesicles with the presynaptic membrane (Söllner *et al*, 1993). This was further developed in a second study, which purified a stable complex consisting of stoichiometric amounts of Synatxin 1, SNAP-25 and VAMP 2 from brain membrane extract. This complex was found to bind both α SNAP and a second protein called Synaptotagmin, believed to be a calcium sensor. By monitoring the association and dissociation of Synaptotagmin with the protein complex, a sequential series of events was postulated, including vesicle fusion, activation and docking (Söllner *et al*, 1993b).

Membrane fusion is a multi-step process, starting with the disassembly of SNARE complexes formed in the previous round of fusion. SNARE complexes are incredibly stable, and thus energy (in the form of ATP) is required to disrupt the complex. After SNARE complex assembly and membrane fusion, N-ethylmaleimide Sensitive Factor (NSF), an ATPase and Soluble NSF Attachment Protein (SNAP) bind to the *cis*-SNARE complex, releasing the SNAREs and allowing another round of fusion to occur (Söllner *et al*, 1993b). The free t-SNAREs are then able to recruit their cognate v-SNAREs causing the vesicle to dock on the plasma membrane.

Upon docking of the vesicle, the t- and v-SNAREs interact to form the stable SNARE complex (Figure 1.3). Elucidation of the crystal structure of the neuronal SNARE complex (consisting of soluble fragments of Syntaxin 1, SNAP-25 and VAMP 2) showed that the SNARE domains of the proteins orientate parallel, with the N-termini at one end of the bundle, and the C-termini at the other (Sutton *et al*, 1998).

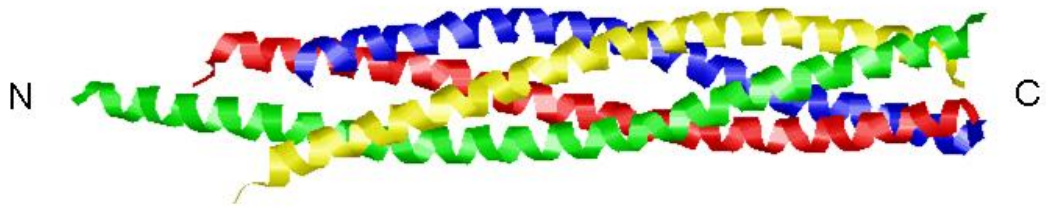

Figure 1.3 The Neuronal SNARE Complex
The 3D structure of a truncated (cytosolic SNARE domains only) neuronal SNARE complex, containing Syntaxin 1 (red), VAMP (blue) and the Qb and Qc domains of SNAP-25 (green and yellow respectively). PDB ID: 1N7S (Ernst & Brunger, 2003).

Further to the main SNARE complex, the high resolution crystal structure highlighted some grooves on the outside of the SNARE complex which, similar to transcription factors with DNA, may indicate binding sites for effector proteins, such as α SNAP (Sutton *et al*, 1998).

1.8 Regulation of SNARE-mediated membrane fusion

Studies using recombinant SNAREs reconstituted into synthetic liposomes identified SNARE complexes as the "minimal machinery" required for bilayer fusion to occur, however the rate observed for these reactions was slower than that observed *in vivo* (hours *in vitro* compared to minutes physiologically), indicating that other factors are necessary to recreate the fast fusion event observed in cells (Weber *et al*, 1998).

1.8.1 NSF and SNAP

NSF was identified as a cytosolic protein which was able to restore vesicle transport to the Golgi apparatus in a cell-free system (Glick & Rothman, 1987). When active, NSF exists as a homo-hexamer with subunits of 76 kDa (Block *et al*, 1988) with each subunit containing two ATP binding sites (Wilson *et al*, 1989). NSF was initially believed to activate membrane fusion (Malhotra *et al*, 1988) however subsequent study showed that its effect on membrane fusion was to disassemble SNARE complexes, priming them for another round of fusion (Söllner *et al*, 1993b; Hayashi *et al*, 1995).

Although implicated in the dissociation of SNARE complexes, NSF does not directly bind to the complex. Instead, it functions through an adapter protein called Soluble NSF Attachment Protein; SNAP (Weidman *et al*, 1989; Clary *et al*, 1990). Upon *cis*-SNARE complex formation and membrane fusion, three SNAP molecules bind to the surface of the SNARE complex (*Rossi et* al, 1997; Wimmer *et al*, 2001). The N-terminus of NSF subsequently binds to the SNAP/*cis*-SNARE complex (Hohl *et al*, 1998), where ATP-hydrolysis dissociates the SNARE bundle, allowing subsequent rounds of fusion to occur (Söllner *et al*, 1993b).

1.8.2 Sec1/Munc-18 (SM) proteins

Sec1/Munc-18 (SM) proteins were initially identified through genetic screening uncoordinated mutants of the nematode *Caenorhabditis elegans* (Brenner, 1974). One of the genes identified encoded the protein *unc*-18, which was discovered to play a role in the transport of acetylcholine in motor neurons (Gengyo-Ando *et al*, 1993). Orthologues of *unc*-18 were subsequently identified in *Saccharomyces cerevisiae* (Novick & Schekman, 1979), *Drosophila melanogaster* (Salzberg *et al*, 1993) and mammalian systems (Hata *et al*, 1993).

SM proteins are 60-70 kDa proteins, found both in the cytosol and associated with membranes via their interaction with membrane-bound proteins. Studies in neuronal tissue identified Syntaxins as major binding partners of SM proteins (Pevsner *et al*, 1994), however defining their role as either positive or negative regulators has been controversial. Initial studies into the functional interactions between the neuronal t-SNARE Syntaxin 1 and its cognate SM partner Munc-18a indicated that the SM protein functioned as a negative regulator, by preventing the SNARE protein from forming SNARE complexes (Dulubova *et al*, 1999). This was supported by *in vivo* studies in 3T3-L1 adipocytes which showed that overexpression of the SM protein Munc-18c inhibited insulin-stimulated GLUT4 translocation (Thurmond *et al*, 1998). However, subsequent studies showed that Munc-18a is essential for neurotransmitter release *in vivo* (Verhage *et al*, 2000).

In order to explain these apparently contradictory functions of SM proteins, it was hypothesised that different SM proteins may bind to their SNARE proteins in different ways. To date, three potential binding modes being identified: a binary interaction between the closed Syntaxin and Munc-18 (Mode 1, Section 1.8.2.1); an interaction between the Syntaxin N-terminal peptide and Munc-18c via a hydrophobic pocket on the SM protein (Mode 2, Section 1.8.2.2); and an interaction between the SNARE complex and the SM protein (Mode 3, Section 1.8.2.3).

1.8.2.1 Mode 1

Elucidation of the crystal structure of Syntaxin 1 bound to Munc-18a (nSec1) led to the identification of the first binding mode between SM proteins and Syntaxins (Misura *et al*, 2000). This structure identified Munc-18a as an arch-shaped molecule with three domains, which contains a 15 Å central cavity. In Mode 1 binding, this cavity "clamps" over the closed Syntaxin molecule, holding it in a non-functional conformation, preventing the SNARE domain from binding to its cognate partners (Figure 1.4).

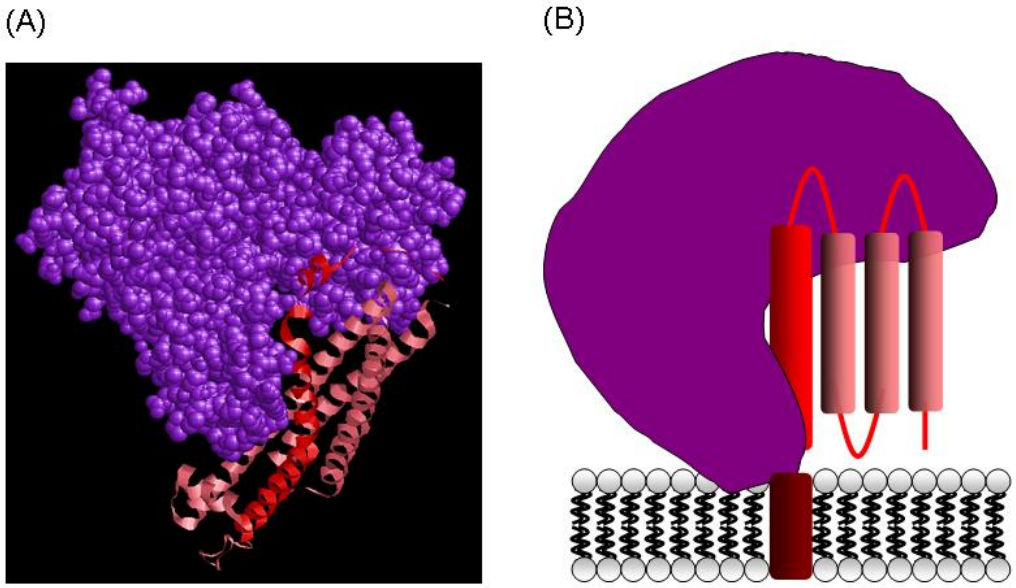

Figure 1.4 Mode 1 binding between Munc-18a and Syntaxin 1
(A) The 3D structure of the SM protein Munc-18a and the cytosolic domain of Syntaxin 1 (PDB ID: 3C98) and (B) a schematic showing how the SM protein "clamps" over the closed Syntaxin, holding it in an inactive conformation. Munc-18a is shown in purple; the SNARE domain of Syntaxin 1 in red and the Habc domain in pink. Figure (A) was created using RasMol software.

This interaction is strong, as a mutant of Syntaxin 1 which is unable to form the "closed" conformation displays reduced binding to Munc-18a (Dulubova *et al*, 1999). Not all Syntaxin/SM protein pairs exhibit Mode 1 binding, as some Syntaxins are unable to form this closed conformation.

1.8.2.2 Mode 2

Determination of the structure of the yeast SM protein Sly1p in complex with the N-terminal peptide of the Golgi Syntaxin Sed5p showed a second mode of binding which did not utilise the central cavity of the SM protein (Bracher *et al*, 2002). Instead, this second binding mode, Mode 2, involved binding of the N-terminal peptide of Sed5p to a small hydrophobic pocket on domain 1 of Sly1p (Figure 1.5). This binding mode has also been observed between the mammalian t-SNARE Syntaxin 4 and Munc-18c (Hu *et al*, 2007).

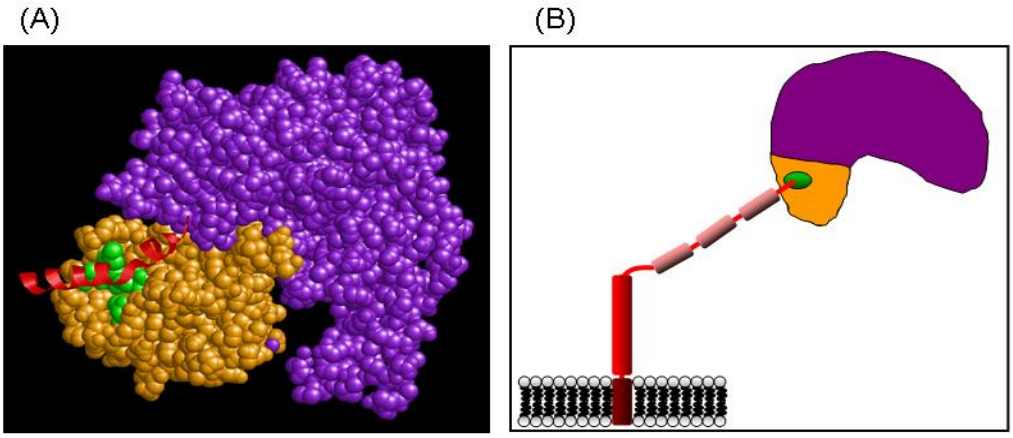

Figure 1.5 Mode 2 binding between Sly1p and Sed5p
(A) The 3D structure of the SM protein Sly1p bound to the N-terminal peptide of Sed5p, a yeast t-SNARE (PDB ID: 1MQS) and (B) a schematic showing the full-length Syntaxin in its "open" conformation, allowing the SM protein to bind to the N-terminus of the protein via its hydrophobic pocket (displayed in green). Residues found in this pocket are conserved between some SM proteins, but not all, suggesting that this binding mode is semi-conserved. Figure (A) was created using RasMol software.

Like Mode 1 binding, Mode 2 binding is not observed between all cognate SNARE/SM pairs. Sequence comparisons have shown that if an SM protein contains a hydrophobic pocket, its cognate SNARE partner will most likely have an N-terminal domain (Hu *et al*, 2007).

Investigations into the functional role of Mode 2 binding showed that by abolishing this binding mode, the function of Sly1p is not affected (Peng *et al*, 2004). This is also true for a second yeast SM protein, Vps55p (Carpp *et al*¸2006). This has implied that this second binding mode is perhaps facilitative, rather than essential (Burgoyne and Morgan, 2007). However, in *Caenorhabditis elegans* a mutant of the protein UNC-18 which disrupts Mode 2 binding (F113R) is unable to rescue neurotransmitter release in unc-18 knockout worms, indicating that in this organism Mode 2 binding is essential for correction neuronal function. The varying results obtained from disruption of Mode 2 binding indicate that the physiological relevance of this binding mode is complex (Munson and Bryant, 2009).

1.8.2.3 Mode 3

Experiments using the yeast t-SNARE Ssop and its cognate SM protein Sec1p showed that the SM protein displayed weak binding to monomeric Ssop; instead it bound to the t-SNARE complex (containing Ssop and Sec9p) and the assembled SNARE complex (Carr *et al*, 1999; Scott *et al*, 2004). Subsequently, it was discovered that although this t-SNARE could adopt an inhibitory "closed" conformation, it was unable to bind the SM protein in this form. This led to the classification of a third binding mode between SNAREs and SM proteins, termed Mode 3. In this mode, the SM protein binds to the ternary SNARE complex, possibly with stimulatory effects (Scott *et al*, 2004). This binding mechanism is the least studied of the three; however it has been discovered that the mammalian SM protein Munc-18c is able to bind its cognate SNARE complex in this manner (Latham *et al*, 2006). Studies using the neuronal SM protein Munc-18a have given contradictory results, with some showing that Munc-18a is able to bind to the ternary SNARE complex (Zilly *et al*, 2006), however others have shown that it is unable to do so (Yang *et al*, 2000).

1.8.2.4 Other SM-SNARE binding modes

As well as binding monomeric t-SNAREs, some SM proteins have been found to interact with v-SNAREs. The yeast SM protein Vps45p, which functions at the TGN/early endosome, has been shown to bind to the v-SNARE Snc2p in a way that can be out-competed with the t-SNARE Tlg2p (Carpp *et al*, 2006). Similarly, Munc-18c can bind to the v-SNARE VAMP 2 (Brandie *et al*, 2008).

1.9 *In vitro* liposome fusion assay

The discovery that SNAREs are able to form stable, exothermic complexes led to the hypothesis that the formation of such complexes would be sufficient to overcome the repulsive forces which prevent fusion. To test this hypothesis, a FRET-based liposome fusion assay was utilised (Struck *et al*, 1981). Full-length t- and v-SNAREs were purified, and reconstituted into two populations of liposomes. t-SNARE complexes were reconstituted into non-fluorescent "acceptor" liposomes,

whilst the v-SNARE was reconstituted into a second, fluorescent "donor" population. This fluorescent population took advantage of the overlap in the excitation/emission spectra of two fluorophores; (N-(7-nitro-2,1,3-benzoxadiazol-4-yl)-1,2-dipalmitoylphosphatidylethanolamine (NBD-DPPE) and (N-(lissamine rhodamine B sulphonyl))-1,2-dipalmitoylphosphatidylethanolamine (Rhodamine-DPPE). These flurophores are attached to the lipid head groups of the donor population, and when excited by light, the energy emitted by the NBD is absorbed by the Rhodamine. If fusion occurs between the two vesicle populations through formation of a functional SNARE complex, then the two flurophores should be diluted in the larger merged lipid membrane, thus preventing FRET from occurring. This allows a direct correlation between rate of fusion and NDB fluorescence (Weber *et al*, 1998; Figure 1.6).

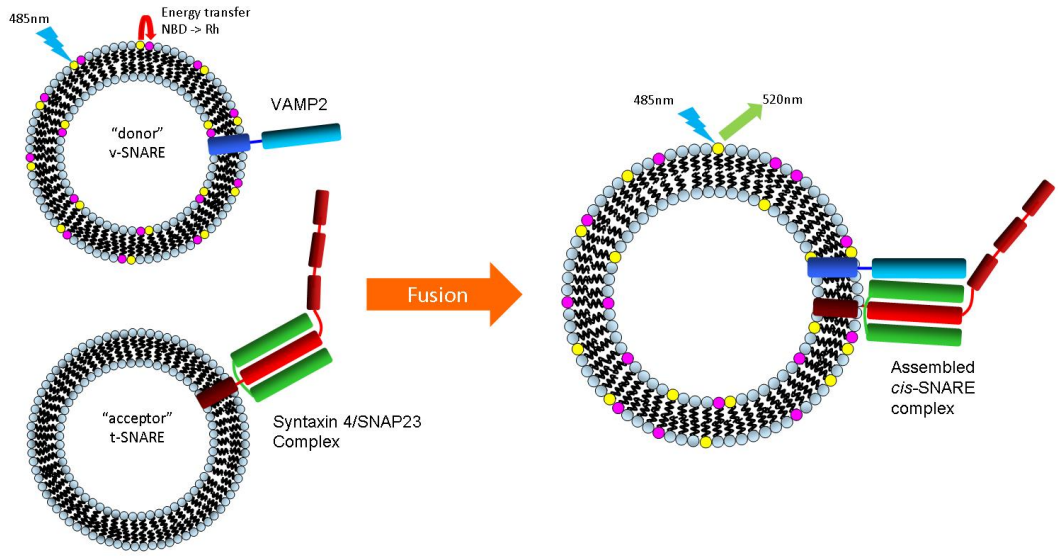

Figure 1.6 Liposome Fusion Assay
The fusion assay utilises two populations of vesicles, one of which contains the flurophores NBD (shown in yellow) and Rhodamine (pink). Before fusion occurs, the flurophores are in close proximity, causing the energy emitted by the NBD to be absorbed by the Rhodamine when excited at 485 nm. After fusion occurs, the flurophores become diluted in the larger population of non-labelled lipids, causing them to separate and the energy emitted by the NBD can be measured at 520 nm.

This technique was used to show that the t-SNAREs Syntaxin 1 and SNAP-25 and the v-SNARE VAMP 2 were the "minimal machinery" required for membrane fusion to occur (Weber *et al*, 1998). The assay can also be developed further to identify the effects of different factors on SNARE complex formation. For example,

addition of Munc-18a to the *in vitro* fusion assay stimulated the rate of SNARE-mediated fusion (Shen *et al*, 2007), with later experiments identifying that the SM protein may function by recruiting VAMP 2 to the t-SNAREs as well as positioning the N-terminal domain of Syntaxin 1 in a position which allows SNARE complex formation to occur (Rodkey *et al*, 2008). The function of other chaperones has also been tested in this manner, for example, Ca^{2+}-dependent activator protein for secretion (CAPS) was shown to bind to Syntaxin 1 and stimulate SNARE complex formation in the presence of Ca^{2+} and synaptotagmin (James *et al*, 2009). It is also possible to alter the lipid composition of the liposomes to better match that found physiologically (Mima *et al*, 2008), making it possible to manipulate the assay to allow for the study of various biological factors which may affect SNARE protein function.

1.10 Glucose transport

Glucose is a monosaccharide which is used as the primary energy source in mammalian cells. As glucose is highly hydrophilic, it is unable to pass through the plasma membrane by simple diffusion; instead a family of specialised glucose transporters (GLUTs) are required to provide cells with this preferred energy source (Bell *et al*, 1990). There are 13 members of the GLUT protein family (Joost *et al*, 2001), which vary in their affinities for glucose and tissue localisation. GLUT4 is the insulin-regulated glucose transporter and is primarily found in muscle and adipose tissue (James *et al*, 1988).

1.11 GLUT4 translocation in response to insulin

1.11.1 Intracellular localisation of GLUT4

Studies in rat adipocytes showed that stimulation with insulin caused a translocation of the glucose transporters within these cells to the plasma membrane (Cushman & Wardzala, 1980; Suzuki & Kono, 1980). cDNA sequence comparison and reaction with a monoclonal antibody identified the transporter as GLUT4 and the primary glucose transporter in muscle and adipose tissue (James *et al*, 1988).

GLUT4 is found in multiple organelles due to its trafficking between different cellular compartments (Bryant *et al*, 2002). Studies into the co-localisation of GLUT4 with the transferrin receptor (TfR, a marker for the recycling endosome) showed that under basal conditions, around 40 % of cellular GLUT4 is found cycling between endosomes and the plasma membrane in the constitutive recycling pathway (Livingstone *et al*, 1996). This leads to the presence of a small amount of GLUT4 on the cell surface, allowing basal glucose uptake under resting conditions. However, chemical destruction of endosomes in adipocytes does not affect insulin-stimulated glucose transport, indicating that this recycling pathway is not responsible for insulin-responsive GLUT4 translocation (Martin *et al*, 1998).

The remaining GLUT4 is found in a second pathway, trafficking between the endosomes and the *trans*-Golgi network (TGN), where it co-localises with the t-SNAREs Syntaxin 6 and 16 but not with the transferrin receptor (Shewan *et al*, 2003). Upon insulin stimulation, this second pool is mobilised to the plasma membrane, increasing the quantity of GLUT4 on the plasma membrane around 10-fold. This allows for increased glucose uptake from the bloodstream, lowering blood-glucose to basal levels. Termination of insulin signalling causes the GLUT4 to again be sequestered away from the plasma membrane, and the levels of glucose uptake to return to basal.

1.11.2 The effect of insulin on GLUT4 trafficking

Unlike GLUT proteins found in other tissues which are constitutively found on the cell surface, GLUT4 sub-cellular distribution in fat and muscle cells is highly regulated; large increases in GLUT4 are observed at the cell surface within minutes of stimulation (Bryant *et al*, 2002). The mechanism by which GLUT4 reaches the plasma membrane is complex, and two theories have been proposed to explain how insulin signalling causes the mobilisation of the transporter: these are termed dynamic exchange and static retention.

The dynamic exchange model proposes that GLUT4 is constantly being cycled between the plasma membrane and intracellular compartments. Upon insulin stimulation, the rate of GLUT4 exocytosis to the cell surface is increased, and the

rate of endocytosis simultaneously decreased, leading to an increase in GLUT4 on the plasma membrane (Karylowski *et al*, 2004).

The second model, static retention, proposes that GLUT4 is instead retained in distinct GLUT4 Storage Vesicle (GSVs) which are responsive to insulin. Thus, upon insulin stimulation, these GSVs are mobilised to the plasma membrane where they dock and fuse, increasing the amount of GLUT4 on the cell surface, and thus glucose transport into the cell with no effect on the kinetics of the recycling pathway (Govers *et al*, 2004; Coster *et al*, 2004).

Although the mechanism by which GLUT4 is excluded from the plasma membrane is still unknown, TIRF (Total Internal Reflection) microscopy has been used to track the movement of fluorescently labelled GLUT4 in cells and pinpoint the location of insulin action. Initial studies showed that GLUT4 moves along a cytoskeletal network adjacent to the plasma membrane. Upon insulin signalling this trafficking slows and the vesicles become tightly tethered to the plasma membrane, suggesting that insulin acts by regulating the tethering of GSVs to the cell membrane (Lizunov *et al*, 2005). These experiments were developed upon by further time-lapse TIRF microscopy, which identified distinct steps in GLUT4 translocation to the plasma membrane in response to insulin: namely docking, priming and finally fusion of the GSVs with the membrane. These experiments also identified that the PKB substrate AS160 is responsible for GSV docking whereas insulin functions to prepare the GSVs for fusion post-docking (Bai *et al*, 2007).

1.11.3 GLUT4 Storage Vesicles (GSVs)

The discovery that ablation of recycling endosomes did not affect insulin-stimulated GLUT4 translocation in 3T3-L1 adipocytes led to the hypothesis that a population of cellular GLUT4 was removed from the endosomal system, in a TfR-negative compartment (Martin *et al*, 1998; Livingstone *et al*, 1996). Early electron microscopy studies indicated that the majority of GLUT4 in basal fat and muscle was located in a tubulo-vesicular system in the cytoplasm of the cells (Slot *et al*, 1991), and that disruption of this cytokeletal system prevented long-range movement of GLUT4 (Fletcher *et al*, 2000). A novel EM technique, which used

intact adipocytes to obtain a 3D structure of organelle, built upon this data and indicated that in rat adipocytes, the majority of GLUT4 was located in vesicles which were distinct from early and late endosomes and the TGN (Ramm *et al*, 2000). Similar observations were made in skeletal muscle, where two pools of GLUT4 exist: one co-localising with the endosomal marker TfR, and one which does not (Aledo *et al*, 1997). However, insulin stimulation was found to decrease the amount of GLUT4 in all intracellular locations, which indicates that the entire GLUT4 population contributes to insulin-stimulated GLUT4 translocation (Malide *et al*, 2000), which matches closer to mathematical models which propose that GLUT4 translocation is not a simple two-pool model (Holman *et al*, 1994).

Further characterisation of the intracellular pool of GSVs indicated that this population may also contain functionally distinct vesicle pools: one containing the protein cellugyrin, and one which does not (Kupriyanova & Kandror, 2000). Cellugyrin is an isoform of Synaptogyrin, a neuronal phosphoprotein which is found in synaptic vesicles and may play a role in synapse plasticity (Baumert *et al*, 1990; Janz *et al*, 1998; 1999). Synaptogyrin I is a potent inhibitor of exocytosis in transfected PC12 cells, suggesting that it functions as an inhibitor of regulated exocytosis (Sugita *et al*, 1999). Similarly, cellugyrin was found in a sub-population of GSVs which do not translocate to the plasma membrane upon insulin stimulation (Kupriyanova *et al*, 2002). This suggests that cellugyrin may also play a role in the regulation of insulin-stimulated GLUT4 translocation.

The formation of insulin-responsive GSVs has also been linked to ubiquitination of GLUT4. Mutation of the seven cytosolic lysine residues on GLUT4 (7K-R) leads to a ubiquitin-resistant protein which is not correctly sorted into the GSV-rich fraction of 3T3-L1 adipocytes (Lamb *et al*, 2010). It is estimated that only 0.1 % of the total GLUT4 in these cells is ubiquitiated at any one time, indicating that this post-translational modification is transient, and that a deubiquitination event is required to prevent the trafficking of these GSVs from the *trans*-Golgi network to the lysosome for degredation (Lamb *et al*, 2010).

1.12 GLUT4-specific SNARE and SM proteins

1.12.1 Syntaxin 4

Syntaxin 4 was first identified as an isoform of the neuronal protein Syntaxin 1, and was found to have a much more ubiquitous distribution within cells, compared to the neuronal (Bennett *et al*, 1993) and, to a lesser extent, renal (Li *et al*, 2003) expression of Syntaxin 1. Syntaxin 4 was found on the plasma membrane of 3T3-L1 adipocytes, and addition of a Syntaxin 4-specific antibody prevented insulin-stimulated GLUT4 translocation, implicating this protein as the Syntaxin isoform involved in the docking and fusion of GSVs with the plasma membrane (Rea *et al*, 1998, Volchuk *et al*, 1996). The importance of Syntaxin 4 was further emphasised by the generation of Syntaxin 4 knockout mice (Yang *et al*, 2001). Homozygotic knockout ($Syn4^{-/-}$) resulted in embryonic lethality, whilst heterozygotic mice ($Syn4^{-/+}$) were viable. However, these mice exhibited a 50 % reduction in glucose uptake, which was linked to a decrease in insulin-stimulated glucose uptake in their skeletal muscle (Yang *et al*, 2001).

Sub-cellular fractionation showed that in red and white skeletal muscle, Syntaxin 4 was located in plasma membrane-enriched fractions (Sumitani *et al*, 1995). In 3T3-L1 adipocytes, around two-thirds of the cellular Syntaxin 4 was located at the plasma membrane, further suggesting that this protein plays a role in regulated exocytosis (Volchuk *et al*, 1996).

1.12.2 SNAP-23

In the SNARE hypothesis, it is proposed that two of the SNARE domains are donated by a SNAP-25 homologue (Söllner *et al*, 1993b). SNAP-25 is predominantly expressed in neuronal tissue (Ravichandran *et al*, 1996) and is not detectable in 3T3-L1 adipocytes (Chen *et al*, 1997), suggesting a role for another family member in GSV translocation. Yeast-two-hybrid assays were used to identify this isoform, and a 23 kDa protein with 59 % sequence similarity to SNAP-25 was located (Ravichandran *et al*, 1996). This protein, SNAP-23, was found ubiquitously expressed and bound tightly to Syntaxin 4 and the cognate v-SNARE VAMP 2,

identifying is as an important regulator of fusion in mammalian cells (Ravichandran *et al*, 1996).

SNAP-23 was linked to insulin-stimulated GSV exocytosis by the addition of a peptide chain comprising the C-terminal 24 residues. Addition of this peptide inhibited around 40 % of GSV translocation to the cell surface in response to insulin, without affecting GLUT1 translocation. The same result is observed when the cells are treated with an anti-SNAP-23 antibody (Rea *et al*, 1998). Redistribution of SNAP-23 within skeletal muscle cells has also been linked to insulin resistance (Boström *et al*, 2007; 2010). In the skeletal muscle of patients with Type 2 diabetes, SNAP-23 was found in microsomal/cytosolic cell fractions compared to the plasma membrane in control patients (Boström *et al*, 2010).

In human neutrophils, a second isoform of SNAP-23 was discovered, named SNAP-23B (Mollinedo *et al*, 1997). This isoform differed from full-length SNAP-23 by the deletion of 153 base pairs, causing omission of residues 90-142. This missing domain of SNAP-23B contains a recognition site for post-translational fatty acid acylation, indicating that this smaller isoform may have limited association with the plasma membrane of the cells (Mollinedo *et al*, 1997).

1.12.3 VAMP 2

VAMP 2 was initially located in synaptic vesicle membranes (Bauert *et al*, 1989), and was found to be part of the 20S particle postulated to be involved in synaptic vesicle fusion (Söller *et al*, 1993). VAMP 2 was the first SNARE protein implicated in the translocation of GLUT4 to the plasma membrane: GLUT4 and VAMP 2 were found to co-localise in transport vesicles in rat adipocytes (Cain *et al*, 1992), and translocated to the plasma membrane with the transporter upon insulin stimulation (Cain *et al*, 1992; Martin *et al*, 1996; 1998). Furthermore, introduction of VAMP 2 peptides into 3T3-L1 adipocytes (Millar *et al*, 1999), or cleavage of the v-SNARE with botulinum toxin D resulted in a reduction in GLUT4 translocation upon insulin stimulation (Cheatham *et al*, 1996).

A second VAMP isoform, cellubrevin (VAMP 3), was also found to co-localise with GLUT4, but there is debate as to whether this v-SNARE is involved in GLUT4 translocation in response to insulin. Addition of VAMP 3 peptides into 3T3-L1 adipocytes did not affect the rate of insulin-stimulated GLUT4 translocation (Millar *et al*, 1999) and did not translocate to the plasma membrane with GLUT4 upon stimulation (Volchuk *et al*¸ 1995; Martin *et al*, 1996) nor appear to regulate GSV fusion at the plasma membrane (Randhawa *et al*, 2000). However, mouse embryonic fibroblasts (MEFs) isolated from VAMP 2 knockout mice showed no decrease in the rate of insulin-stimulated GLUT4 translocation, with GLUT4 translocation only being completely abolished with the disruption of VAMP 3 and VAMP 8 (Zhao *et al*, 2009). It has been postulated that these two pools of GSVs, one containing VAMP 2 and the other VAMP 3, are derived from two different compartments: one from an exocytotic compartment and one derived from the endosome (Martin *et al*, 1996). The results from these studies suggest some redundancy in the requirement for a specific v-SNARE in the insulin-stimulated translocation of GLUT4.

1.12.4 Munc-18c

Screening of a 3T3-L1 adipocyte cDNA library with a oligonucleotides corresponding to the 5' and 3' termini of rat brain Munc-18 identified the presence of three Munc-18 isoforms: Munc-18a, -18b and -18c (Tellam *et al*, 1995). Early experiments into the function of the SM proteins identified Munc-18c as having potential involvement in GSV translocation and fusion as it is able to bind to Syntaxin 4, which is found in 3T3-L1 adipocytes (Tellam *et al*, 1997). Binding between Syntaxin 4 and Munc-18c was further characterised and it was shown that the SM protein is able to bind to both the closed conformation of Syntaxin 4, and also a constitutively open (L173A/E174A) mutant (D'Andrea-Merrins *et al*, 2007). The binding between the open mutant and SM protein is mediated by the N-terminal domain of Syntaxin 4, and also appears to be stabilised by an interaction between the SNARE domain of Syntaxin 4 and Munc-18c (Hu *et al*, 2007). It has also been demonstrated that Munc-18c is able to bind to the assembled Syntaxin 4/SNAP-23/VAMP 2 SNARE complex (Brandie *et al*, 2008).

Although it has been shown that Munc-18c and Syntaxin 4 are able to interact, assigning functional significance to this interaction has been difficult. Initial experiments identified that binding of Munc-18c to Syntaxin 4 prevents the Syntaxin from binding to its cognate v-SNARE VAMP 2, suggesting that the SM protein may negatively regulate SNARE complex formation (Tellam *et al*, 1997). However, like most SM proteins, the role of Munc-18c in GLUT4 translocation is somewhat controversial. *In vitro* characterisation of Munc-18c aimed to assign the SM protein a function in fat and muscle cells: overexpression of Munc-18c in 3T3-L1 adipocytes resulted in a decrease in insulin-stimulated GLUT4 translocation, confirming a negative role for the SM protein (Tamori *et al*, 1998). However, further testing revealed that overexpression of Munc-18c in 3T3-L1 adipocytes resulted in the SM protein co-localising with Syntaxin 4 under basal conditions, however the complex between the two proteins dissociated upon insulin stimulation (Thurmond *et al*, 1998). This suggests that Munc-18c functions as a negative regulator of fusion under basal insulin conditions, preventing Syntaxin 4 and VAMP 2 from forming fusogenic complexes in the absence of insulin.

As understanding of SM/Syntaxin binding developed, the function of Munc-18c during insulin-stimulated GLUT4 translocation became less clear, and data began to suggest that Munc-18c may act as a positive regulator of GSV translocation and fusion. Homozygous knockout mice (Munc-18c $^{-/-}$) were embryonic lethal, however heterozygous mice (Munc-18c $^{-/+}$) were viable and displayed decreased insulin sensitivity and a large decrease in insulin-stimulated GLUT4 translocation compared to wild-type mice (Oh *et al*, 2005). Further to this, heterozygous Munc-18c knockout was found to also inhibit glucose-stimulated insulin secretion in mouse islet cells (Oh & Thurmond, 2009). Disruption of the interaction between endogenous Munc-18c and Syntaxin 4 was also found to cause a decrease in the fusion of GSVs with the plasma membrane (Thurmond *et al*, 2000).

The complexity of the interactions between Munc-18c and its cognate SNARE proteins have been subject to various studies which have tried to link the multiple binding modes observed between the proteins to the different functions observed within cells. Single-cell analysis using Fluorescence Correlation Spectroscopy

(FCS) showed that Munc-18c is able to bind to Syntaxin 4 in cells under basal and insulin-stimulated conditions; however insulin-signalling caused repositioning of the SM protein on the Syntaxin, allowing the recruitment of other proteins involved in vesicle fusion (Smithers *et al*, 2008). This repositioning hypothesis is further supported by the observation that Mode 2 binding (between the SM protein and the N-terminal peptide of the Syntaxin) is the least specific binding mode, and confers minimal binding between the two proteins (Dulubova *et al*, 2003); and also the 3D structure of the Syntaxin 4/ Munc-18c complex which shows that stabilisation of Mode 2 binding (between the SM protein and the N-terminus of the Syntaxin) requires an interaction with the SNARE domain of the Syntaxin protein (Hu *et al*, 2007).

Munc-18c is also regulated at a post-translational level. Using a full-length Munc-18c probe, a cDNA screen was performed using human brain tissue; this identified the Protein Kinase C isoform zeta (PKCζ) as a binding partner of Munc-18c, with the interaction between the proteins becoming three times stronger upon insulin stimulation (Hodgkinson *et al*, 2005). Developing on this, more phosphosites were discovered on Munc-18c, including Tyrosine 219 and Tyrosine 521 (Oh & Thurmond, 2006; Umahara *et al*, 2008). More recently, the insulin receptor has been linked as a direct kinase of Munc-18c residue Tyr521 in an insulin-dependent manner, which also disrupts Munc-18c/Syntaxin 4 complexes (Jewell *et al*, 2011).

1.12.5 Link with Type II diabetes

Diabetes mellitus is a metabolic condition which is characterised as an inability of the body to clear high blood glucose after a meal. The condition was linked to a specific area of the pancreas, termed the Islets of Langerhans, and more specifically the beta cells in this region. The condition is sub-divided into two types (Himsworth, 1936); Type 1 diabetes is an autoimmune condition where the beta cells of the pancreas are destroyed, resulting in insulin deficiency; whilst Type 2 diabetes is characterised as insulin resistance, rather than underproduction, as the

body is still able to produce insulin but cells, in particular within fat, muscle and liver tissue, are unable to respond to this signal.

Around 346 million people worldwide have diabetes, with 90 % of these having Type 2 (WHO estimate, 2011). In recent years, Type 2 diabetes has been increasingly linked to sedentary lifestyle, in particular a rise in the prevalence of obesity. However, the link between obesity and the development of Type 2 diabetes is complex, with more than one factor appearing important in the development of the disease. It has been proposed that an intake of fatty acids in the diet can affect the fatty acid composition of the cell membrane, and thus could potentially affect the function of the cell membrane and its components, including binding of insulin to its receptor, translocation of glucose transporters and second messenger signalling (Storlien *et al*, 1996; Vessby, 2000).

The link between Type 2 diabetes, obesity and perturbed function of SNARE and SM proteins has not been fully characterised, however data is emerging identifying possible links between disease phenotype and SNARE/SM protein function. When fed a normal diet, heterozygous knockout (KO) mice were able to clear glucose from the bloodstream at a similar rate to wild-type mice; however when switched to a high fat diet the heterozygous KO mice showed low insulin sensitivity compared to wild-type mice on an identical high-fat diet, suggesting that a decrease in Munc-18c protein levels may lead to an increased susceptibility of developing Type 2 diabetes when a high fat diet is consumed (Oh *et al*, 2005). Furthermore, knockdown of the SNAREs involved in GLUT4 fusion with the plasma membrane indicate that Syntaxin 4 and SNAP-23 are indispensable for the tethering of GSVs to the plasma membrane in response to insulin (Kawaguchi *et al*, 2010).

1.13 Aims of this thesis

The aim of this project was to characterise the interactions between the SM protein Munc-18c and its cognate SNARE proteins, the v-SNARE VAMP 2 and the t-SNAREs Syntaxin 4 and SNAP-23.

The first stage of this investigation was to reconstitute the SNAREs into liposomes, and to test the fusogenic ability of these proteins using an *in vitro* liposome fusion assay (Section 1.9 and Chapter 3).

The second stage of this project involved assessing the fusion between the t- and v-SNARE vesicles in the presence of wild-type and mutant Munc-18c. Point mutations were made in Munc-18c with the aim of disrupting Mode 3 binding. The function of these mutants was assessed using both the liposome fusion assay and *in vitro* pull down assays using individual SNAREs and assembled SNARE complex. This aimed to narrow down the residues in the SM protein which are important in this (proposed) positive binding mode (Chapter 4).

The final aim of this project was to establish a liposome fusion assay using proteins isolated from the plasma membranes of 3T3-L1 adipocytes, rather than recombinant proteins. This technique has been performed using SNAREs purified from primary rat adipocytes; however the aim was to establish this assay using a cell line so that any changes in the fusogenic abilities of SNARE proteins based on the knockdown of other proteins (which is easier to accomplish using cell lines than knocking out the gene in an animal) could be assessed (Chapter 5).

2 Materials and Methods

2.1 Materials

2.1.1 General reagents

Avanti Polar Lipids, Alabaster, USA

1,2-dioleoyl phosphatidyl serine (DOPS)
(N-(7-nitro-2,1,3-benzoxadiazol-4-yl)-1,2-dipalmitoylphosphatidylethanolamine (NBD)
1-palmitoyl-2-oleoyl phosphatidyl choline (POPC)
(N-(lissamine rhodamine B sulphonyl))-1,2-dipalmitoylphosphatidylethanolamine (Rhodamine)

Applied Biosystems, Warrington, UK

Nuclease-free Water

BioRad Laboratories Ltd., Hemel Hempstead, Hampshire, UK

BioBeads
EcoPac Disposable Chromatography Columns
Quick Start Bradford 1x Dye Reagent
Broad Range Protein Markers

Fischer Scientific UK Ltd., Loughborough, Leicestershire, UK

2-[4-(2-hydroxyethyl)-1-piperazine] ethanesuphonic acid (HEPES)
Chloroform
Ethanol
Ethidium Bromide
Glycine
Tris(hydroxymethyl)aminoethane Base (Tris Base)

Formedium Ltd., Hunstanton, Norfolk, UK

Bacterial Agar
Tryptone
Yeast Extract Powder

GE Healthcare BioSciences, Chalfont, Buckinghamshire, UK

Glutathione-S-Sepharose 4B

Invitrogen Ltd., Paisley, UK

One Shot Chemically Competent BL21 (DE3) *E. coli*
One Shot Chemically Competent TOP10 *E. coli*

Kodak, Hemel Hempstead, Hertfordshire, UK

X-ray film

Melford Laboratories Ltd., Chelsworth, Ipswich, UK

Dithiothreitol (DTT)
Isopropyl-β-D-thiogalactopyranoside (IPTG)

New England Bioscience (UK) Ltd., Hitchin, Hertfordshire, UK

1 kb DNA Ladder
100 bp DNA Ladder
6x DNA Loading Buffer
10x T4 DNA Ligase Buffer
T4 DNA Ligase

Premier Foods, Long Sutton, Spalding, Linconshire, UK

Marvel Dried Milk Powder

Promega, Southampton, UK

100 mM dNTPs (dATP, dTTP, dGTP, dCTG)
Alkaline Phosphatase (Shrimp)
DpnI
NcoI
NdeI
NheI
Taq buffer
Taq DNA Polymerase
Wizard® Plus SV Minipreps DNA Purification System
XhoI

Qiagen Ltd., Crawley, West Sussex, UK

Ni-NTA Agarose
QIAfilter™ Plasmid Maxi Kit
QIAquick Gel Extraction Kit

Roche Diagnostic Ltd., Burgess Hill, UK

Agarose MP
Complete™ Protease Inhibitor Cocktail Tablets
Complete™ EDTA-free Protease Inhibitor Cocktail Tablets

Severn Biotech Ltd., Kidderminster, Worcestershire, UK

30 % Acrylamide [Acrylamide: Bis-acrylamide ratio 37.5:1]

Sigma-Aldrich Ltd., Gillingham, Dorset, UK

((5-[*N*-(2,3-dihydroxypropyl)acetamido]-2,4,6-triiodo-*N*,*N*'-bis(2,3-dihyrdoxypropyl)isophthalamide)) (Histodenz™)
Ammonium Persulphate
Ampicillin
β-mercaptoethanol
Bovine Serum Albumin (BSA)
Brilliant Blue^{R}
Bromophenol Blue
Dimethyl Suphoxide (DMSO)
Ethylenediaminetetracetic Acid (EDTA)
Ficoll
Gelatin from Cold Water Fish Skin
Glycerol
Imidazole
Isopropanol
Kanamycin
Methanol
N,N,N',N'-Tetramethylethylenediamine (TEMED)
n-octyl-β-D-glucopyranoside (OG)
Phenylmethylsulphonyl fluoride (PMSF)
Polyoxyethylene Sorbitan Monolaurate (Tween20)
Ponceau Stain
Potassium Hydroxide (KOH)
Reduced Glutathione
Sodium Dodecyl Sulphate (SDS)
Thrombin (Bovine)
Triton-X100

Spectrum Europe BV., Breda, The Netherlands

Float-a-lyzer, 5 ml 5 kDa MWCO
Float-a-lyzer, 5 ml 10 kDa MWCO
Float-a-lyzer, 5 ml 50 kDa MWCO

VWR International Ltd., Lutterworth, Leicestershire, UK

Formaldehyde
Glacial Acetic Acid
Disodium hydrogen orthophosphate (Na_2HPO_4)
Potassium Acetate
Potassium Chloride (KCl)
Potassium dihydrogen orthophosphate (KH_2PO_4)
Silver Nitrate ($AgNO_3$)
Sodium Carbonate (Na_2CO_3)
Sodium Thiosulphate ($Na_2S_2O_3$)
Sodium Chloride (NaCl)

2.1.2 General cell culture reagents

Dulbecco's Modified Eagle Medium (DMEM), Newborn Calf Serum (NCS) and Foetal Bovine Serum (FBS) were purchased from Invitrogen Ltd, Paisley. Porcine insulin, 3-isobutylmethylxanthine (IBMX) and Dexamethasone were purchased from Sigma-Aldrich Ltd.

2.1.3 Escherichia coli strains

All bacterial strains used are modfications of *E. coli*

TOP10	F´ *mcr*A Δ(*mrr-hsd*RMS-*mcr*BC) φ80*lac*ZΔM15 Δ*lac*X74 *rec*A1 *ara*D139 Δ(*ara-leu*) 7697 *gal*U *gal*K *rps*L (Str^R) *end*A1 *nup*G λ-
BL21 (DE3)	F- *ompT hsd*SB (rB-mB-) *gal dcm rne131*(DE3)

2.1.4 Primary antibodies

Rabbit polyclonal Syntaxin 4 antiserum was purchased from Synaptic Systems (#110042)

Rabbit polyclonal SNAP-23 antibody was purchased from Synaptic Systems (#111203)

Rabbit polyclonal VAMP 2 antibody was purchased from Abcam (#ab18014)

Rabbit polyclonal GLUT4 antibody was purchased from Synaptic Systems (#235003)

Mouse monoclonal Munc-18c antibody was purchased from Abcam (#ab117632)

2.1.5 Secondary antibodies

Anti-rabbit and anti-mouse secondary antibodies were purchased from GE Healthcare (Buckinghamshire, UK) and used at a dilution of 1:2000.

2.1.6 General solutions

Breaking Buffer	50 mM HEPES-KOH (pH 7.4), 400 mM KCl, 10 % (w/v) Glycerol, 4 % (v/v) Triton-X100, 2 mM β-mercaptoethanol
DNA Loading Buffer	40 % Ficol (w/v), 0.25 % Bromophenol Blue
Coomassie Brilliant Blue Solution	0.25 g Coomassie Brilliant Blue^{R} in H_2O: Methanol: Glacial Acetic Acid (4.5:4.5:1 v/v/v)
Destain Solution	5 % (v/v) Methanol, 10 % (v/v) Glacial Acetic Acid
ECL Solution A	100 mM Tris-HCl (pH 8.5), 2.25 mM Luminol, 0.4 mM p-Coumaric Acid, 1.4 % (v/v) DMSO
ECL Solution B	100 mM Tris-HCl (pH 8.5), 0.018 % (v/v) H_2O_2
Exchange/Reconstitution Buffer	25 mM HEPES-KOH (pH 7.4), 100 mM KCl, 10 % (w/v) Glycerol, 1 % (w/v) n-octyl-β-D-glucopyranoside, 2 mM β-mercaptoethanol
GST Elution Buffer	50 mM Tris (pH 8.8), 200 mM NaCl, 25 mM Reduced Glutathione
HES Buffer	20 mM HEPES-KOH (pH 7.4), 225 mM Sucrose, 1 mM EDTA, EDTA-free Complete™ Protease Inhibitor Tablets

High Sucrose HES Buffer	20 mM HEPES-KOH (pH 7.4), 1.12 M Sucrose, 1 mM EDTA, EDTA-free Complete™ Protease Inhibitor Tablets
Phosphate Buffered Saline (PBS)	136 mM NaCl, 10 mM Na_2HPO_4, 2.5 mM KCl, 1.8 mM KH_2PO_4 pH 7.4
PBS-T	PBS, 0.1 % (v/v) Tween-20
SDS PAGE Electrode Buffer	25 mM Tris base, 190 mM Glycine, 0.1 % (w/v) SDS
SDS PAGE Loading Buffer	9.3 mM Tris-HCl (pH 6.8), 1 mM Sodium EDTA, 10 % (w/v) Glycerol, 2 % (w/v) SDS, 0.002 % (w/v) Bromophenol Blue, 20 mM DTT
SOC Media	2 % (w/v) Typtone, 0.5 % (w/v) Yeast Extract, 20 mM Glucose, 20 mM $MgSO_4$, 10 mM NaCl, 2.5 mM KCl, 10 mM $MgCl_2$
Superbroth	3.2 % (w/v) Tryptone, 2 % (w/v) Yeast Extract, 5 % NaCl
TAE	40 mM Tris-acetate, 1 mM EDTA (pH 7.8)
Terrific Broth	1.2 % (w/v) Tryptone, 2.4 % (w/v) Yeast extract, 0.4 % (v/v) Glycerol, 2.3 % (w/v) KH_2PO_4, 12.5 % (w/v) K_2HPO_4
Thrombin Cleavage Buffer	50 mM Tris-HCl (pH 8.0), 150 mM NaCl, 2.5 mM $CaCl_2$

Transfer Buffer	192 mM Glycine, 25 mM Tris Base, 20 % (v/v) Methanol
Wash Buffer	25 mM HEPES-KOH (pH 7.4), 400 mM KCl, 10 % (w/v) Glycerol, 1 % Triton-X100, 2 mM β-mercaptoethanol
2 YT Medium	1.6 % (w/v) Tryptone, 1 % (w/v) Yeast Extract, 0.5 % (w/v) NaCl
2 YT Agar	1.6 % (w/v) Tryptone, 1 % (w/v) Yeast Extract, 0.5 % (w/v) NaCl, 2 % (w/v) Agar

2.2 Methods

For all buffer compositions, please refer to Section 2.1.6.

2.2.1 General Molecular Biology

2.2.1.1 DNA amplification by Polymerase Chain Reaction (PCR)

Appropriate forward and reverse oligonucleotide primers were designed to amplify the DNA sequence of interest and also containing the appropriate restriction sites. Primers were synthesised by York Bioscience Ltd, and routinely diluted to 50 pM with sterile water and stored at -20 °C. PCR reactions were set up on ice in thin walled PCR tubes using existing plasmid or genomic DNA as a template. The following general protocol was followed:

Template DNA (~1 μg/μl)	1 μl
Forward Primer (5 pM)	1.5 μl
Reverse Primer	1.5 μl
10x DNA Polymerase buffer (containing 20 mM $MgSO_4$)	5 μl
dNTP Mix (10mM each dATP, dTTP, dGTP, dCTP)	1 μl
Pfu Polymerase	1 μl
Nuclease Free Water	39 μl

PCR reactions were carried out in a thermocycler using the following standard conditions:

95 °C (initial denaturing)	2 min	
94 °C (denature)	1 min	25-35 cycles
55 °C (primer annealing)	1 min	
72 °C (elongation)	2 min/kb	
72 °C (final elongation)	10 min	
4 °C (chill)	HOLD	

The melting temperature of the primers had to be taken into account when selecting the annealing temperature: the optimal annealing temperature is generally 5 °C lower than the lowest melting temperature of the primers. After the PCR was finished a sample of the reaction was run on an agarose gel to check if the correct size product was formed.

2.2.1.2 Site Directed Mutagenesis

The desired mutations were incorporated into the forward and reverse primers, and a standard PCR was carried out with a few alterations: the elongation step was reduced to 68 °C for 1 min/kb and only 18 cycles were performed. After the reaction was complete 1 µl of DpnI was added to the SDM mixture and incubated at 37 °C for 1 h to digest any methylated parental DNA. 10 µl of the reaction mix was then transformed into TOP10 *E. coli* cells. Successful mutants were selected on antibiotic agar plates, and the DNA isolated from single colonies by small-scale DNA preparations (Section 2.2.1.6) and the mutant confirmed by DNA sequencing.

2.2.1.3 DNA agarose Gel Electrophoresis

Agarose powder (0.8 % w/v) was dissolved in TAE buffer by boiling in a microwave oven. Once the powder was totally dissolved the solution was allowed to cool to ~50 °C before 10 µl Ethidium Bromide (1 % w/v) was added from a dropper bottle. This was mixed and then poured into a gel casting cassette containing the

appropriate loading comb, where it was left to polymerise. Once set, the gel was transferred to a horizontal gel tank containing TAE buffer. DNA samples were prepared in 6x DNA Loading Buffer (40 % (w/v) Ficoll, 0.25 % (w/v) Bromophenol Blue) were loaded into the wells alongside 0.5 µg of 1 kb DNA ladder (New England Biolabs). Electrophoresis was carried out at 100 volts and the gel visualised and recorded using a BioRad Molecular Imager ChemiDoc XRS+ System.

2.2.1.4 Gel extraction/purification

DNA samples were separated by agarose gel electrophoresis and products of the correct size were identified under UV light. Bands of interest were excised using a clean scalpel blade and placed in sterile eppendorf tubes. The DNA was then purified using the QIAGEN Gel Extraction Kit following the manufacturer's instructions. Typically, 600 µl of solubilisation buffer QC was added to each gel slice and the samples heated at 50 °C for 10 mins or until the gel slice had completely dissolved. Then, 200 µl isopropanol was added and the solution transferred to a QIASpin Column. The column was spun at 14000*g* for 1 min and the flow through discarded. 750 µl wash buffer PE was added and the column spun for a further minute and the flow through discarded. To remove any residual ethanol the column was spun for another minute before being transferred to a sterile eppendorf tube. 30 µl nuclease free water was added to the centre of the column and incubated at room temperature for 1 min to maximise the amount of DNA eluted. The column was spun for 1 min at 14000*g* to collect the eluted DNA, which was typically stored at -20 °C.

2.2.1.5 Transformation of *E. coli* cells

Chemically competent cells were defrosted on ice for 15 mins. DNA was added (1-10 µl) and the cells incubated on ice for a further 15 mins. The cells were then heat shocked for 1 min at 42 °C before recovering on ice for a further minute. 250 µl SOC media was added and the tubes incubated at 37 °C for at least 1 h with shaking. After incubation, the mixture was plated onto agar plates containing the appropriate antibiotic. The plates were inverted and incubated overnight at 37 °C.

2.2.1.6 Small-scale DNA preparations from *E. coli* (Miniprep)

A single colony from a fresh bacterial transformation was used to inoculate 5 ml 2 YT media containing the appropriate antibiotic, and the culture grown overnight with shaking at 37 °C. DNA purification was carried out using Promega Wizard® Plus SV Miniprep Kit. Cells were collected by centrifugation at 3000*g* for 5 mins in a refrigerated bench top centrifuge. The pellet was then resuspended in 250 µl cell resuspension buffer and transferred to a sterile eppendorf tube. 250 µl cell lysis buffer was added and the tubes mixed by inversion 4 times. Then, 10 µl alkaline protease solution was added and the tubes again mixed by inversion. The mixture was incubated at room temperature for 5 mins. After this incubation, 350 µl neutralisation solution was added and the sample mixed by inversion before being spun for 10 mins at 14000*g* in a microfuge. The cleared lysate was transferred to a Wizard® Plus spin column and centrifuged for 1 min at 14000*g*. The flow through was discarded and the column washed with firstly 750 µl column wash solution (containing ethanol), then 250 µl column wash solution, with the flow though being discarded after each spin. The columns were then spun for an additional 2 mins to remove any residual column wash solution. The columns were then placed in sterile eppendorf tubes and 50 µl nuclease free water was added to the centre of the column. These were then spun for 1 min to elute the DNA from the column. DNA concentration was determined using a spectrophotometer set at 260 nm and the DNA was generally stored at -20 °C.

2.2.1.7 TOPO®-TA cloning

High fidelity proof-reading PCR was used to amplify DNA, which was subsequently gel purified. Taq polymerase possesses terminal transferase activity which allows it to generate adenosine overhangs to the PCR product, allowing it to be cloned into linearised pCR®2.1-TOPO® vector (Invitrogen), which contains overhanging deoxythymidine residues. Reactions were set up as outlined:

Gel purified DNA	10 µl
10x Mg-free buffer	1 µl
$MgCl_2$	0.6 µl
Taq polymerase	0.4 µl
dNTPs	0.4 µl

The reactions were incubated at 72 °C for 20 mins. 2 µl of the mixture was cloned into the pCR2.1®-TOPO® vector using the pCRII-TOPO® kit (Invitrogen). The ligation mixture was then transformed into TOP10 cells and successful transformation selected for on 2 YT agar plates containing the appropriate antibiotic and X-Gal at a concentration of 0.04 µg/ml. The DNA from white colonies was isolated by mini DNA preparation and sequenced to ensure the correct sequence was cloned.

2.2.1.8 Sequencing

Sequencing of DNA samples was carried out by the University of Dundee Sequencing Service and was generally performed after the generation of new DNA (PCR, SDM).

2.2.1.9 Restriction endonuclease digestion

A pair of enzymes was usually chosen to cut plasmid DNA or PCR product. Enzymes were chosen based on the restriction sites of interest and reactions were carried out in an appropriate buffer which retained 75-100 % of enzyme activity. Reactions were set up in eppendorf tubes, for example:

DNA (~0.5-1 µg/µl)	5 µl
10x buffer	1 µl
Restriction Enzyme #1	1 µl (20 units)
Restriction Enzyme #2	1 µl (20 units)
Sterile water	2 µl

Samples were mixed and spun briefly before incubation at 37 °C for 3-4 h. After the digestion was complete, the product was analysed using agarose gel electrophoresis.

2.2.1.10 Ligation reactions

The target vector and vector containing the desired insert were restriction digested using the same restriction enzymes as outlined in Section 2.2.1.9. The required fragments (insert and linearised target vector) were isolated by gel extraction (Section 2.2.1.4). The linearised vector was treated with Shrimp Alkaline Phosphatase (Promega) for 30 mins at 37 °C to remove any phosphate groups from the 5' end of the plasmid. The alkaline phosphatase was the inactivated by incubation at 65°C for a further 30 mins. Ligation reactions were carried out in thin-walled PCR tubes and set up on ice:

Linearised Vector DNA (0.5 μg/μl)	2 μl
Insert DNA (0.5 μg/μl)	6 μl
10x T4 DNA Ligase Buffer	1 μl
T4 DNA Ligase (NEB)	1 μl

Vector only, insert only, and DNA-free controls were also set up. The reactions were incubated at 16 °C overnight. The reaction mixture was the transformed into TOP10 cells and plated on the appropriate antibiotic.

2.2.2 General biochemical methods

2.2.2.1 SDS Polyacrylamide Gel Electrophoresis (SDS-PAGE)

SDS PAGE was used to resolve proteins on the basis of size, using Tris-HCl gels. 30 % acrylamide was used to form a 5 % stacking layer in stacking buffer (25 mM Tris-HCl (pH 6.8), 0.2 % (w/v) SDS) and a resolving layer (75 mM Tris-HCl (pH 8.8), 0.2 % (w/v) SDS), which ranged in acrylamide content from 8-15 %, depending on the protein being studied. Gels were polymerised by addition of Ammonium Persulphate and N,N,N',N'-Tetramethylethylenediamine (TEMED). Protein samples were prepared in an equal volume of SDS-PAGE Loading Buffer and incubated for 5 mins at 95°C. Gels were run in BioRad Mini PROTEAN-III apparatus. The samples were loaded into the lanes of the gel alongside 5 μl of BioRad Broad Range Protein Marker. Gels were run at 80 volts until the samples had cleared the separating gel, at which point the voltage was increased to 150 volts

and the gels run until the markers had separated adequately and the dye-front had cleared the bottom of the gels.

2.2.2.2 Western blotting

Following SDS PAGE, proteins were transferred to nitrocellulose membrane. Gels were separated from their glass plates, and the stacking gel removed, before being submerged in transfer buffer for 2 mins, along with Whatman 3 mm Filter Paper, nitrocellulose membrane (45 μm pore size) and two sponge pads. The system was set up as follows (cathode to anode): sponge pad, Whatman filter paper, nitrocellulose membrane, gel containing electrophoresed samples (Section 2.2.2.1), Whatman filter paper, and sponge pad. The assembly was encased in a cassette and inserted into a BioRad Mini Tras-Blot cell filled with Transfer Buffer. The proteins were transferred onto the membrane at room temperature for 2 h at 200 mA or overnight at 40 mA.

2.2.2.3 Immundetection of proteins

Following western blotting, proteins transferred to nitrocellulose were visualised by Enhanced Chemiluminescence (ECL). After transfer, membranes were removed from the cassette and washed briefly in PBS-T. Non-specific binding of the antibody was minimised by blocking membranes in PBS-T containing 5 % dried milk powder for 30 mins. Membranes were briefly washed again, and primary antibody (diluted to an appropriate concentration in 1 % PBS-T/dried milk) was added before incubation for 1 h at room temperature, or at 4°C overnight with rolling. Unbound antibody was removed by washing membranes three times in PBS-T over the course of 30 mins. Secondary IgG Horseradish Peroxidase conjugated antibodies (IgG-HRP) were diluted to an appropriate concentration in 5 % PBS-T/dried milk and incubated with membranes for 1 h at room temperature. Membranes were then washed a further three times in PBS-T . Labelled proteins were visualised using the ECL system. ECL solutions A (100 mM Tris-HCl (pH 8.5), 2.25 mM Luminol, 0.4 mM p-Coumaric Acid, 1.4 % (v/v) DMSO) and B (100 mM Tris-HCl (pH 8.5), 0.018 % (v/v) H_2O_2) were mixed in a 1:1 ratio and incubated

with membranes for 1 min. The membrane was then exposed to X-Ray film in a lightproof cassette and processed in a Kodak X-Omat processor.

2.2.2.4 Coomassie staining

To detect proteins on an SDS PAGE gel, Coomassie Blue Stain solution was used. After removal from the glass plates, the gel was immersed in Coomassie stain for at least 1 h with gently agitation. After this, the stain was poured off, and the gel washed in distilled water. To remove the excess stain from the gel and allow visualisation of the proteins, the gel was submerged in Destain Solution, typically overnight.

2.2.2.5 Silver staining

Silver staining was used to detect low levels (0.5-5 ng) of protein on an SDS PAGE gel. The gel was first submerged in fixer solution (40 % ethanol, 10 % acetic acid, 50 % H_2O) for 1 h with gentle agitation. The gel was then washed 6x 10 mins to remove excess acetic acid. Then, the gel was sensitised using 0.02 % sodium thiosulphate for one minute, before being incubated for 20 mins in ice cold silver nitrate solution (0.1 % silver nitrate, 0.02 % formaldehyde added just before use). After staining, the gel was washed three times in water before being transferred to a second staining tray. The gel was developed using 3 % sodium carbonate (0.05 % formaldehyde added just before use). Staining was terminated by washing once in water, followed by incubation with 5 % acetic acid for 5 mins. The gel was then photographed and stored at 4 °C in 1 % acetic acid in case further analysis was required.

2.2.3 General protein methods

2.2.3.1 Expression of recombinant proteins

A single colony from a fresh transformation was used to inoculate 400 ml of 2 YT containing the appropriate antibiotic. The culture was incubated overnight at 37 °C with shaking. The next morning, the cells were collected by centrifugation at 1000*g* for 15 mins and typically resuspended in 6 L of Terrific Broth and incubated at 37 °C

with shaking until an OD_{600} of 0.8 was reached. Expression was induced by addition of 1 mM sopropyl-β-D-thiogalactopyranoside (IPTG) at 37 °C for 4 h. Cells were collected by centrifugation at 3000*g* for 15 mins. Cell pellets were typically resuspended in 120 ml of cold PBS containing two Complete™ protease inhibitor tablets. This was homogenised using a blender, and the cells lysed by one pass through a Microfluidics M-110P cell disruptor at 10 kpsi. The lysate was clarified by centrifugation at 15000*g* at 4°C for 15 mins in a Beckman JA-25.5 rotor. The clarified lysate was then incubated with the appropriate beads, which had been washed in Breaking Buffer, and incubated overnight at 4 °C on a roller.

2.2.3.2 Purification of His-tagged proteins

E. coli cells producing His-tagged recombinant protein were resuspended in PBS containing EDTA-free Complete™ protease inhibitor tablets and clarified lysate was obtained as described in Section 2.2.3.1. The lysate was incubated overnight with Ni-NTA agarose beads which had been washed in PBS containing 25 mM Imidazole. The beads were harvested the next day by collection in an EcoPac disposable chromatography column. The beads were washed ten times with 10 ml of PBS containing 25 mM Imidazole. The protein was then eluted from the beads on a linear gradient from 50 mM-500 mM Imidazole. 1 ml elutions were typically collected and a sample from each eluate was run on an SDS PAGE gel (Section 2.2.2.1). The most abundant protein fractions were pooled, and dialysed against 4 L PBS overnight at 4 °C to remove any Imidazole. The sample was then split into aliquotes, snap-frozen in liquid nitrogen and stored at -80 °C.

2.2.3.3 Purification of GST-tagged proteins

E. coli cells producing GST-tagged proteins were resuspended in PBS containing Complete™ protease inhibitor tablets and clarified lysate was obtained as outlined in Section 2.2.3.1. The lysate was incubated overnight with Glutathione Sepharose 4B beads which had been washed with PBS. The next day the beads were harvested by collection in an EcoPac disposable chromatography column. The beads were washed ten times with 10 ml of PBS. The protein was either eluted from the beads by incubation with reduced Glutathione or the affinity tag removed by Thrombin

cleavage. For elution by reduced Glutathione the beads were incubated in a suitable volume of GST Elution Buffer for 15 mins at room temperature. The elution was separated from the beads and the supernantent retained. The elution step was usually repeated 3 times to maximise the amount of protein eluted. Samples from each elution were run on an SDS PAGE gel (Section 2.2.2.1) before being split into aliquots and stored at -80°C. If Thrombin cleavage was required the beads were incubated in a suitable volume of Thrombin cleavage buffer containing 100 units of Thrombin and incubated at room temperature for 4 h. After this time, the Thrombin was inactivated by the addition of 0.2 mM PMSF. The eluted protein was the separated from the beads by centrifugation at 14000*g* at 4 °C for 3 mins in a benchtop microfuge. The supernatant was retained, and the sample dialysed against 4 L PBS overnight at 4 °C to remove the Reduced Glutathione. The sample was split into aliquots, snap-frozen and stored at -80°C.

2.2.3.4 Analysis of protein concentration

The concentration of proteins in recombinant and whole-cell lysates samples was assessed by Bradford analysis. Bovine Serum Albumin (BSA) was used to prepare standards ranging from 0-6 µg/ ml. The amount of sample assayed varied, however usually a 1:300 dilution of protein was prepared in water. 150 µl of standard and sample was analysed in triplicate in a 96-well plate. 150 µl of Bradford reagent was added to each well and the plate incubated at 37 °C for 1 h. After incubation, the samples were analysed in a FLUOstar Optima Plate reader set to 595 nm. Protein concentrations were calculated using a standard curve derived from the BSA standards.

2.2.4 Mammalian cell culture

2.2.4.1 Culture of 3T3-L1 murine fibroblasts and adipocytes

3T3-L1 fibroblasts were cultured in Dulbecco's modified Eagle Medium (DMEM) supplemented with 10 % (v/v) Newborn Calf Serum (NCS) and 1 % (v/v) penicillin and streptomycin. Fibroblasts were maintained at sub-confluency in a 10 % CO2 incubator at 37 °C. Fibroblasts were differentiated into adipocytes 3 days post-confluency by addition of DMEM containing 10 % (v/v) Foetal Bovine Serum (FBS),

1 % (v/v) penicillin and streptomycin, 1.25 µM dexamethasone, 0.5 mM 3-isobutyl-1-methylxanthine (IBMX) and 1 µg/ µl insulin. After 3 days, the differentiation media was replaced with DMEM containing 10 % FBS, 1 % penicillin and streptomycin and 1 µg/µl insulin. Differentiated adipocytes were fed with DMEM containing 10 % FBS and 1 % penicillin and streptomycin every three days and harvested for experimentation 8-12 days post-differentiation.

2.2.4.2 Sub-cellular fractionation of 3T3-L1 adipocytes

Ten 10 cm2 plates of confluent adipocytes were washed three times in chilled HES buffer containing EDTA-free protease inhibitor tablets (HES + PI). The cells were then scraped in 1 ml chilled HES + PI on ice and homogenised by ten passes through a 25G needle and two passes through a 26G needle. All centrifugation steps were carried out at 4 °C. Cell debris was pelleted by centrifugation at 500*g* in a chilled bench microfuge. The supernatant was retained and spun at 6000*g* in a TLA 110 rotor for 10 mins. At this stage, the supernatant and pellet were retained for separate fractionation steps.

2.2.4.2.1 Isolation of Cytosol, High-Density Microsome (HDM) and Low-density microsome (LDM) fractions

The retained supernatant (Section 2.2.4.2) was spun at 9400*g* for 17 mins in a TLA 110 rotor. The pellet, which contained the high-density microsome (HDM) was resuspended in 100µl HES + PI. The supernatant was centrifuged at 104300*g* for 75 mins in a TLS 55 rotor. The supernatant, containing the cytosol, was removed and retained; whist the pellet contained the low-density microsome (LDM) fraction and was resuspended in 100 µl HES + PI. All fractions were snap-frozen and stored at -20 °C until use.

2.2.4.2.2 Isolation of Plasma Membrane (PM) and Nuclear/Mitochondrial (N/M) fractions

The pellet retained after centrifugation at 6000*g* (Section 2.2.4.2) was resuspended in 4 ml HES + PI and centrifuged again at 6000*g* for 12 mins in a TLA 110 rotor. The supernatant was discarded and the pellet resuspended in 1 ml HES + PI and layered

over 1 ml high sucrose HES containing protease inhibitors. This gradient was centrifuged at 42000*g* for 1 h in a TLS 55 rotor. The pellet obtained contained the nuclear/mitochondrial fraction and was resuspended in 100 µl HES + PI. The plasma membrane (PM) fraction was collected from the layer above the high sucrose HES + PI and mixed with 3 volumes of HES + PI. This was centrifuged at 9400*g* for 15 mins in a TLA 110 rotor and the pellet, containing the PM fraction, resuspended in 100 µl HES + PI containing 0.8 % (w/v) n-octyl-β-D-glucopyranoside to solubilise the membrane proteins. Samples were snap-frozen and stored at -20 °C until use.

2.2.5 Liposome Fusion Assay

2.2.5.1 Purification of recombinant SNARE proteins

Full-length SNARE proteins were purified separately: Syntaxin 4 and SNAP-23 were co-expressed from the vector pETDuet-1, and VAMP 2 from pQE30. Overnight cultures of each construct were set up in 2 YT containing the appropriate antibiotic. This overnight culture was then used to inoculate 8 L of Superbroth containing antibiotic. Proteins were expressed and harvested essentially as described in Section 2.2.3.1, however the cell pellet was resuspended in 160 ml Breaking Buffer containing 3 Complete™ Protease Inhibitor tablets. Cells were lysed by one pass through a Microfluidics M-110P cell disruptor at 10 kpsi. Lysates were clarified as described previously and incubated overnight with 4 ml of the appropriate affinity beads. The next day, the beads were isolated by collection in an EcoPac disposable chromatography column and washed 5 times in Wash Buffer. For His-tagged proteins, this wash included 25 mM Imidazole. The Triton-X100 was exchanged for n-octyl-β-D-glucopyranoside by washing 5 times in Exchange/Reconstitution Buffer containing 0.8 % (w/v) n-octyl-β-D-glucopyranoside. His-tagged proteins were eluted from the beads on a linear gradient of Imidazole in Exchange/Reconstitution Buffer containing 0.8 % (w/v) n-octyl-β-D-glucopyranoside. GST-tagged proteins were cleaved from their affinity tag by incubation with 125 units of Thrombin in 4 ml Exchange/Reconstitution buffer for 4 h at room temperature. The thrombin was inactivated by incubation with 0.2 mM PMSF and the elution isolated from the beads and analysed by SDS-

PAGE and/or western blotting. The protein sample was then concentrated (if necessary) and snap-frozen and stored at -80 °C.

2.2.5.2 Preparation of lipid stocks

A 15 mM lipid stock of acceptor liposomes was made up containing 85 mol % POPC and 15 mol % DOPS in Chloroform. For donor liposomes, a 3 mM and 15 mM stock was made up containing 82 mol % POPC, 15 mol % DOPS, 1.5 mol % NBD-DPPE and 1.5 mol % Rhodamine-DPPE in Chloroform. Lipid stocks were stored under nitrogen at -80 °C.

2.2.5.3 Formation of proteoliposomes

100 µl of unlabelled acceptor liposomes, for t-SNAREs, and 500 µl of donor liposomes were added to 12x75 mm glass tubes and dried under nitrogen for 15 mins. The samples were further dried in a vacuum desiccator for 30 mins to remove any traces of chloroform. 500 µl of purified t- or v-SNARE protein (Section 2.2.5.1) containing 0.8 % n-octyl-β-D-glucopyranoside was added to the appropriate tube and the lipid film resuspended with the protein by vortexing for 5 mins. After resuspension, 1 ml of Exchange/Reconstitution Buffer containing 1 mM DTT was added drop-wise to each tube while vortexing in order to dilute the detergent below its critical micellar concentration (CMC). The samples were transferred to 3 ml Float-a-lyzer tubes and dialysed overnight in 4 L of Exchange/Reconstitution buffer containing 4 g BioBeads to absorb any detergent. Samples were collected the following day and stored on ice before proteoliposome recovery by gradient centrifugation.

2.2.5.4 Proteoliposome recovery by gradient centrifugation

Proteoliposomes were isolated by floatation of a three step ((5-[N-(2,3-dihydroxypropyl)acetamido]-2,4,6-triiodo-N,N'-bis(2,3-dihyrdoxypropyl)isophthalamide)) (Histodenz™) gradient. Each 1.5 ml dialysate was added to 1.5 ml 80 % Histodenz™ containing 1 mM DTT and mixed extensively. This was carefully overlaid with 1.5 ml 30 % Histodenz™ containing 1 mM DTT. Finally, 250 µl of glycerol free Exchange/Reconstitution buffer was

layered on top. Gradients were centrifuged for 4 h at ~375 000*g*. 400 µl of proteoliposomes were recovered from the top of each gradient and transferred into screw-cap eppendorf tubes. The protein content of the liposomes was assessed by SDS-PAGE analysis and the samples stored at -80 °C.

3 Development of an *in vitro* liposome fusion assay to study SNARE protein function

3.1 Introduction

In 1981, Struck and colleague developed an assay which utilised lipid-conjugated fluorophores to measure the rate of fusion between two vesicle populations. This assay is dependent on the Fluorescence Resonance Energy Transfer (FRET) that occurs between the fluorophores NDB ((N-(7-nitro-2,1,3-benzoxadiazol-4-yl)) and Rhodamine ((N-(lissamine rhodamine B sulphonyl)).

FRET is the transfer of energy from a donor fluorophore (in this case, NBD) to an acceptor (rhodamine): when excited, the donor fluorophore emits a photon which, when in close proximity is absorbed by the second (acceptor) fluorophore. The transfer of energy in this way is dependent on the distance between fluorophores and the overlap between the emission spectrum of the donor and excitation spectrum of the acceptor fluorophore (Förster, 1948; Stryer, 1978). When utilised in the *in vitro* fusion assay, two populations of vesicles are used. Acceptor vesicles are produced using non-fluorescent lipids, whilst donor vesicles are produced using lipid-conjugated fluorophores. Before fusion occurs, the flurophores present in the donor vesicles are in close proximity to one another, allowing FRET to occur between the NBD and rhodamine. Upon fusion, the fluorophores are spatially separated as they are diluted within the larger (non-fluorescent) lipid volume. This prevents the rhodamine from absorbing the photons emitted from the excited NBD, allowing levels of fusion to be measured as an increase in NBD fluorescence (Struck *et al*, 1981; Figure 3.1).

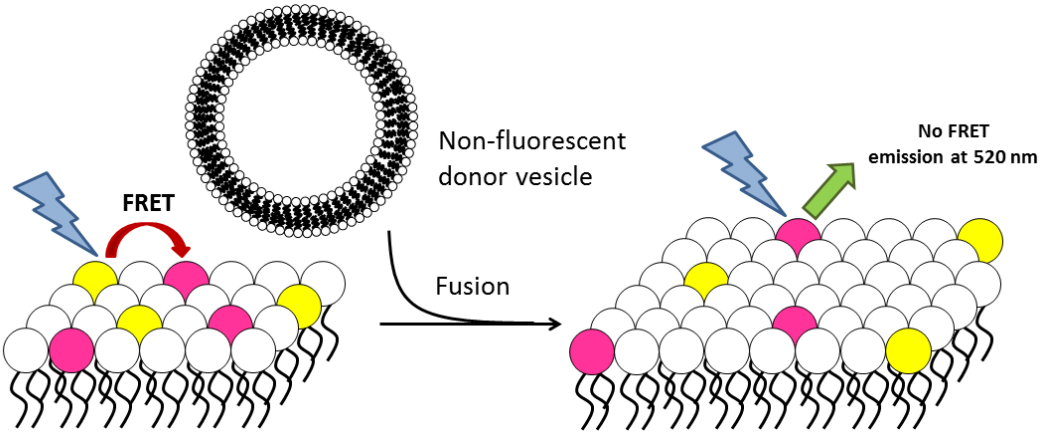

Figure 3.1 The mechanism of FRET in the *in vitro* fusion assay
In order for FRET to occur between NBD and rhodamine, the fluorophores must be within 4-7 nm of one another (Wolf *et al*, 1992). Upon fusion between the two liposome populations in the *in vitro* fusion assay, FRET is unable to occur between the fluorophores as they are diluted in the larger (unlabelled) membrane of the donor vesicle. This allows the levels of fusion between the two vesicle populations to be measured as an increase in NDB fluorescence.

This *in vitro* fusion assay was further developed by Weber and colleagues in 1998, whereby they reconstituted full-length neuronal t-SNAREs (Syntaxin 1 and SNAP-25) into unlabelled vesicles and full-length VAMP 2 into fluorescence vesicles, allowing them to measure the rate at which the SNARE complex fused the two populations of liposomes (Weber *et al*, 1998).

Once established, the *in vitro* fusion assay can be used to study the interactions between SNARE proteins and their effectors, for example signalling molecules or SM proteins, in order to determine the function of any interactions between the proteins. For example, the yeast SM protein Sec1p was added to a liposome fusion assay where it was found predominantly to interact with the t-SNAREs Sso1p and Sec9c and the ternary SNARE complex where it stimulated fusion between the two vesicle populations (Scott *et al*, 2003).

The v-SNARE VAMP 2 is known to form functional SNARE complexes with the t-SNAREs Syntaxin 4 and SNAP-23, and formation of this ternary complex is responsible for the fusion of GSVs with the plasma membrane in adipose and muscle cells in response to insulin (Rea *et al*, 1998). Although this SNARE complex forms the basis of GSV fusion, many other factors are involved, including the

signalling molecules PKB and PI-3-K (Holman *et al*, 1997; Jiang *et al*, 2003), and the SM protein Munc-18c (Tellam *et al*, 1997).

3.2 Aims of this chapter

The aim of this chapter was to purify and reconstitute the full-length SNARE proteins Syntaxin 4, SNAP-23 and VAMP 2 into proteoliposomes in order to establish an *in vitro* fusion assay as a method to study the regulation of membrane fusion by this SNARE complex. This assay would then be further used to assess the effect of regulatory SM proteins on SNARE complex formation.

This assay was previously established in our lab by Dr Fiona Brandie (Brandie *et al*, 2008), however problems with reconstitution and SNARE complex formation necessitated that the assay be re-established and re-optimised. We were able to optimise the assay in order to produce adequate levels of fusion, similar to those found in literature (Brandie *et al*, 2008; Ji *et al*, 2010).

3.3 Results

3.3.1 Purification of full-length and cytosolic VAMP 2

Full-length VAMP 2 was expressed as an N-terminally His_6-tagged protein from the vector pQE30 (QIAGEN) in BL21 (DE3) *E. coli* cells. Ni-NTA agarose chromatography was used to purify the protein, which was eluted from the beads using a linear Imidazole gradient from 50-500 mM. A sample from each fraction was analysed by SDS PAGE analysis and Coomassie staining. A typical purification is shown in Figure 3.2.

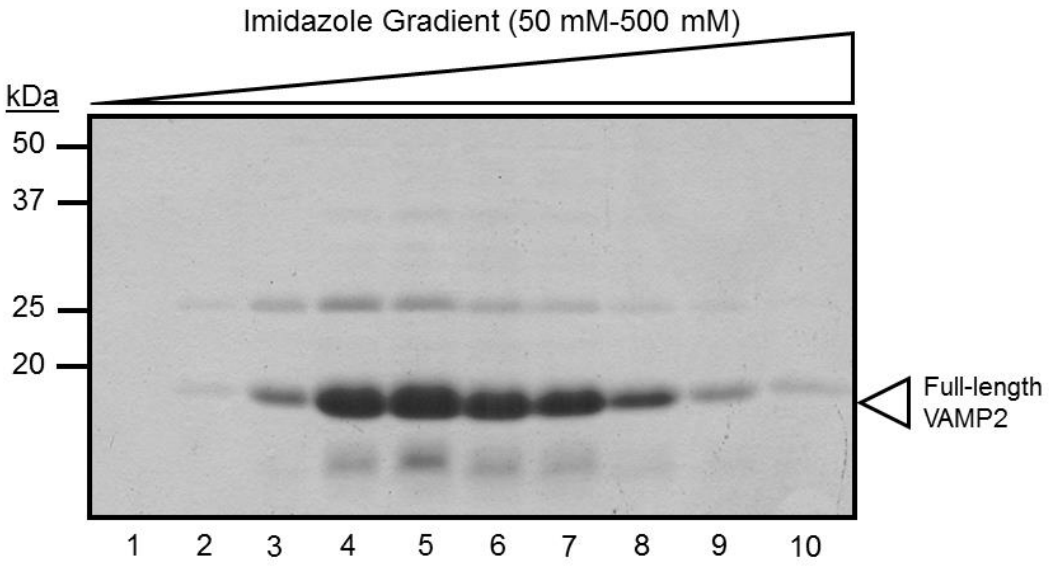

Figure 3.2 Purification of full-length VAMP 2
Full-length VAMP 2 was expressed from the vector pQE30 in BL21 (DE3) *E. coli* cells. The protein was purified using an N-terminal His_6 tag as described as in Section 2.2.5.1, using 3 ml Ni-NTA agarose. 6 L of bacteria were grown to an OD_{600} of ~0.8 before induction with 1 mM IPTG for four hours. After elution using a linear Imidazole gradient, 5 µl of each fraction was analysed for protein content on an 18 % SDS PAGE gel and the largest yielding fractions were combined and concentrated, usually to a volume of 1 ml. Molecular weight markers are indicated.

By combining the highest yielding elutions of VAMP 2 (lanes 4-7) were able to obtain a sufficient concentration of protein to continue with reconstitution into proteoliposomes for the *in vitro* fusion assay.

Cytosolic VAMP 2 was required as a control for the *in vitro* fusion assay: this protein contains the SNARE domain of the v-SNARE but not the transmembrane domain. By adding the protein to a mixture of t- and v-SNARE proteoliposomes, the cytosolic VAMP 2 is able to bind to the binary t-SNARE complex, preventing the v-SNARE in the donor vesicles from binding and forming a fusogenic SNARE complex. This allows us to ensure that fusion observed is the result of SNARE complex formation, and not simply spontaneous fusion of the vesicles. Cytosolic VAMP 2 was also expressed as an N-terminally His_6-tagged protein from pQE30 (QIAGEN) and was purified in an similar manner to the full-length v-SNARE, except Triton X-100 and n-octyl-β-D-glucopyranoside were omitted from the buffers. Data from a typical purification is shown in Figure 3.3.

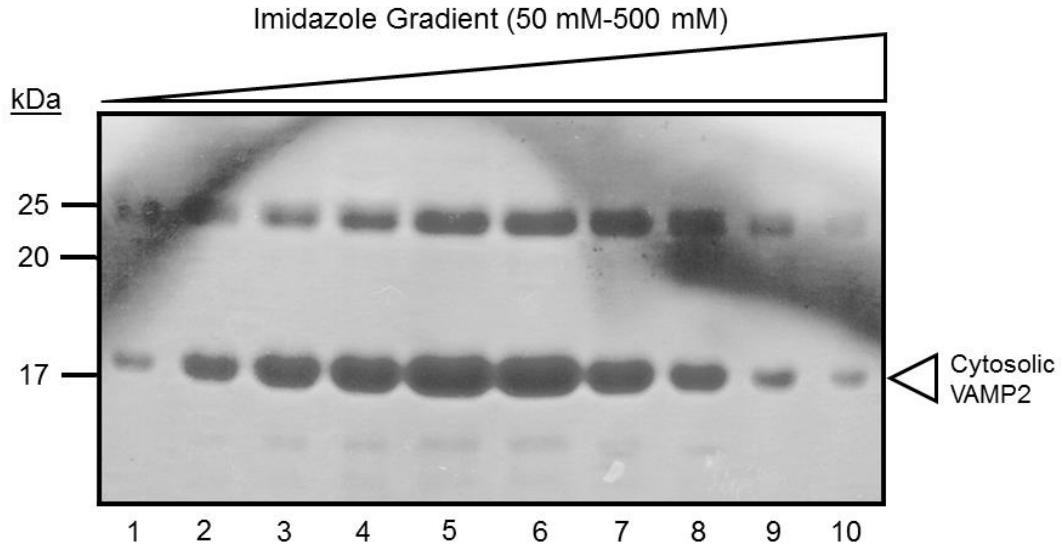

Figure 3.3 Purification of cytosolic VAMP 2
The cytosolic domain of VAMP 2 was expressed from the vector pQE30, and purified as outlined in Section 2.2.5.1. 5 µl of each elution was analysed on an 18 % SDS PAGE gel and Coomassie stained to visualise the protein. The highest yielding fractions were pooled and concentrated to 1 ml before being split into aliquots and stored at -80 °C. Molecular weight markers are indicated, and this figure represents a typical purification.

As shown in Figure 3.3, although high levels of cytosolic VAMP 2 were produced, a second band can be seen on the gel with a similar elution profile as the v-SNARE. Interestingly, a band of similar molecular weight (~25 kDa) was observed in cytosolic v-SNARE preparations by previous students in our lab who studied both the mammalian (Dr V. Aran-Ponte) and yeast (Dr C. MacDonald) fusion systems, however the presence of this band did not appear to effect cytosolic v-SNARE functioning as a control for the *in vitro* fusion assay (Brandie *et al*, 2008). Again, combining the highest yielding elutions (lanes 4-7) allowed us to obtain sufficient cytosolic VAMP 2 protein to use as a control in our experiments.

3.3.2 Initial purification of the t-SNARE Syntaxin 4/SNAP-23 complex

Early fusion assay studies into neuronal SNARE complex function used reconstituted t-SNARE complexes that were purified from co-transformed bacteria: that is, both t-SNAREs (Syntaxin 1 and SNAP-25) were expressed from two different plasmids which were co-transformed into the same BL21 (DE3) *E. coli* and selected using dual antibiotic resistance (Weber *et al*, 1998). t-SNARE complexes could then be purified via the GST-tag on SNAP-25 and both t-SNAREs

reconstituted as a complex. Indeed, initial studies into the insulin-responsive SNAREs in our lab used this same technique (Brandie *et al*, 2008).

Full-length Syntaxin 4 was expressed as an untagged protein from the vector pQE30 (QIAGEN). Full-length SNAP-23 was expressed as a Thrombin-cleavable GST-tagged protein from the vector pET41A (Novagen). Both plasmids were co-transformed into BL21 (DE3) *E. coli* cells and successful transformations selected for on dual antibiotic (Ampicillin and Kanamycin) agar plates.

t-SNARE complexes were purified utilising the C-terminal GST tag present on SNAP-23. After incubation overnight with Glutathione Sepharose 4B beads (GE Healthcare) the sample was washed and cleaved from the beads using 100 units of Thrombin (Sigma-Aldrich). Aliquots of the wash steps and elution were analysed by SDS PAGE and Coomassie staining, as shown in Figure 3.4.

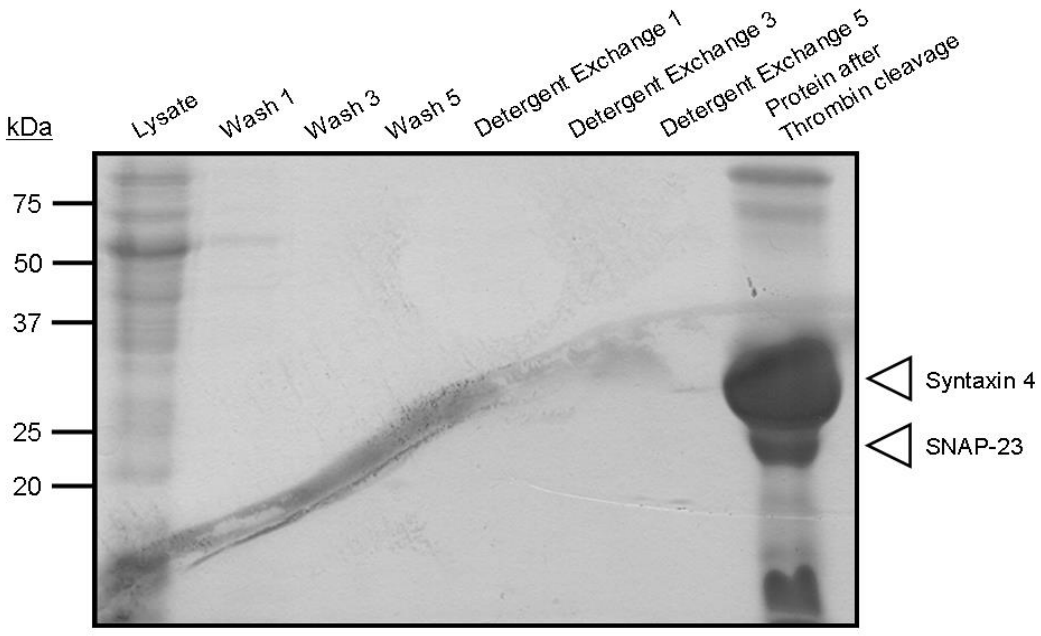

Figure 3.4 Purification of t-SNARE complexes
Syntaxin 4/SNAP-23 t-SNARE complexes were purified in BL21 (DE3) *E. coli* which had been co-transformed with both pQE30 and pET41A plasmids. Usually 8 L of bacteria was grown to OD_{600} of 0.8 before 4 hour induction with 1 mM IPTG. Molecular weight markers are indicated, and data is representative of a standard purification.

As Figure 3.4 shows, there appears to be an excess of Syntaxin 4 protein compared to SNAP-23. Ideally these proteins should form a binary t-SNARE complex with 1:1 stoichiometry. As the complex is purified using the C-terminal GST tag present on

the SNAP-23, it is assumed that 1:1 t-SNARE complexes would be isolated, since the Syntaxin 4 is purified via the interaction between the SNARE domains of the two t-SNAREs. Since both proteins are expressed from different plasmids, it is plausible that one protein is being over-expressed relative to the other, which would explain why more Syntaxin 4 is present. This theory appears plausible as Syntaxin 4 is expressed from the vector pQE30, which is under the control of the T5 promoter, whilst SNAP-23 is expressed from the vector pET41A, under the control of the T7 promoter. Study of QIAGEN literature indicates that for best expression of the protein, the plasmid should be transformed into *E. coli* cells expressing the repressor plasmid pREP4: the T5 promoter is known to exhibit high levels of basal expression, and this plasmid is designed to regulate and repress this. Therefore, it is perhaps unsurprising that high levels of Syntaxin 4 are obtained. However, as the complex is purified as a whole, the excess Syntaxin 4 suggests that more of this t-SNARE is binding to the SNAP-23 than the 1:1 ratio we would expect to see *in vivo*. This correlates with data published by Ji *et al* (2010), who noted that the neuronal t-SNAREs Syntaxin 1a and SNAP-25 are able to form 2:1 complexes, where the second Syntaxin molecule functions in place of VAMP 2, which in turn lowers the rate of fusion observed. It is, therefore, possible that similar complexes are forming between Syntaxin 4 and SNAP-23, accounting for the greater amount of Syntaxin purified.

We decided to continue and reconstitute these complexes into vesicles in order to test whether the ratio of Syntaxin 4 to SNAP-23 is altered by the reconstitution procedure.

3.3.3 Preparation of lipid stocks

Lipid stocks were obtained from Avanti Polar Lipids (Alabaster, AL, USA) and prepared in chloroform. Two populations of liposomes were required for this study: and unlabelled acceptor mix and a second fluorescently labelled donor mix.

Acceptor liposomes were made by mixing 85 mol % 1-palmitoyl-2-oleoyl phosphatidylcholine (POPC) and 15 mol % 1,2-dioleoyl phosphatidylserine (DOPS) to a final lipid concentration of 15 mM. Fluorescent donor liposomes were made by

decreasing the amount of POPC to 82 mol % and adding the lipid-conjugated fluorophores NBD-DPPE and Rhodamine-DPPE at 1.5 mol % each to a final lipid concentration of 15 mM. Historically, t-SNARE complexes are reconstituted into acceptor liposomes, and v-SNAREs into donor, however fusion also occurs if proteins are reconstituted into the "opposite" liposomes (Scott et al, 2003). Lipid stocks were generally made to a volume of 3 ml and stored under nitrogen at -80 °C until use.

3.3.4 Reconstitution of SNAREs into liposomes

SNARE proteins/complexes were reconstituted into liposomes as specified in Section 2.2.5.3. Briefly, dried acceptor or donor lipid films were resuspended in 500 µl t-SNARE complex or VAMP 2 protein containing 0.8 % n-octyl-β-D-glucopyranoside respectively. 1 ml Exchange/Reconstitution buffer was added drop-wise while vortexing the samples in order to dilute the detergent below its CMC and form proteoliposomes. The samples were dialysed overnight in 4 L Exchange/Reconstitution buffer containing 4 g Biobeads (BioRad) to absorb any detergent.

Reconstitution efficiency was assessed by running samples of protein before reconstitution alongside a sample of the proteoliposomes recovered after gradient centrifugation (Section 2.2.5.4). Figure 3.5 shows data from a standard reconstitution.

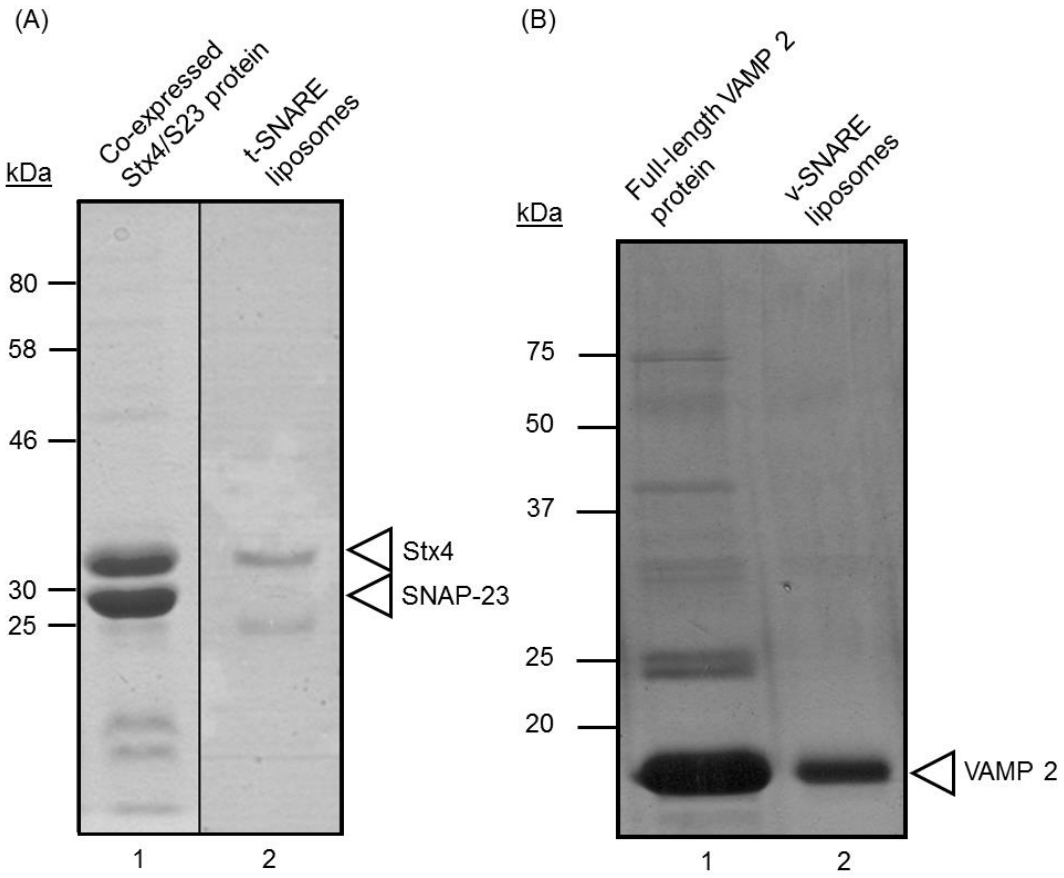

Figure 3.5 Reconstitution of full-length SNARE proteins
500 µl of (A) t-SNARE or (B) v-SNARE protein was reconstituted into proteoliposomes as described. Proteoliposomes were purified using a 3-step Histodenz™ gradient. The 1.5 ml dialysate was mixed with 1.5 ml 80 % Histodenz™ in Exchange/Reconstitution buffer, before being overlayed with 1 ml of 30 % Histodenz™ in Exchange/Reconstitution buffer. Finally, 250 µl of Buffer (without glycerol) was overlayed. The gradients were spun for 4 hours at ~375000 *g* in a Beckman SW60 rotor. 400 µl proteoliposomes were harvested from the top of the gradient (the interface between the 0 % and 30 % layers). A sample of each proteoliposome population was analysed by SDS PAGE along with a sample of protein retained before reconstitution.

As shown in Figure 3.5A, the Syntaxin 4 protein appears to reconstitute into the liposomes, whilst the levels of reconstituted SNAP-23 protein are low (lane 2). It is perhaps unsurprising that the Syntaxin reconstitutes more efficiently than SNAP-23 as it contains a transmembrane domain which can be inserted into the lipid bilayer of the vesicles, whilst SNAP-23 is palmitoylated *in vivo* and is reconstituted into the vesicles by its interaction with Syntaxin 4 (much in the same way Syntaxin 4 is purified in complex with SNAP-23).

To ensure that SNAP-23 was being reconstituted, the samples were subjected to Western Blot analysis, as shown in Figure 3.6.

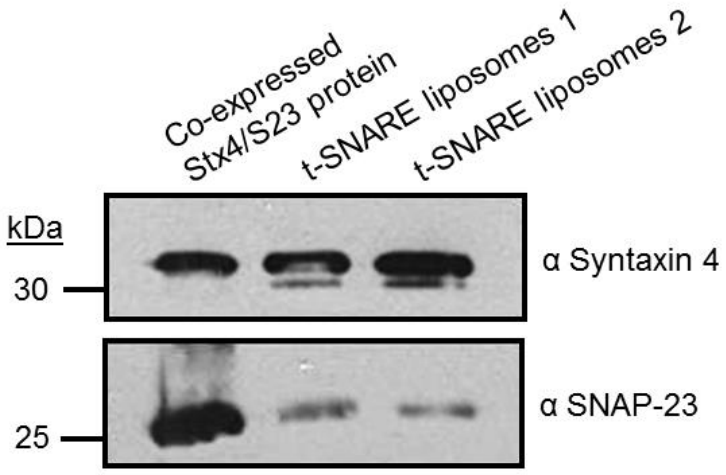

Figure 3.6 Western blot analysis of acceptor liposomes
A 5 µl sample of protein retained before reconstitution was analysed alongside 5 µl of two proteoliposome populations to check for levels of t-SNARE reconstitution. After transfer, the nitrocellulose membrane was cut into strips, and blotted for t-SNARE proteins using the antibodies specified.

Analysis of the proteoliposomes by western blotting confirms that there is SNAP-23 protein in the vesicles; however the levels appear much lower than Syntaxin 4, although this could be attributed to a lower affinity of the antibody for SNAP-23. We decided to continue with the assay, as there was t-SNARE protein present in the vesicles and, even at these somewhat low levels, this may be enough to stimulate fusion between the vesicle populations.

3.3.5 Initial fusion assays

The reconstituted acceptor and donor proteoliposomes were used in an *in vitro* fusion assay. A control reaction was set up in addition to the fusion assay to ensure that any observed fusion was due to the formation of SNARE complexes and not spontaneous fusion of the vesicles. For the control reaction, 45 µl of acceptor (t-SNARE) liposome was mixed with 5 µl of VAMP 2 cytosolic domain and incubated for 15 minutes on ice in one well of a white-bottomed 96-well plate. After this incubation, 5 µl of donor (v-SNARE) liposome was added. 45 µl of acceptor liposomes was added to a second well of the 96-well plate, and to this 5 µl of Exchange/Reconstitution buffer was added along with 5 µl of donor liposome. The plate was covered and incubated overnight at 4 °C to induce pre-docking of the SNARE complexes.

The next day, the plate was warmed in to 37 °C in a FLUOstar Optima spectrophotometer for 15 minutes in order to bring the plate to reaction temperature. Fluorescence was measured every two minutes for 2 hours, at which point 10 µl of 2.5 % (w/v) n-dodecylmaltoside was added in order to lyse the vesicles and allow for measurement of the maximum NBD fluorescence of the donor liposomes. Fluorescence was measured for a further 40 minutes, after which the data was collated. Data was normalised (for this and future experiments) by assigning the lowest fluorescence reading to 0 % and maximal readings after detergent addition as 100 %, with data plotted as a percentage of this maximum fluorescence, as shown in Figure 3.7.

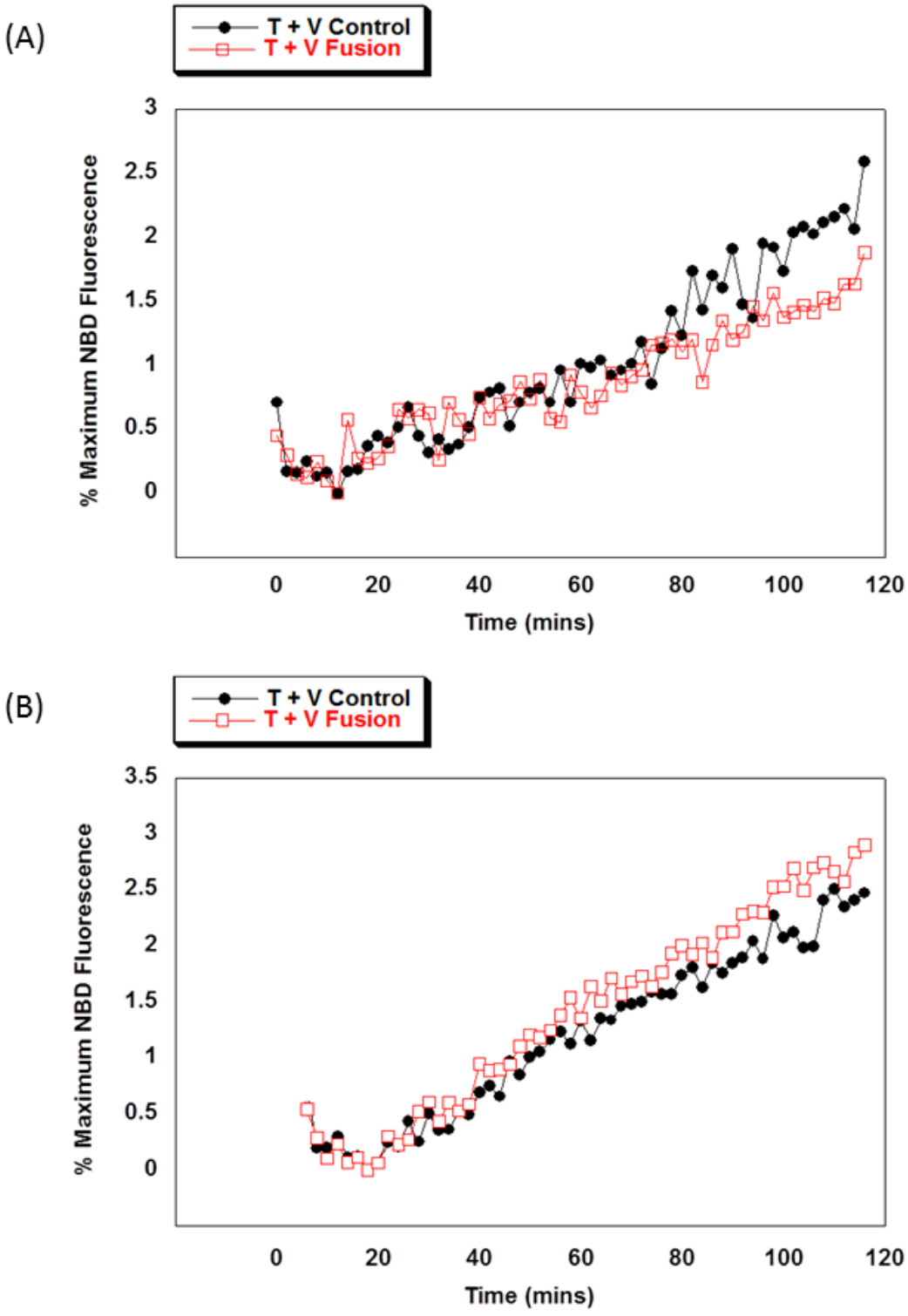

Figure 3.7 Initial Fusion Assays
45 µl of t-SNARE liposome was mixed in the presence (black circles) or absence (red squares) of 5 µl of the cytosolic SNARE domain of VAMP 2 – this functions as a control by binding to the t-SNARE proteins in the acceptor liposomes preventing fusion with the VAMP 2 present in the donor liposomes. Fusion was measured over a two hour period, and maximum NBD fluorescence obtained by lysis of the donor vesicles with detergent. Figures (A) and (B) show normalised data obtained from two separate protein purifications and reconstitutions, and are representative of data obtained from these experiments.

As Figure 3.7 shows, we were able to obtain moderate (~3 %) fusion between the two vesicle populations, although this level was lower than data previously produced in our lab (Brandie *et al*, 2008). Given that there are low levels of SNAP-23 being purified and reconstituted (as shown in Figure 3.4 and Figure 3.5), there are a few possible reasons that little fusion is occurring. Firstly, as suggested previously in Section 3.3.2, it is possible that the increased amounts of Syntaxin 4 protein relative to SNAP-23 is causing non-functional SNARE complex formation. It is also possible that the low levels of SNAP-23 in the vesicles is limiting the amount of binary t-SNARE complexes that can fuse with the v-SNARE donor vesicles, leading to low levels of fusion.

Furthermore, there was little difference between the control reaction (containing cytosolic VAMP 2) and the fusion reactions, suggesting that the cytosolic VAMP 2 was not functioning as an adequate control reaction for this experiment. Cytosolic VAMP 2 was added in excess to the control reaction, and should have been sufficient to inhibit fusion as it has done in previous experiments (Weber *et al*, 1998; Brandie *et al*, 2008; Ji *et al*, 2010).

We decided at this point to investigate other methods of t-SNARE protein purification and reconstitution in order to increase the amount of binary complex in our liposomes and, in theory, increase the levels of fusion.

3.3.6 Formation of t-SNARE binary complexes for reconstitution

In an attempt to solve the issue of low fusion, t-SNARE binary complexes were formed in solution by mixing protein from separate t-SNARE purifications. By mixing the t-SNAREs in a 1:1 molar ratio, it was hoped that this would help prevent the formation of non-functional t-SNARE complexes which we hypothesised may responsible for the low levels of fusion obtained in previous assays (shown in Figure 3.7).

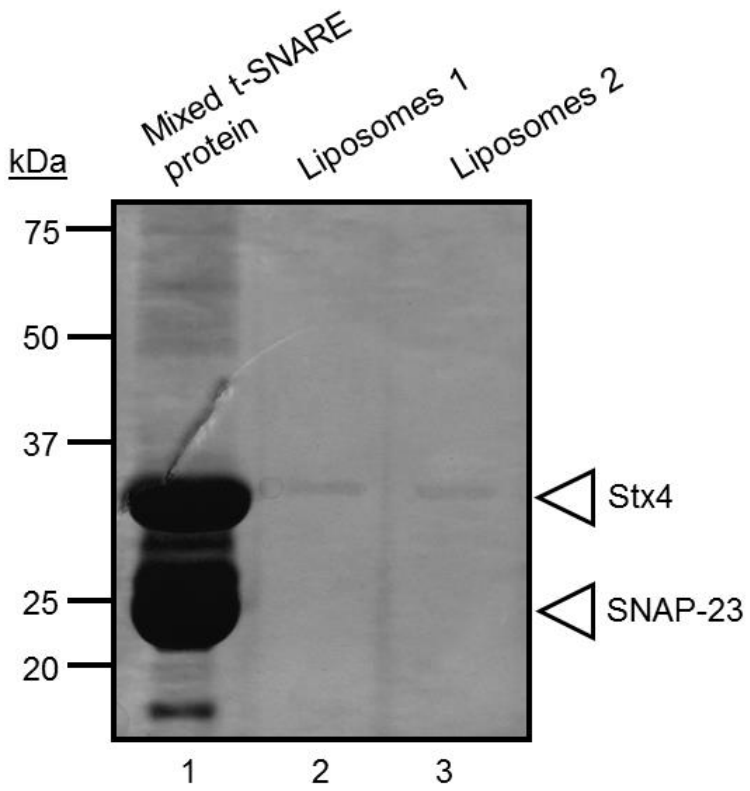

Figure 3.8 Mixing t-SNARE proteins before reconstitution
His-tagged Syntaxin 4 was expressed from the vector pQE30, and GST-tagged SNAP-23 was purified from pET41A. After elution from Ni-NTA and Glutathione Sepharose 4B respectively, the proteins were mixed overnight at 4 °C in a molar ratio of 1:1. The next day, proteoliposomes were formed by resuspension of the lipid film in the protein mixture and, after overnight dialysis; proteoliposomes were recovered by gradient centrifugation (Sections 2.2.5.3 and 3.3.4).

Although both t-SNAREs were present in the pre-reconstitution protein mix, only Syntaxin 4 appeared to be reconstituted into the liposomes (Figure 3.8lanes 2 and 3). This suggests that the binary t-SNARE complex was not forming, preventing SNAP-23 from being reconstituted along with the Syntaxin 4. As these proteins were expressed from the same plasmids as the co-expression experiments (Section 3.3.2), this suggests that the reason we are not obtaining much SNAP-23 reconstitution is because the binary t-SNARE complex is not forming between the proteins. At this stage, we decided to investigate new methods for purifying recombinant t-SNARE complexes.

3.3.7 pETDuet-1 purification and reconstitution of t-SNARE complexes

As previously discussed in Section 3.3.5, there was no difference in the rate of fusion obtained between the control and fusion reactions, and the overall rate of fusion is moderate (~3 %). Previously published data show that it is possible to obtain a rate of 10-20 % fusion (Ji *et al*, 2010). These higher rates allow for a better analysis of the effects of proteins, for example SM proteins, on the rate of fusion as there is a greater difference between the rate of fusion, and the rate of the control (~0-1 %).

In order to address the issue of binary t-SNARE complex formation, we located a construct containing Syntaxin 4 and SNAP-23 which had been generated in our lab by Dr Fiona Brandie. This utilised the two multiple cloning sites in the vector pETDuet-1 (Novagen) – both cloning sites are under the control of the T7lac promoter, meaning that both genes expressed in the vector are transcribed and translated at a similar rate. This construct contained an N-terminally His-tagged Syntaxin 4 in multiple cloning site 1 (MCS1) and a C-terminally GST-tagged SNAP-23 in the second multiple cloning site (MCS2). Protein was purified in an identical manner to the co-expressed t-SNARE complexes; however Kanamycin was omitted from the growth media as this vector only confers Ampicillin resistance. The complexes were thrombin-cleaved from Glutathione Sepharose 4B beads and an aliquot from the wash steps and elution analysed by SDS-PAGE and Coomassie staining.

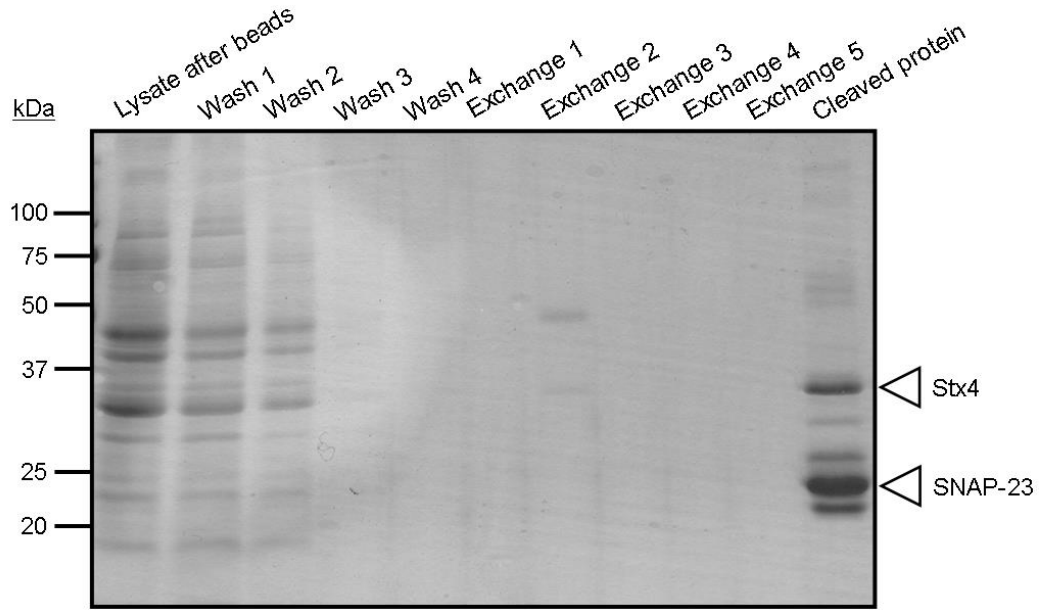

Figure 3.9 Purification of t-SNARE complex from pETDuet-1
pETDuet-1 was used to express full-length t-SNAREs in complex via a C-terminal GST-tag on SNAP-23. Protein was purified as described in Section 2.2.5.1 using 4 ml of Glutathione Sepharose 4B beads. Usually 8 L of bacterial culture was grown to an OD_{600} of ~0.8 before induction of protein expression for 4 hours with 1 mM IPTG. After thrombin cleavage of the complexes, a 5 µl aliquot of the elution was analysed alongside the wash/detergent exchange fractions on a 15 % SDS-PAGE gel. The cleaved protein was generally concentrated to a volume of 500 µl and snap-frozen in liquid nitrogen.

As shown in Figure 3.9, using pETDuet-1 to express the t-SNARE proteins resulted in a more equal expression of the t-SNARE proteins compared to co-expressing separate plasmids. Once purified, these t-SNARE complexes were reconstituted into acceptor liposomes as outlined in Sections 2.2.5.3 and 2.2.5.4.

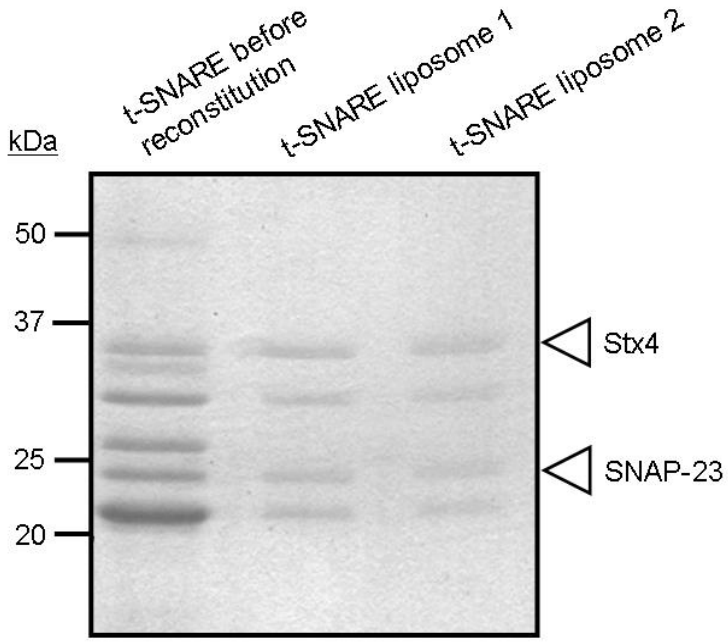

Figure 3.10 Reconstitution of t-SNARE proteins
500 µl purified t-SNARE complex was used to resuspend 100 µl 15 mM acceptor lipid mix before overnight dialysis to remove detergent. Proteoliposomes were recovered by floatation on a Histodenz™ density gradient. Two liposome populations are shown, both reconstituted from the shown protein sample.

As Figure 3.10 shows, the t-SNARE proteins expressed from pETDuet-1 reconstitute evenly, suggesting that binary t-SNARE complexes are forming. It is important to note the two contaminant bands in the protein preparation that are reconstituted into the liposomes alongside the full-length SNARE proteins. These are postulated to be degradation products of the SNARE proteins: in particular with the Syntaxin 4 degradation product, it is postulated to be N-terminal degradation as the C-terminal transmembrane domain is required for successful reconstitution. As it is theorised that the N-terminal peptide of Syntaxin is required for SNARE complex regulation (Hu *et al*, 2007; Section 1.8.2.2) it is possible that these proteins may inhibit SNARE complex formation.

The fusogenic properties of these liposomes could then be assessed using the *in vitro* fusion assay.

3.3.8 Fusion assays

Acceptor t-SNARE liposomes prepared from the plasmid pETDuet-1 were used in a fusion assay with donor v-SNARE vesicles. The experimental setup was similar to that described previously (Section 3.3.5), however the donor vesicles were produced using 100 µl of a 3 mM lipid mix rather than 500 µl (covered in detail in Section 3.3.9) and fluorescence readings were measured every two minutes for 2 hours before addition of detergent to lyse the vesicles in order to obtain maximum NBD fluorescence readings. As before, data was normalised and plotted as a percentage of the maximum observed NBD fluorescence.

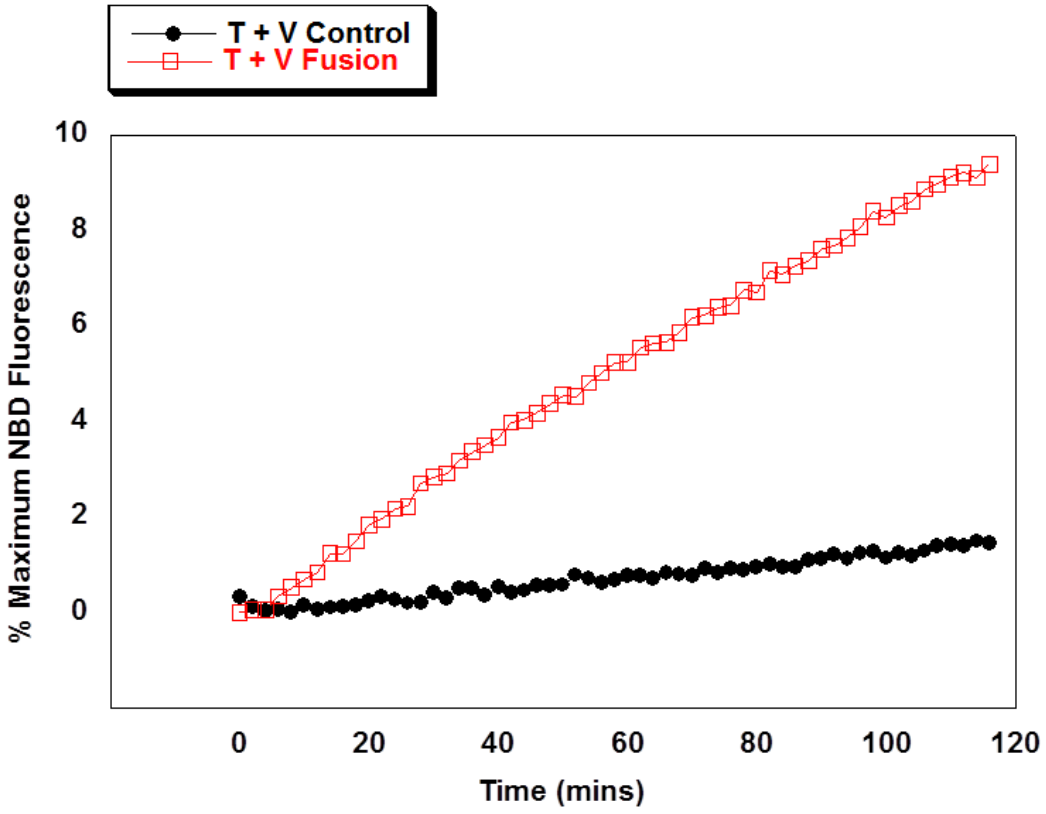

Figure 3.11 pETDuet-1 Fusion Data
45 µl t-SNARE liposome was mixed with 5 µl v-SNARE donor liposome in the presence (black circles) or absence (red squares) of 5 µl of the cytosolic SNARE domain of VAMP 2. Fusion was measured over a two hour period, and maximum NBD fluorescence obtained by lysis of the donor vesicles with detergent. This figure shows representative data from three independent experiments.

As Figure 3.11 shows, we are now able to show fusion between our t- and v-SNARE vesicles, indicating that the complexes formed using the vector pETDuet-1 are

stable and functional, and that fusion between the two vesicle populations is SNARE dependent. All future *in vitro* fusion assay experiments were performed using t-SNARE proteins expressed from this vector.

3.3.9 Functional significance of lipid content of donor vesicles

While researching possible solutions to overcome the low levels of fusion being observed in the assay (Section 3.3.5), it was discovered that it is possible to reconstitute v-SNAREs into liposomes containing only 20 % of the usual donor lipid level, whilst still maintaining fusion (Vicogne & Pessin, 2008).

Studies into the structure and function of the v-SNARE VAMP 1 indicated that the protein was sensitive to protein-lipid interactions, especially in the transmembrane domain of the protein (Yassine *et al*, 2010). To test whether the lipid content of the vesicles affects the function of VAMP 2, v-SNARE protein was reconstituted into vesicles using either 100 µl or 500 µl fluorescent donor lipid stock, and their ability to fuse with t-SNARE liposomes was assessed using the *in vitro* fusion assay.

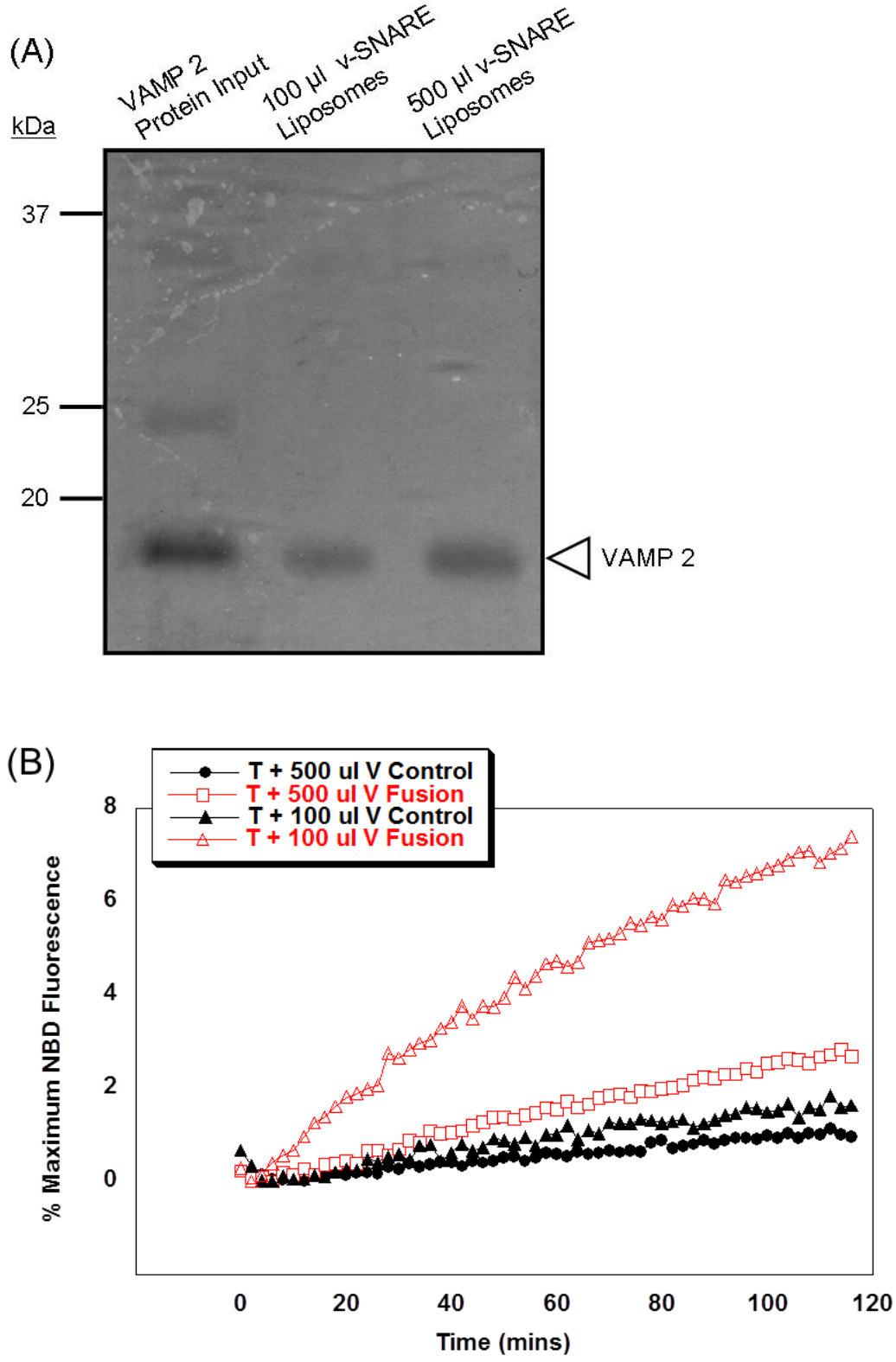

Figure 3.12 Test of v-SNARE protein reconstitution and function
(A) 500 µl v-SNARE protein was reconstituted into liposomes using either 100 µl or 500 µl fluorescent lipid mix. Levels of protein reconstitution were tested by running 5 µl protein input alongside 5 µl of each liposome population on an SDS PAGE gel and Coomassie staining. (B) 45 µl t-SNARE liposome were mixed with 5 µl v-SNARE donor liposome in the presence (black triangles/circles) or absence (red triangles/circles) of cytosolic VAMP 2. Fusion was measured over a two hour period, and maximum NBD fluorescence obtained by lysis of the donor vesicles with detergent. This figure shows representative data from three independent experiments.

Although the vesicles with a lower lipid:protein ratio contain slightly lower levels of VAMP 2 protein, as shown in Figure 3.12A, they are able to sustain higher levels of SNARE-mediated membrane fusion, leading to around a 4-fold increase in the final fluorescence percentage (Figure 3.12B). This appears to support the previous observations regarding VAMP 1 (Yassine *et al*, 2010), and extends the model to VAMP 2, although further studies would be required to determine how the lipids are affecting VAMP 2 function and/or structure.

3.3.10 Characterisation of proteoliposome size

Critics of the *in vitro* fusion assay argue that the reconstitution method used to incorporate the SNARE proteins into the vesicles results in small (<20 nm) liposomes, which have a tendency to spontaneously fuse due to high membrane curvature (Chen *et al*, 2006). To ensure that our vesicles were within the generally accepted diameter range of 20-100 nm, Transmission Electron Microscopy was used to estimate the size of the t- and v-SNARE vesicles. Samples of proteoliposome were diluted 1/10 in reconstitution buffer and imaged at 16000x magnification.

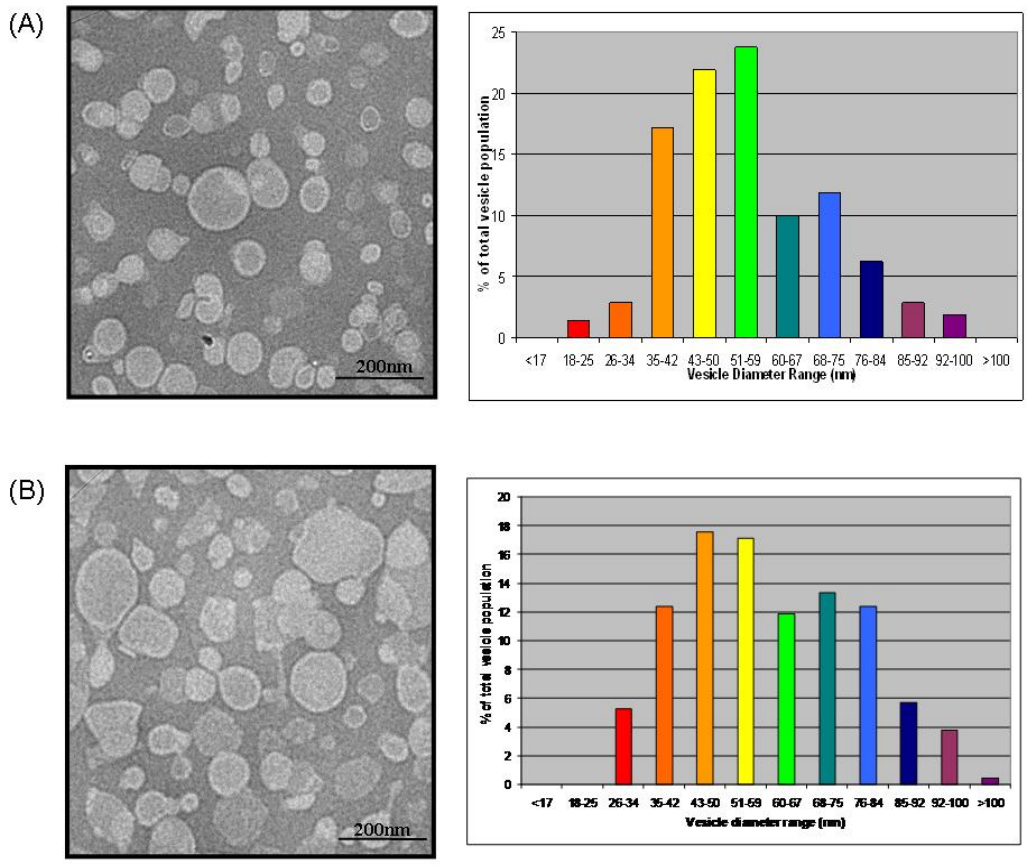

Figure 3.13 Transmission EM of (A) t- and (B) v-SNARE proteoliposomes
Diluted samples of SNARE proteoliposomes were applied to a glow-discharged copper grid before 1 % methylamine vanadate was applied as a negative stain. Samples were imaged at 120 kV. SIS iTEM imaging software (Olympus) was used to directly measure the liposome diameter from multiple grids before calculating the percentage of total population for each diameter range.

As Figure 3.13 shows, both the t- and v-SNARE vesicles fall within the 20-100 nm diameter range, indicating that high membrane curvature is not a factor in our assay, and that the levels of fusion we observed are due to SNARE complex formation, as fusion between the vesicles is blocked by the addition of the cytosolic domain of VAMP 2 (Figure 3.11 and Figure 3.12B).

3.4 Conclusions

Whilst the *in vitro* fusion assay is a useful tool for studying the fusogenic properties of SNARE proteins, establishing this assay to study the SNAREs involved in the fusion of GSVs with the plasma membrane has been difficult. Using a standard co-expression method (with each t-SNARE in a separate vector, but transformed into

the same *E. coli* cells) we observed the formation of non-functional SNARE complexes, possibly due to the different levels of translation of the t-SNAREs, as Syntaxin 4 appeared to be produced in vast excess to SNAP-23 (Figure 3.4To overcome this, both t-SNAREs were expressed from one vector which contains two multiple cloning sites (pETDuet-1, Novagen). Using this vector, we were able to produce t-SNARE complexes with similar levels of each t-SNARE, thus preventing (or reducing) non-functional complex formation (Figure 3.9

These protein complexes were then reconstituted into acceptor liposomes in order to test their ability to fuse with VAMP 2-containing donor vesicles. Experiments using the initial t-SNARE complexes resulted in moderate levels of fusion (Section 3.3.5). Experiments using the complexes purified from pETDuet-1 showed higher levels of fusion compared to the control experiment (Figure 3.11), indicating that protein expression from pETDuet-1 resulted in formation of functional binary t-SNAREs which were able to from SNARE complexes with VAMP 2.

Once the *in vitro* fusion assay was established, we were able to use it to test the importance of the protein/lipid ratio in the donor v-SNARE vesicles. Altering the amount of lipid used to reconstitute the vesicles showed that higher levels of fusion are obtained with lower lipid concentrations in the donor vesicles, despite slightly less protein being reconstituted in comparison to the vesicles with a higher lipid:protein ratio (Figure 3.12). Based on these findings, we chose to continue the experiments using donor liposomes reconstituted using 100 µl of lipid stock.

Finally, we tested the physical properties of the liposomes by measuring their diameter using transmission electron microscopy. It is argued that vesicles smaller than 20 nm have a tendency to spontaneously fuse (Chen *et al*, 2006), however analysis of our vesicles showed that the majority of both donor and acceptor vesicles have a diameter greater than 20 nm, indicating that membrane curvature should not be a contributing factor to fusion in our assay.

4 The effect of Munc-18c on SNARE-mediated membrane fusion

4.1 Introduction

The rate of fusion observed in *in vitro* experiments, such as the liposome fusion assay, are many times slower than those observed *in vivo*, indicating an additional level of regulation than SNARE proteins alone. One such family of proteins identified as regulators of SNARE-mediated fusion are the Sec1/Munc-18 (SM) family of proteins, with Munc-18c being implicated in the regulation of GLUT4 exocytosis (Tellam *et al*, 1995, 1997).

The exact function of SM proteins is highly debated, as many of these proteins exhibit different functions depending on the experimental conditions. There are, however, three widely-accepted modes of binding observed between SM proteins and their cognate SNARE partners, outlined in Figure 4.1.

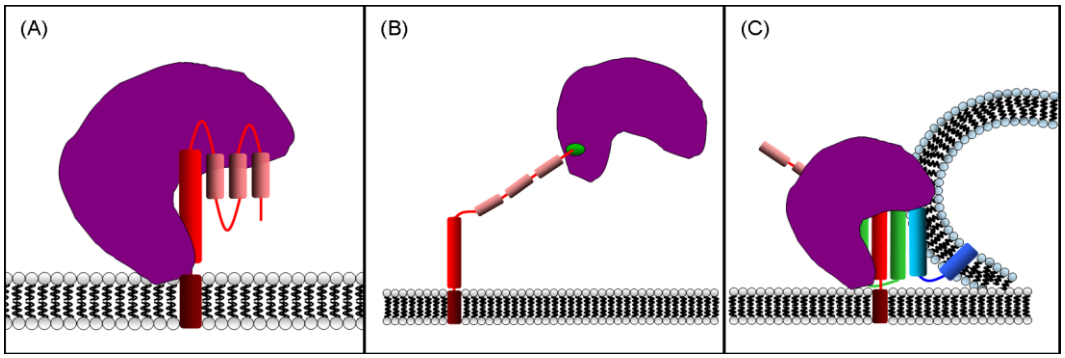

Figure 4.1 Binding modes between SNARE and Sec1/Munc-18 proteins
Three binding modes have been shown to exist between SM proteins and their SNARE partners. (A) Binding between the "closed" conformation of Syntaxin (red) and the SM protein (purple) is termed Mode 1. (B) Binding between the N-terminus of the Syntaxin and a pocket on the outside of the SM protein is Mode 2. (C) Binding between the assembled SNARE complex (SNAP-23 green, VAMP 2 blue) and the SM protein is Mode 3. Not all SM/SNARE partners exhibit all modes of binding.

Mode 3 binding between SM and SNARE proteins has been characterised in yeast, where the SM protein Sec1p was shown to co-precipitate with its cognate SNAREs, and is localised to areas in the plasma membrane where SNARE complexes are believed to assemble and function (Carr *et al*, 1999). However,

studies in mammalian systems have been less conclusive and conflicting data exists as to whether mammalian SM proteins are able to bind their cognate SNARE complexes in this manner. Initial studies identified that the neuronal SM protein Munc-18a was only able to bind its cognate Syntaxin, and that this binding (presumed to be Mode 1 binding) prevented the Syntaxin forming a SNARE complex with SNAP-25 and VAMP 2 (Yang *et al*, 2000). In contrast, subsequent studies showed that in PC12 cells, Munc-18a-bound Syntaxin is able to form SNARE complexes with its cognate SNARE partners, and that Munc-18a is involved in SNARE complex formation (Zilly *et al*, 2006).

It has previously been shown in our lab that Munc-18c is able to bind to both the v-SNARE VAMP 2 and the t-SNARE Syntaxin 4 (Brandie *et al*, 2008; Aran *et al*, 2009). Mutants of Syntaxin 4 were generated that were unable to exhibit the "closed" conformation (L173A/E174A); were missing the N-terminal peptide (ΔN36) or both (ΔN36/LE) in order to test the interactions between Syntaxin 4 and Munc-18c. Using pull-down assays and Surface Plasmon Resonance (SPR) experiments, the interactions between wild-type/mutant Syntaxin 4 and Munc-18c were further characterised, and it was shown that Syntaxin 4 and Munc-18c exhibit both Mode 1 and Mode 2 binding (Aran *et al*, 2009). Low-resolution structural studies have also indicated that the N-terminal peptide of Syntaxin 4 is critical in binding to Munc-18c, regardless of binding mode (Christie *et al*, 2012). Furthermore, it has been shown that Munc-18c is also able to bind to the SNARE complex consisting of Syntaxin 4, SNAP-23 and VAMP 2 (Latham *et al*, 2006); however this interaction has not yet been investigated on a molecular level.

In order to characterise Mode 3 binding between SM proteins and SNARE complexes, point mutations have been made to the SM proteins at key residues which are believed to have involvement in the interactions involved in these complexes. The residues are labelled according to the position of the amino acid in the protein studied – the homologous position in Munc-18c (based on sequence alignment) is given in parenthesis.

Analysis of the structure of the Munc-18a/SNARE complex produced by Nuclear Magnetic Resonance (NMR) imaging shows that formation of the complex requires the Syntaxin N-terminal peptide, the Habc domain and the SNARE bundle (Dulubova *et al*, 2007; Deák *et al*, 2009). Based on this structure, mutations were made in the sequence of Munc-18a that targeted residues that interact with these domains, and are conserved between homologous SM proteins. Glutamic Acid 59 (E63) makes contact with the Habc domain of the Syntaxin, whilst Glutamic Acid 66 (E70) contacts both the Habc and N-terminal domains of the Syntaxin. These residues were mutated to Alanine and Lysine respectively, and both were found to retain tight binding to Syntaxin 1a in the "closed" conformation (Mode 1) but binding between the SM protein and the SNARE complex (Mode 3) was decreased leading to a decrease in vesicle priming, but not to vesicle fusion (Deák *et al*, 2009).

Studies using the nematode worm *Caenorhabditis elegans* identified a residue in the SM protein unc-18 which also impairs binding of the SM protein to its cognate SNARE complex. Using pull-down assays, it was observed that a mutation of Aspartic Acid 214 (D222) to Asparagine caused a decreased in binding to the SNARE proteins involved in complex formation with no effect on binding to Syntaxin in either its "open" or "closed" conformations (Graham *et al*, 2009).

4.2 Aims of this chapter

This chapter aimed to generate recombinant wild-type and mutant Munc-18c (E63K, E70A and D222N) and to test the function of these proteins through pull-down assays and the *in vitro* fusion assay.

4.3 Results

4.3.1 Purification of N- and C-terminally tagged Munc-18c

With several binding modes between Syntaxin and SM proteins being identified, and each of these binding modes utilising a different domain of the SM protein, it is plausible that N- and C-terminally located purification tags on the SM protein may interfere with or alter binding between the proteins. Therefore, it was important to

firstly determine whether the location of the polyhistidine affinity tags affected the ability of Munc-18c to bind to SNAREs and the SNARE complex. Indeed, earlier work in our lab has established that the location of GST purification tags on Syntaxin 4 can affect its binding to Munc-18c (Aran *et al*, 2009); however reciprocal experiments on the SM protein have not been performed as yet.

Previous experiments in our laboratory utilised full length murine Munc-18c cloned into the QIAGEN vector pQE30 to generate an N-terminally polyhistidine tagged protein. This construct was then transformed into bacterial cells containing a plasmid expressing the chaperone protein GroEL, which was thought to aid protein folding and stability. Although the addition of GroEL may aid in the overall purification of the SM protein, it is very difficult to remove from the final protein solution, even after extensive washes with Mg-ATP (Hu *et al*, 2003, Aran *et al*, unpublished).

In order to eliminate (or reduce) the need for GroEL, full-length Munc-18c was cloned into a new vector, pET28B (Novagen). This vector is able to create both N- and C-terminally His_6-tagged proteins, depending on the restriction sites used. Two full-length murine Munc-18c constructs were generated by PCR; N-terminally tagged Munc-18c (NHis M18c) was cloned between the NheI and XhoI sites and C-terminally tagged Munc-18c (CHis M18c) was cloned between the NcoI and XhoI sites (all oligonucleotide sequences used in this study are presented in the Appendix).

After successful cloning was confirmed by sequencing, full-length SM proteins were purified as outlined in Section 2.2.3.2, without co-expressed GroEL. Briefly, ~200 ml clarified *E. coli* lysate was incubated overnight at 4^0C with 3 ml Ni-NTA agarose washed in PBS. The next morning, the lysate was applied to an EcoPac disposable chromatography column and washed 10 times with 10 ml PBS containing 25 mM Imidazole. Protein was eluted from the column using a linear gradient of Imidazole, and each fraction analysed by SDS PAGE and Coomassie staining. Peak fractions were combined and dialysed overnight to remove any traces of Imidazole.

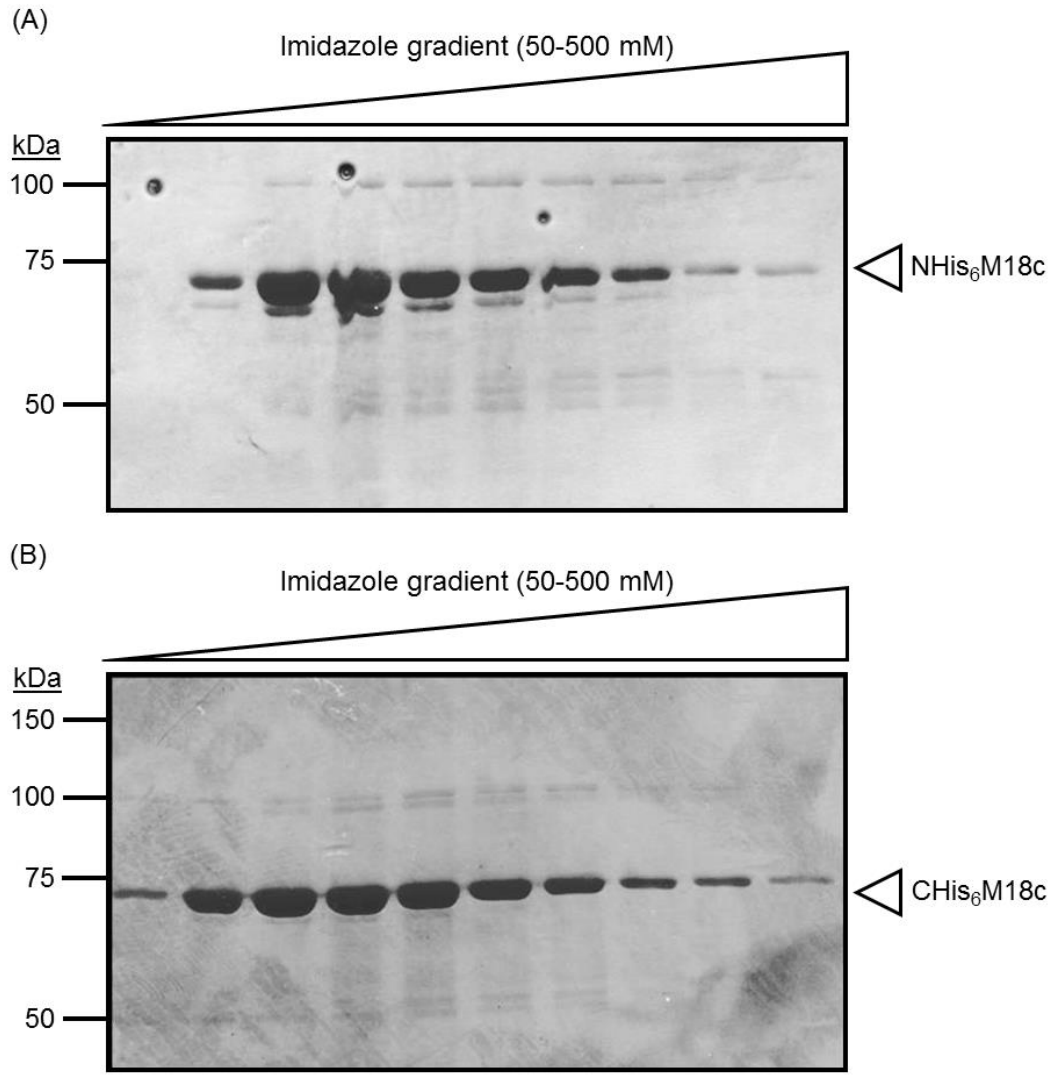

Figure 4.2 Purification of (A) N- and (B) C-terminally tagged Munc-18c
Full-length N- and C-terminally tagged Munc-18c was produced in BL21 (DE3) *E. coli* cells. Purification utilised the polyhistidine tags on the termini of the proteins using 3ml Ni-NTA agarose (QIAGEN). Typically 6 L of bacteria were grown to an OD_{600} of ~0.8 before overnight induction with 1 mM IPTG at 22 °C. After purification using a linear Imidazole gradient a 5 µl sample of each fraction was run on an 10 % SDS PAGE gel, and the highest yielding fractions combined, and dialysed against either PST + 10 % glycerol, or Exchange/Reconstitution buffer before concentration to ~1 ml.

Unlike our previous pQE30 construct, co-expressed GroEL was not required to express the protein, and sufficient levels of Munc-18c could be produced from the pET28B vector in BL21 (DE3) *E. coli*. Both pQE30 and pET28b are derived from the vector pBR222 (Bolivar *et al*, 1977), however pET28b is controlled by the T7 promoter and is a medium-copy number plasmid, whilst pQE30 is a low-copy number plasmid (*The Qiaexpressionist*, QIAGEN). Both proteins also appeared to be

purified to similar levels, suggesting that the tag location does not affect binding to Ni-NTA agarose.

4.3.2 The effect of purification tags on wild-type Munc-18c function

In order to test for any functional consequences of His_6-tag location on the SM protein, we performed GST pull-down assays using the two wild-type Munc-18c proteins and Syntaxin 4, as this is the best characterised of our SNARE/SM protein binding pairs. Further to this, we added both wild-type SM proteins into our *in vitro* fusion assay to assess whether and differences occur in their ability to regulate SNARE-mediated membrane fusion.

4.3.2.1 GST pull-down assays to assess binding between wild-type Munc-18c and Syntaxin 4

In order to assess binding between the wild-type SM proteins and Syntaxin 4, a 1:1 molar ratio of recombinant Syntaxin 4 and Munc-18c was incubated overnight at 4 °C in a final volume of 500 µl PBS with rotation. The next day, 20 µl Glutathione Sepharose 4B beads (50 % slurry in PBS) was added to each tube and incubated at room temperature for 1 hour with rotation. The beads were harvested by centrifugation at 14000*xg* for 2 minutes and washed 5 times with 1 ml PBS + 10 % glycerol. After the final wash all supernatant was carefully removed and 20 µl 2xLSB added. The samples were boiled at 95 °C for 5 minutes and the beads collected by centrifugation at 14000*xg* for 5 minutes. A sample of supernatant was run on a 15 % SDS PAGE gel, along with an input sample for each experiment, and proteins visualised using Coomassie staining.

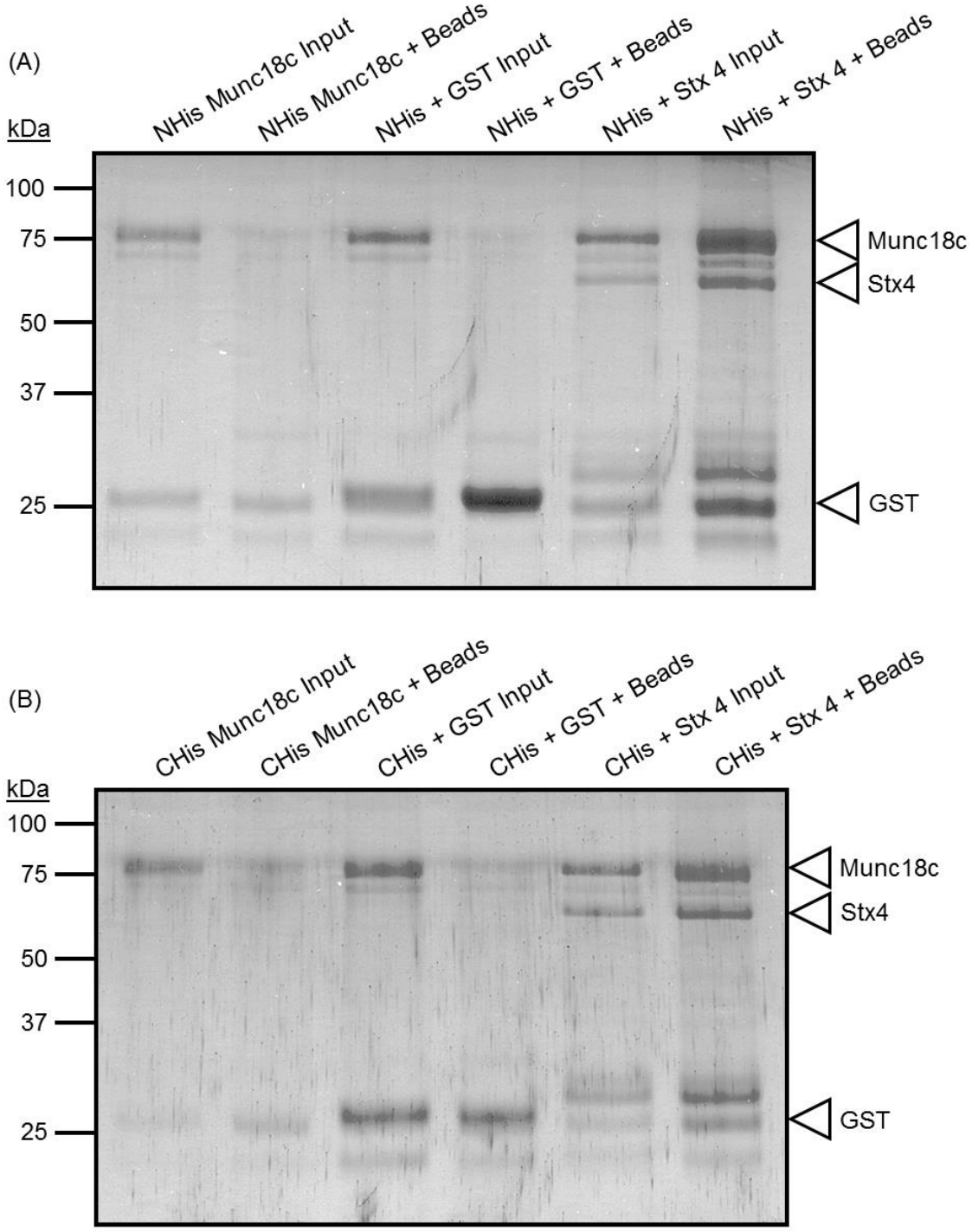

Figure 4.3 Syntaxin 4/GST Pull-down of (A) N- and (B) C-terminally tagged Munc-18c
40 µg full-length (A) N- and (B) C-terminally His_6-tagged Munc-18c was incubated with 20 µg cytosolic Syntaxin 4 or GST overnight at 4 °C. After incubation the next morning with 20 µl Glutathione Sepharose 4B for 1 hour at room temperature, the beads were washed and boiled with 2x LSB. 15 µl of input sample was run alongside 10 µl pull-down supernatant.

As Figure 4.3 shows, both Munc-18c constructs bind to the C-terminally tagged cytosolic Syntaxin 4 after overnight incubation, with limited binding to the beads and GST controls. This suggests that the location of the purification tag has no effect on the ability of the SM proteins interactions with Syntaxin 4. In order to test any functional differences between the proteins, both constructs were analysed using the *in vitro* fusion assay.

4.3.2.2 The effect of Munc-18c on the liposome fusion assays

As our *in vitro* liposome fusion assay was now functional, as outlined in Chapter 3, we were able to use it to investigate the effect of Munc-18c on SNARE-mediated membrane fusion.

During this time, experiments were underway for Chapter 5, where I was attempting to establish a fusion assay utilising proteins isolated from the plasma membrane of 3T3-L1 adipocytes. During the optimisation for this assay, we discovered that the cytosolic domain of VAMP 2 was an ineffective control (see Chapter 5 for further details). We chose at this stage to use a different control, using protein-free donor vesicles. As these vesicles do not contain any v-SNARE, they should not fuse with the t-SNARE containing acceptor vesicles, indicating that fusion between the vesicle populations is SNARE-dependent. This control was tested in the initial SNARE-mediated *in vitro* fusion assay, where the protein-free vesicle control was shown to exhibit similarly low levels of fusion to adding cytosolic VAMP 2 (Weber *et al*, 1998).

To test whether the N- and C-terminally located purification tags conferred different functional effects, both proteins were added to the fusion assay. t- and v-SNARE-containing liposomes were incubated overnight in the presence (triangles) or absence (squares) of wild-type Munc-18c. After heating to 37 °C, fluorescence readings were obtained every two minutes for two hours before addition of n-dodecylmaltoside in order to lyse the donor vesicles and obtain a maximum NBD fluorescence level. Data was normalised (as outlined in Chapter 3) and expressed as a percentage of maximum NBD fluorescence.

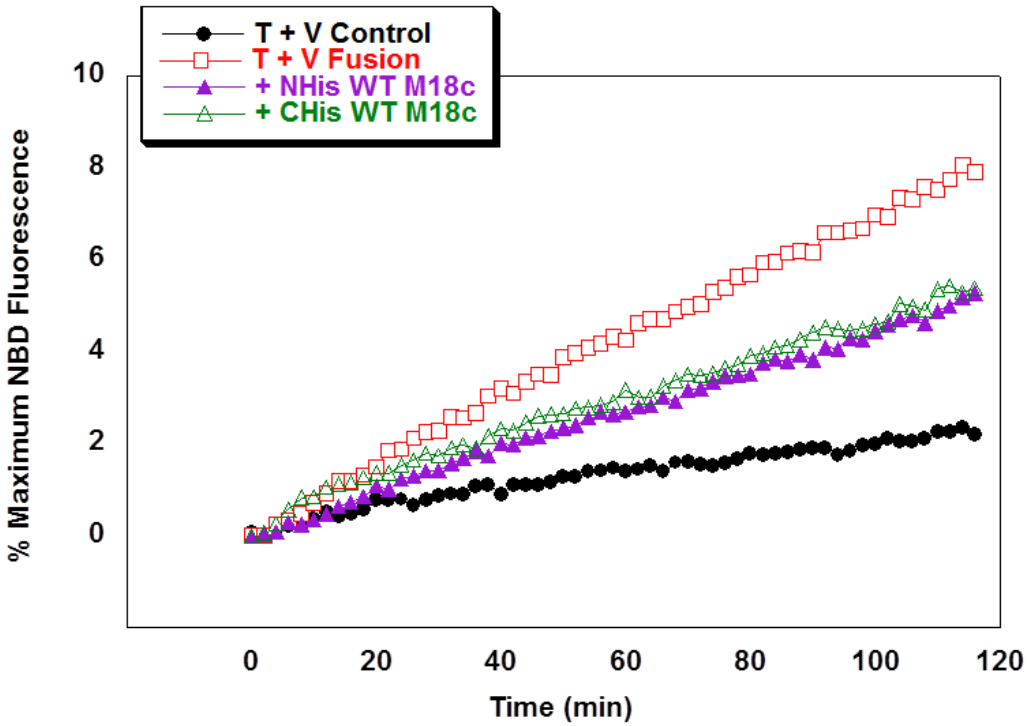

Figure 4.4 The effect of wild-type Munc-18c on SNARE-mediated liposome fusion
45 µl t-SNARE liposomes was incubated overnight in the presence of VAMP 2-containing (red squares) or empty (black circles) donor vesicles. N-terminal (purple triangles) or C-terminal (green triangles) wild-type Munc-18c was added to two of the fusion wells in a 1:1 molar ratio with the t-SNAREs, with Exchange/Reconstitution buffer added to the control and fusion reactions to account for volume. Fusion was measured over a two hour and maximum NBD fluorescence obtained by lysis of the donor vesicles with detergent. This figure shows representative data from three independent protein purifications and reconstitutions.

As shown in Figure 4.4, both wild-type Munc-18c constructs cause a decrease in the rate of SNARE-mediated liposome fusion in our *in vitro* fusion assay. This supports previous data produced in our lab which indicated that N-terminally tagged Munc-18c acts as an inhibitor of SNARE-mediated fusion (Brandie *et al*, 2008), and indicates that the C-terminally tagged Munc-18c also functions as a negative regulator of SNARE-mediated membrane fusion.

4.3.3 Munc-18c Site-Directed Mutagenesis

As previously described, three residues (E63, E70 and D222) were selected for mutation in Munc-18c based on studies into Mode 3 binding in homologous systems. The mutants were generated using site-directed mutagenesis (SDM) as outlined in Section 2.2.1.2, using the N-terminally tagged wild-type Munc-18c as a template. We chose to perform the mutagenesis in this context as the information

for the pET28B plasmid claimed that the N-terminal His_6 tag was Thrombin cleavable. Unfortunately, we subsequently discovered that, despite multiple optimisation attempts, we were unable to remove the polyhistidine tag by Thrombin cleavage. However as we observed no functional difference between the N- and C-terminally tagged wild-type proteins (Figure 4.4), we hypothesised that the location of the purification tag would not affect the proteins' function.

Mutagenesis was performed using the Platinum® *Pfx* DNA polymerase kit (Invitrogen). Due to the large size of Munc-18c (1.8 kbp) and the large size of the pET28B vector (5.4 kbp), the mutants were generated in the vector pCR®2.1-TOPO®, as this vector is significantly smaller than pET28B. Successful clones were identified by sequencing, excised from the carrier vector and sub-cloned into pET28B.

Full-length proteins were purified as described for the wild-type SM protein (Sections 2.2.3.2 and 4.3.1), and eluted from Ni-NTA agarose using a linear imidazole gradient before analysis by SDS PAGE and Coomassie staining (Figure 4.5).

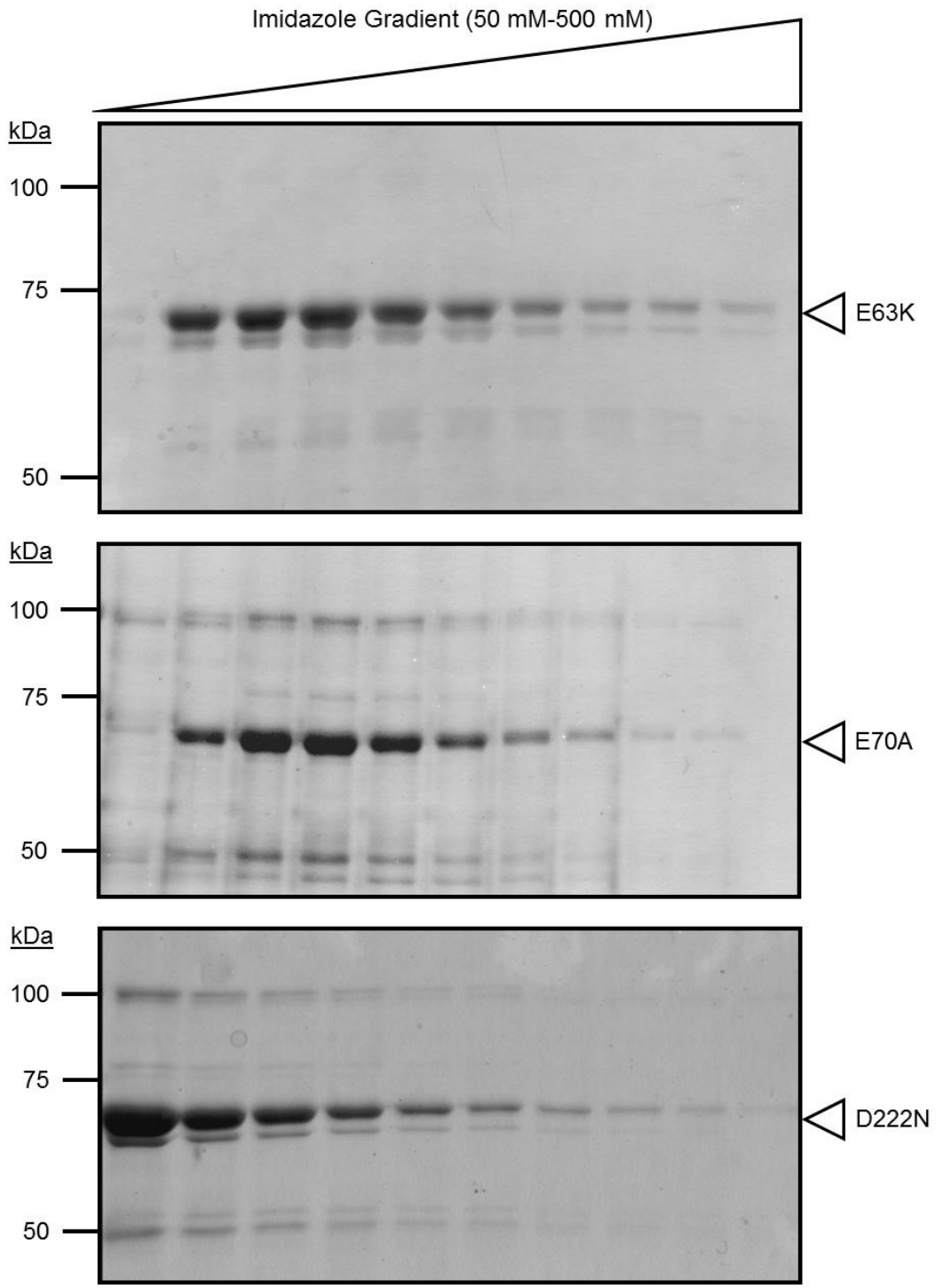

Figure 4.5 Purification of Munc-18c point mutants
Full-length (A) E63K (B) E70A and (C) D222N Munc-18c was produced in BL21 (DE3) *E. coli* cells. Purification utilised N-terminal polyhistidine tags on the proteins using Ni-NTA agarose. After elution from the beads using a linear Imidazole gradient a 5 µl sample of each fraction was run on an 10 % SDS PAGE gel, and the most pure, highest yielding fractions combined and dialysed against either PST + 10 % glycerol, or Exchange/Reconstitution buffer. This figure is representative of typical purifications. Molecular weight markers are indicated.

Like the wild-type SM protein, the mutant Munc-18c proteins were expressed without the chaperone GroEL. The mutant proteins were also expressed and purified to similar levels as the wild-type protein, although the D222N protein appears to elute from the Ni-NTA column at a lower concentration of Imidazole than the other constructs.

4.3.4 Effect of Munc-18c point mutants on protein function

We chose two experimental systems to test the effect of the selected point mutations on the function of Munc-18c. Firstly, we tested the ability of the wild-type and mutant SM proteins to bind to their cognate SNAREs to assess whether the mutant proteins have a different affinity to the SNAREs compared to wild-type Munc-18c. Secondly, we assessed the ability of the mutant proteins to regulate SNARE-mediated membrane fusion in our newly established *in vitro* fusion assay.

4.3.4.1 Test of Munc-18c antibody specificity

Previous work in our lab showed that an α Syntaxin 4 antibody bound with 10-fold greater affinity to wild-type Syntaxin 4 than to the "open" L173A/E174A mutant (Dr Fiona Brandie, unpublished data), highlighting the importance of analysing ability of antibodies to bind both wild-type and mutant proteins. As it was possible that the mutations made to our SM protein may cause small structural changes, we tested three commercially available α Munc-18c antibodies for their ability to detect wild-type and mutant SM proteins with equal affinities. A known amount of wild-type and mutant Munc-18c was run on an SDS PAGE gel. The samples were then analysed by Coomassie staining and western blotting to test antibody affinities, as shown in Figure 4.6.

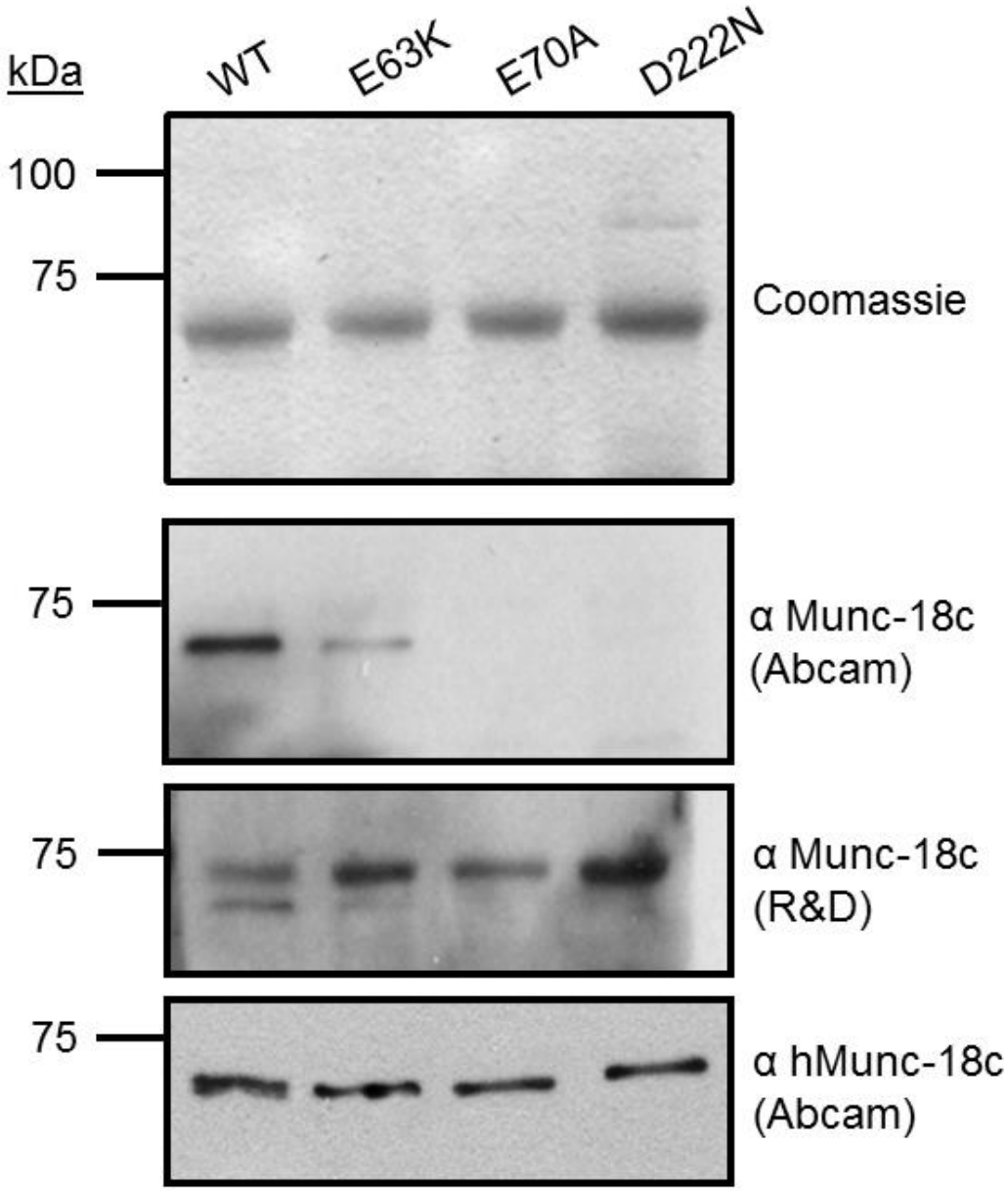

Figure 4.6 Test of Munc-18c antibody specificity
1 μg wild-type and mutant Munc-18c were run on 10 % SDS PAGE gels. One set of samples was stained with Coomassie, to ensure equal loading of the proteins. The other samples were transferred to nitrocellulose and subjected to western blotting using different Munc-18c antibodies. Molecular weight markers are shown.

Of all the antibodies tested, the α-human Munc-18c (Abcam) antibody appears to bind to the wild-type and mutant SM proteins with similar affinities, and thus was used in our further studies.

4.3.4.2 GST pull-down assays

In order to test the function of the mutant Munc-18c proteins, their ability to bind to SNARE proteins was assessed. As these mutations are postulated to inhibit Mode 3 binding (i.e. to the assembled SNARE complex), we first attempted to form recombinant SNARE complexes, and to assess the mutant proteins' ability to bind to them.

The SNARE hypothesis postulates that for every membrane fusion event, there is a specific pairing of SNARE proteins which form a functional SNARE complex, providing specificity to the membrane fusion event (Söllner et at, 1993). Functional SNARE complexes can be identified by their resistance to denaturing by SDS (Hayashi et al, 1994); a characteristic that has been observed in complexes consisting of Syntaxin 4, SNAP-23 and VAMP 2 (Kawanishi et al, 2000). To form recombinant SNARE complexes, bacterial lysates were produced expressing Syntaxin 4/SNAP-23 binary complexes, cytosolic VAMP 2 or GST. Lysate containing cytosolic VAMP 2 was incubated overnight at 4 °C with GST lysate (as a control) or t-SNARE complex lysates. The next day, Glutathione Sepharose 4B was added to each mixture, and further incubated overnight at 4 °C. The beads were isolated and washed 5 times with 1 ml Exchange/Reconstitution buffer containing 1 % Triton X-100. After washing, a sample of the beads was analysed by SDS PAGE and western blotting: in order to identify successfully formed SNARE complexes, samples were analysed for the presence of two of the SNARE proteins (SNAP-23 and VAMP 2), as shown in Figure 4.7A.

Once complexes had been assembled, they were used in pull-down assays. GST alone (control) or SNARE complex beads were incubated overnight at 4 °C with bacterial lysate expressing wild-type Munc-18c. The next day, beads were washed 5 times with 1 ml Exchange/Reconstitution buffer containing 1 % Triton-X100, and binding of Munc-18c was analysed by SDS PAGE and western blotting.

.

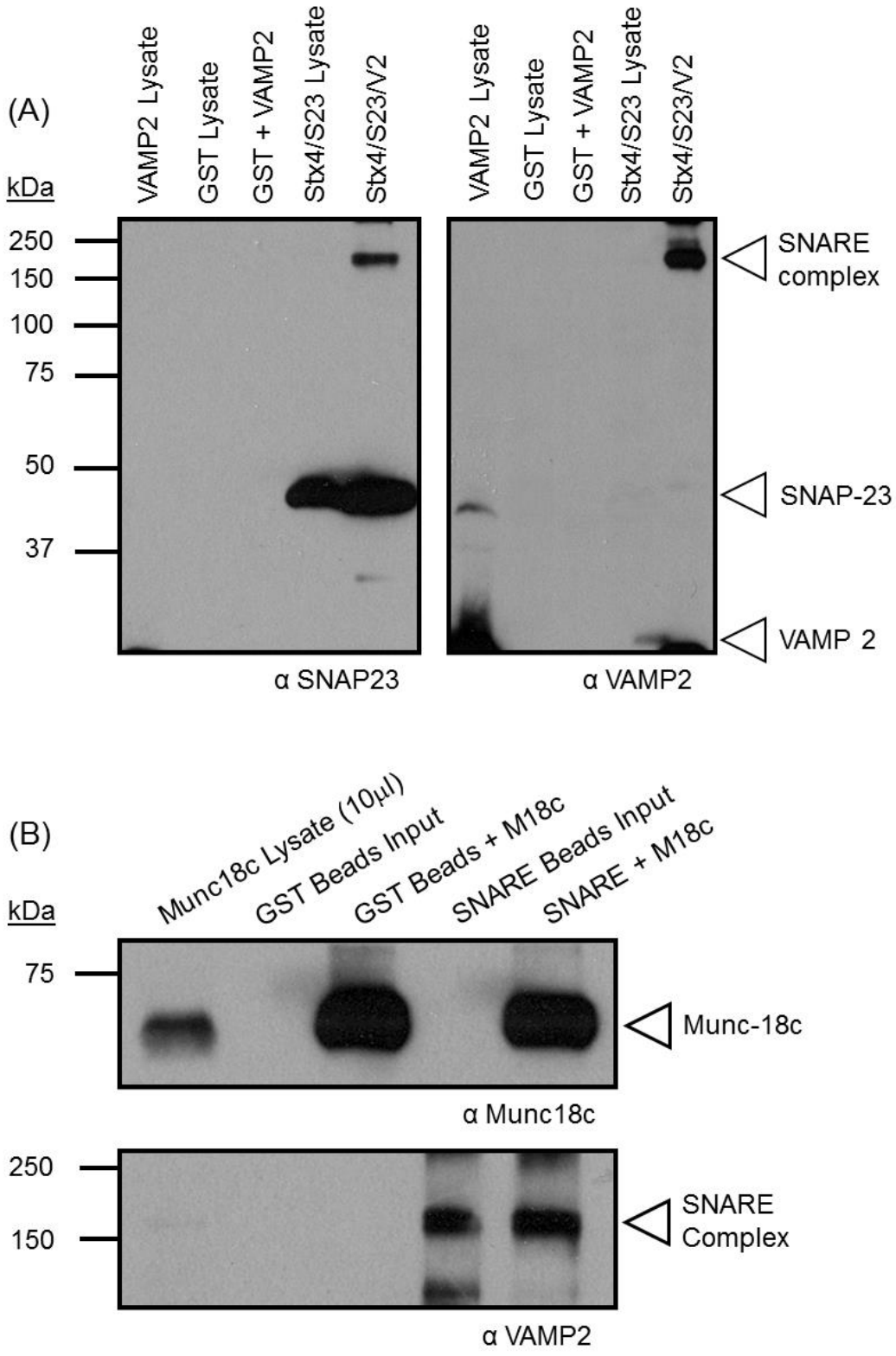

Figure 4.7 Binding of wild-type Munc-18c to assembled SNARE complexes
(A) Bacterial lysates containing GST and VAMP 2 (control reaction) or Syntaxin 4, SNAP-23 and VAMP 2 were mixed overnight at 4 °C in order to assemble recombinant SNARE complexes. Assembled complexes were isolated on Glutathione Sepharose beads and, after washing, were analysed for the presence of SNARE proteins in the assembled complex. (B) Wild-type Munc-18c was incubated overnight with GST (control) or SNARE complex bound to Glutathione Sepharose 4B. After washing, binding of the SM protein was analysed by western blotting with the specified antibodies.

Our attempts to optimise this pull-down assay using assembled SNARE complexes proved unsuccessful, as we encountered high levels of binding between the wild-type SM protein to the GST-only control, as shown in the top panel of Figure 4.7B. As it appeared difficult to assess binding of the SM protein to the assembled SNARE complexes, we chose to assess whether binding to the individual SNARE proteins was compromised. Using our previous method for pull-down assays (described in Section 4.3.2.1), we witnessed high levels of mutant Munc-18c/GST interaction in our negative control. In order to minimise this binding, we altered the assay and used *E. coli* lysates expressing recombinant SNARE proteins and Munc-18c, hypothesising that the proteins present in the bacterial lysates may act as a block, minimising non-specific binding to the GST control.

1 mg GST-SNARE or GST alone *E. coli* lysates were incubated overnight with 1 mg wild-type or mutant Munc-18c lysate, in a total volume of 1 ml Exchange/ Reconstitution buffer containing 1 % Triton-X100. The next day, 40 µl Glutathione Sepharose 4B (as a 50 % slurry in PBS) was added to each tube and incubated at room temperature for 1.5 hours. The beads were then harvested by centrifugation at 14000*xg* for 90 seconds and washed 5 times with 1 ml PBS + 10 % glycerol. After the final wash all supernatant was carefully removed and 20 µl 2xLSB added. The samples were boiled at 95 °C for 5 minutes and the beads collected by centrifugation at 14000*xg* for 5 minutes. A sample of supernatant was run on an SDS PAGE gel along with an input sample for each experiment.

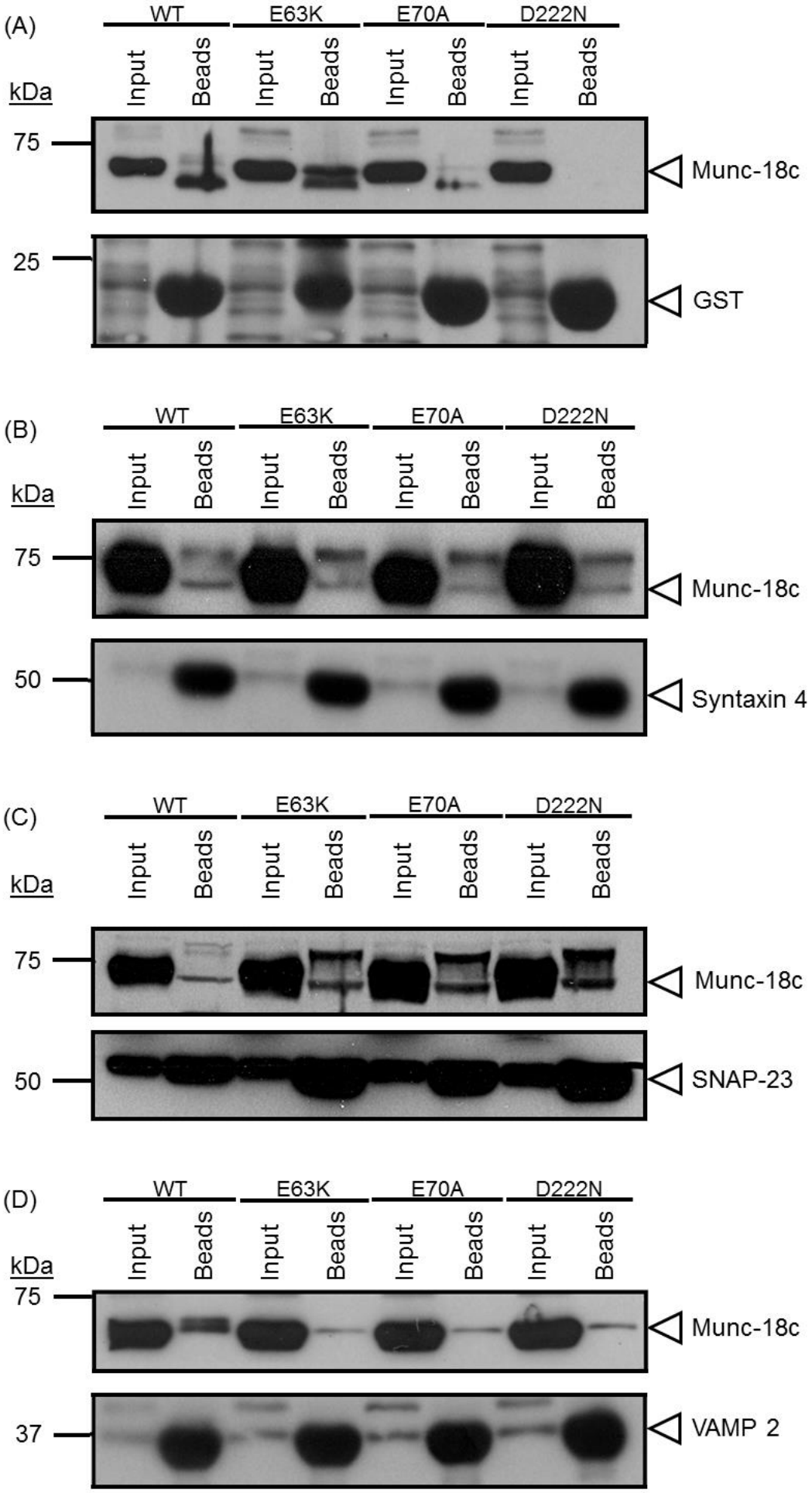
(A)
WT
E63K
E70A
D222N
Input
Beads
kDa
75
Munc-18c
25
GST
(B)
50
Syntaxin 4
(C)
SNAP-23
(D)
37
VAMP 2

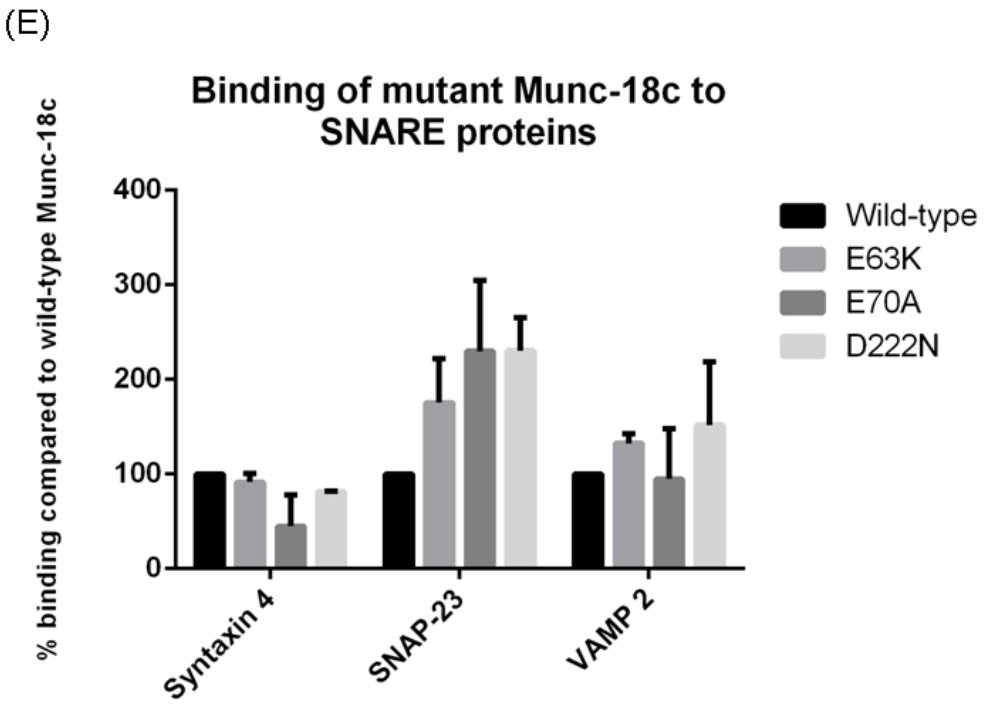

Figure 4.8 Binding of Munc-18c mutants to SNARE proteins
E. coli lysates expressing SNARE and SM proteins were incubated together overnight at 4 °C. The next morning and input sample of the protein mixture was retained and protein complexes were isolated using Glutathione Sepharose 4B. After washing, a sample of the beads was analysed by SDS PAGE and western blotting using the specified antibodies – A-D represent a sample from the same Munc-18c lysate preparation incubated with the individual SNARE lysates. Protein inputs are shown as "Input" samples; isolated complexes are shown as "Beads" samples. ImageJ software (NIH) was used to quantitatively analyse the amount of Munc-18c bound to each SNARE protein, expressed as a percentage of the wild-type binding. Error bars represent the standard deviation of the mean binding values, where n=2.

As Figure 4.8A shows, the wild-type, E63K and E70A Munc-18c proteins bind to the GST control to varying degrees, with the E63K mutant showing the strongest binding. In contrast, the D222N mutant does not bind the GST control, however it does exhibit binding to all three SNARE proteins (Figure 4.8B, C and D). D222N Munc-18c binds Syntaxin 4 with similar affinity to the wild-type SM protein; however it exhibits higher levels of binding to both SNAP-23 and VAMP 2, as quantified in Figure 4.8E. These results partially confirm those observed in studies utilising Munc-18a, where D216N Munc-18a exhibited similar levels of binding to Syntaxin 1a, however reduced binding to SNAP-25 and VAMP 2 (Graham *et al*, 2009). It is perhaps unsurprising that we observed these results, as these proteins are hypothesised to interfere with binding to the assembled SNARE complex, rather than individual SNAREs. This is not to say that the mutations only affect Mode 3 binding, and therefore what we observe may be a secondary effect of the

mutations. Ideally, we would hope to investigate the binding of the mutant SM proteins to the assembled SNARE complex, and with continued optimisation of our complex binding assay, it may be possible to assess the effect of SM protein binding to the assembled SNARE complex in this manner.

4.3.4.3 Effect of mutant Munc-18c on SNARE-mediated membrane fusion

Although our pull-down assays failed to highlight any functional significance of the Mode 3 mutations on the interactions between SNAREs and the SM protein (with the exception of the D222N mutant), we conducted further analysis into their function by adding the proteins to the *in vitro* fusion assay. As the point mutants we were investigating are hypothesised to interfere with binding to the assembled SNARE complex (Mode 3) we designed an alternative assay, in which the t- and v-SNARE liposomes are pre-incubated overnight in order to induce pre-docking of SNARE complexes before addition of the SM protein the next morning (unlike previous experiments, where all components of the assay were incubated together overnight, outlined in Section 4.3.2.2). As before, t-SNARE protein concentration was quantified by amido black protein assay, and Munc-18c was added in a 1:1 molar ratio.

After addition of SM protein, the plate was warmed to 37 °C for 15 minutes to bring it to reaction temperature. Fluorescence was measured every two minutes for 2 hours, before addition of 10 µl n-dodecylmaltoside detergent in order to lyse the vesicles and obtain a maximum NBD fluorescence reading. Data was normalised and plotted as a percentage of the maximum NBD fluorescence.

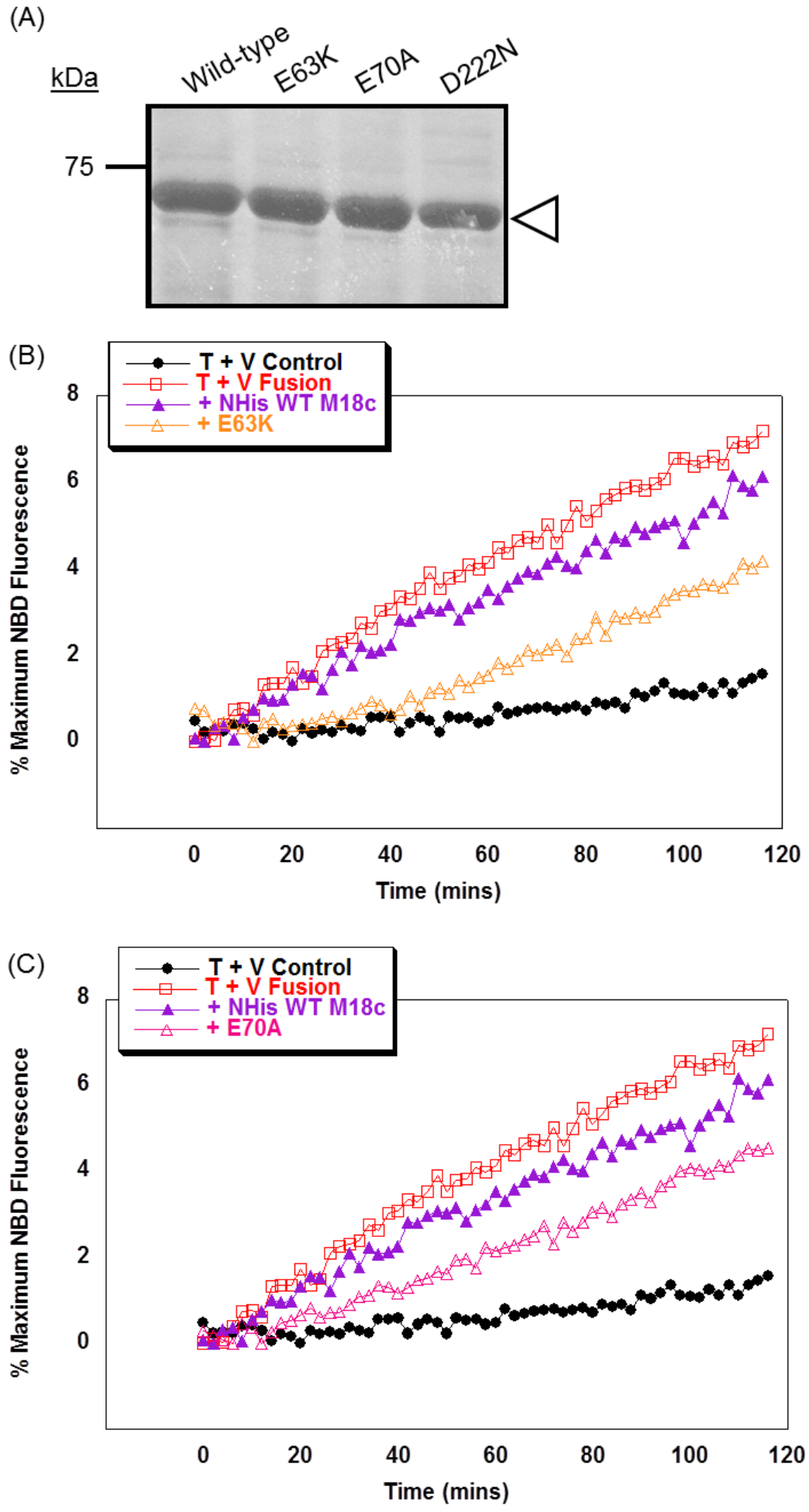
(A)
kDa
Wild-type
E63K
E70A
D222N
75
(B)
T + V Control
T + V Fusion
+ NHis WT M18c
+ E63K
% Maximum NBD Fluorescence
0
2
4
6
8
0
20
40
60
80
100
120
Time (mins)
(C)
T + V Control
T + V Fusion
+ NHis WT M18c
+ E70A
% Maximum NBD Fluorescence
0
2
4
6
8
0
20
40
60
80
100
120
Time (mins)

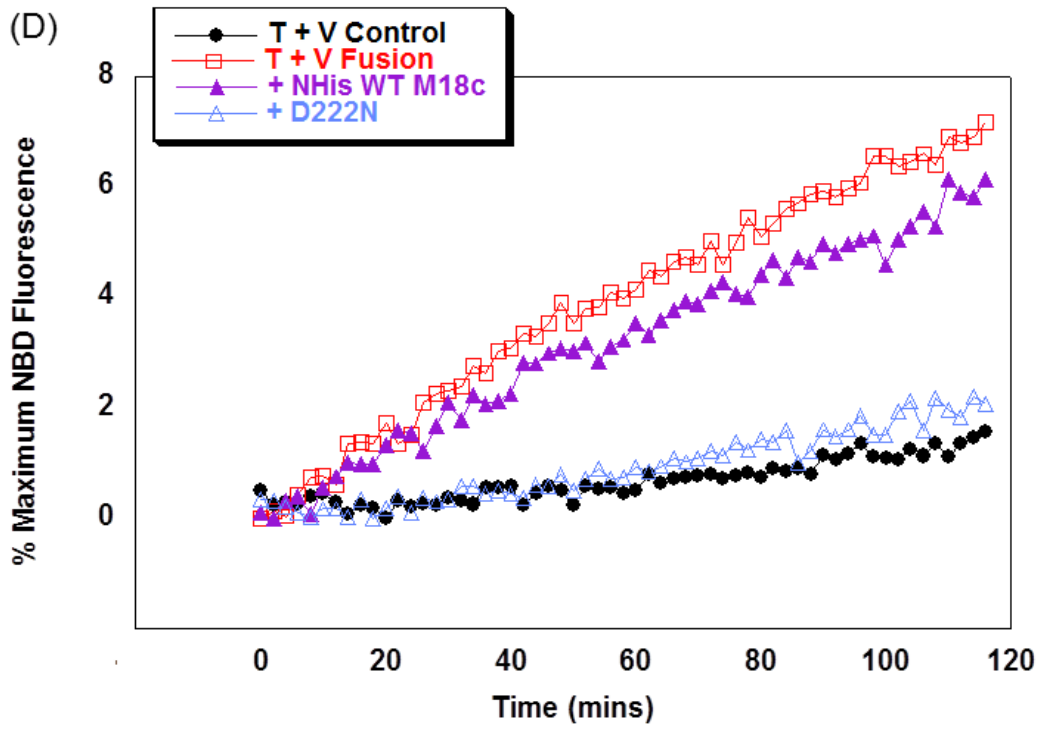

Figure 4.9 The effect of mutant Munc-18c on the *in vitro* fusion assay
(A) 2 µg of wild-type, E64K, E70A and D222N Munc-18c was analysed by SDS PAGE and Coomassie staining to ensure equal loading. 45 µl t-SNARE liposome and 5 µl v-SNARE (red squares) or empty donor (black circles) liposomes were incubated overnight at 4 °C in order to pre-dock SNARE complexes. The next morning, either wild-type or (B) E63K (C) E70A or (D) D222N mutant Munc-18c protein was added to the liposomes in a 1:1 molar ratio with the binary t-SNARE complex. After warming to reaction temperature, fluorescence readings were measured for 2 hours. Figure shows representative data from these experiments.

The fusion data from these experiments shows that when added to pre-docked SNARE complexes, wild-type Munc-18c decreases the rate of fusion between SNARE-containing vesicles, as shown in Figure 4.9. The three point mutations we investigated appear to further inhibit the rate of fusion compared to wild-type, with the D222N mutation showing the most pronounced effect (Figure 4.9D), indicating that these mutations in the SM protein confer a dominant negative effect. This is perhaps surprising as experiments using the E63K and E70A mutations in the neuronal SM protein Munc-18a showed that these mutations caused no change in the rate of vesicle fusion compared to wild-type (Déak *et al*, 2009).

Furthermore, studies using Munc-18c knockout mice suggested that the SM protein has a positive regulatory role in SNARE-complex formation and/or vesicle

fusion as these heterozygous knockout mice (Munc-18c $^{-/+}$) display reduced insulin sensitivity and decreased insulin-stimulated GLUT4 translocation to the plasma membrane (Oh *et al*, 2005). Previous experiments in our lab indicated that Munc-18c was able to interact with Syntaxin 4 via Mode 1 and Mode 2 binding, with Mode 1 conferring a negative regulatory role (Brandie *et al*, 2008). Experiments performed in this study confirmed this observation (Section 4.3.2.2), and we hypothesised that Mode 3 interactions between Munc-18c and the SNARE complex may confer the positive regulatory role indicated by previous knockout mice studies (Oh *et al*, 2005).

In order to further dissect our results, we decided to reassess the ability of the C-terminally tagged wild-type Munc-18c in our "Mode 3 *in vitro* fusion assay", where the SM protein is added to the liposomes after they have been incubated together overnight at 4°C to induce pre-docking of the SNARE complexes. As before, t- and v-SNARE containing liposomes were incubated overnight at 4°C, before addition of N- or C-terminally tagged wild-type Munc-18c in a 1:1 molar ratio (relative to the binary t-SNARE complex). Fusion was measured every two minutes for 2 hours and plotted as a percentage of the maximum NBD fluorescence obtained after vesicle lysis.

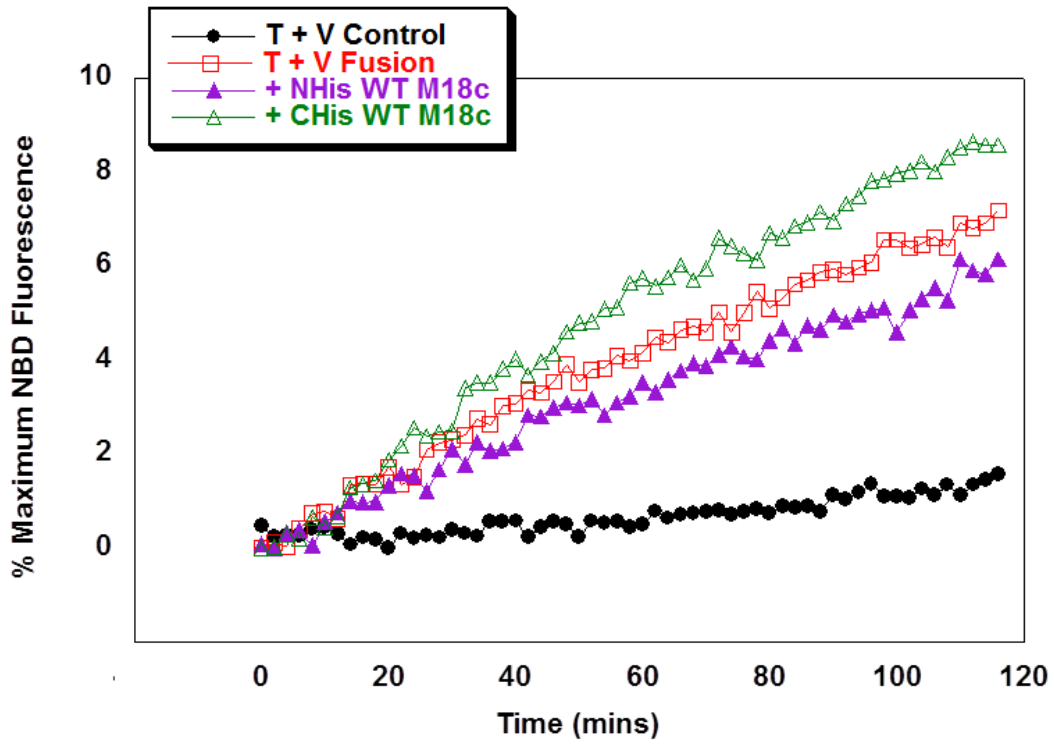

Figure 4.10 Effect of His-tag location on wild-type SM protein Mode 3 fusion
45 µl t-SNARE vesicles was incubated with 5 µl v-SNARE containing (red squares) or protein-free (black circles) donor vesicles overnight at 4 °C. The next morning, N- (purple triangles) or C- (green triangle) terminally tagged Munc-18c was added and fluorescence measured for two hours. Vesicles were lysed with 10 µl n-dodecylmaltoside and fluorescence measured for 40 minutes. Data was plotted as a percentage of maximum NBD fluorescence. Figure shows representative data for these experiments.

Unlike our previous experiment where N- and C-terminally tagged Munc-18c was incubated with the t- and v-SNARE overnight, when C-terminally tagged Munc-18c was added to assembled SNARE complexes, the rate of fusion increases (Figure 4.10, green triangles). Although we were unable to measure the exact change in fusion rate (as the absolute levels of fluorescence vary for each reconstitution), we have qualitatively observed this increase in at least three experiments, and the trend is maintained. This supports the expected results (discussed above), but raises concern with regards to the location of purification tags on recombinant SM proteins, as studies into SM protein function have used tags on both termini (N-terminal: Brandie *et al*, 2008; Scott *et al*, 2004; C-terminal: Rodkey *et al*, 2008).

4.4 Conclusions

After establishing the *in vitro* fusion assay (discussed in Chapter 3), we were able to use it to study the effects of the SM protein Munc-18c on the rate of SNARE-mediated membrane fusion. Previous experiments in our lab have indicated that this SM protein is a negative-regulator of SNARE mediated fusion (Brandie *et al*, 2008), however the existence of a positive regulatory role in fusion has been suggested by knockout studies using mice (Oh *et al*, 2005).

Our initial experiments using N- and C-terminally His_6-tagged Munc-18c indicated that the purification tag did not affect the interaction between Syntaxin 4 and the SM protein (Figure 4.3); and both constructs equally inhibited the rate of Syntaxin 4/ SNAP-23/VAMP 2-mediated fusion of the two liposome populations to a similar extent (Figure 4.4).

We generated three point mutants of Munc-18c based on similar studies in homologous fusion systems. The effect of these point mutants was analysed by pull-down assay and addition to the *in vitro* fusion assay. Initial experiments using recombinant assembled SNARE complexes displayed high levels of non-specific binding between the SM protein and the complex (Figure 4.7), so we investigated binding between the individual SNAREs and wild-type/mutant Munc-18c.

In order to prevent non-specific binding between the SNARE and SM proteins, we used bacterial lysates clarified from *E. coli* expressing the SM and SNARE proteins of interest: the bacterial proteins present in the lysates were intended to act as a blocking agent, binding to GST and the Glutathione Sepharose 4B beads preventing the SM proteins from binding non-specifically. Utilising this method, we were able to observe binding between the SM proteins and individual SNAREs, but no overall pattern was observed, and the SM proteins bound to the SNARE proteins with differing affinities (Figure 4.8).

Although these initial binding studies did not indicate any functional differences between the wild-type and mutant Munc-18c with regards to binding individual SNARE proteins, we further analysed the mutant SM proteins by addition into the

in vitro fusion assay (Section 4.3.4.3). In order to assess the effect of the proteins on Mode 3 binding (to the assembled SNARE complex), we altered our protocol, adding the SM protein after overnight pre-incubation of the t- and v-SNARE liposomes in order to induce complex formation. In this instance, the mutant proteins decreased the rate of SNARE-mediated membrane fusion compared to the wild-type Munc-18c (Figure 4.9). This was a surprising observation, as studies in homologous systems indicated that the E63 and E70 mutations did not affect the rate of vesicle fusion in the neuronal system (Déak *et al*, 2009). The D222N mutant showed the greatest levels of inhibition, which suggests that this residue is important in the interactions between the SM protein and SNARE complex.

In order to understand our findings, we added the C-terminally tagged Munc-18c into the *in vitro* fusion assay using our modified "Mode 3" protocol, and observed that this protein was able to increase the rate of SNARE-mediated membrane fusion (Figure 4.10). This calls into question previous studies performed not only on Munc-18c but on other SM proteins which have been purified using an N-terminal polyhistidine tag. Although the N-terminally tagged construct causes a decrease in SNARE-mediated membrane fusion regardless of when it is added to the assay, the location of the C-terminal tag appears to have a different functional effect. It could be that the location of the N-terminal tag prevents access to a binding pocket, or possibly masks an important residue for interactions between the SM/SNARE proteins. Further structural and binding studies, including NMR and Surface Plasmon Resonance could be of interest to investigate why the location of the polyhistidine tag causes such a drastic effect.

5 The effect of insulin on the plasma membrane of 3T3-L1 adipocytes

5.1 Introduction

The presentation of GLUT4 on the plasma membrane of muscle and adipose tissue is the end result of a complex signalling pathway which begins with insulin binding to its receptor in response to an increased blood glucose concentration, and culminates with the transport of GLUT4 from an intracellular store to the cell surface (Cushman *et al*, 1980; Suzuki and Kono, 1980). It has been difficult to locate the exact site of insulin action on this trafficking pathway, or to resolve each of the steps leading up to GLUT4 storage vesicle (GSV) fusion with the plasma membrane, in particular the final fusion event itself (Bai *et al*, 2007).

In adipocytes, insulin was found to restrict the movement of GSVs located on a microtubule network close to the plasma membrane (Lizunov *et al*, 2005). Indeed, early studies implicated insulin in the recruitment of the exocyst – a tethering complex which may be involved in targeting GLUT4 to the cell surface (Inoue *et al*, 2003) and tethering of the GSVs in response to insulin (Inoue *et al*, 2006). In an attempt to resolve the steps of this regulated exocytosis event, high-resolution total internal reflection (TIRF) microscopy has been used to visualise fusion events within 100 nm of the plasma membrane. Using this live-cell imaging technique, it was observed that the docking of GSVs at the cell membrane was not regulated by insulin, but that a post-docking "priming" step appeared to be the insulin-regulated step at the plasma membrane (Bai *et al*, 2007). This high-resolution data helped further confirm the earlier observation that fusion of GSVs with the plasma membrane is not constitutive, rather it is stimulated eight-fold by insulin, leading to the plasma membrane of rat adipocytes being described as the location of the "key regulated step in stimulation of fusion" (Koumanov *et al*, 2005).

TIRF microscopy studies have further resolved the function of insulin at the plasma membrane. Using fluorescently-tagged GLUT4, it was observed that under basal conditions, GLUT4 appears to cluster at distinct sites in the plasma membrane. These sites were also observed to recruit clathrin (a coat protein involved in the

formation of endocytotic vesicles), and thus are likely sites of GLUT4 internalisation. It is believed that this clustering is dependent on insulin, and mediates GLUT4 delivery to and removal from the plasma membrane (Stenkula *et al*, 2010). This study also observed that upon insulin stimulation, two linked events occur at the plasma membrane: in addition to the expected increase in GSV exocytosis there is an increase in the dispersal of GLUT4 within in the plasma membrane. Furthermore, three minutes post-insulin the rate of GSV fusion with the plasma membrane returns to around basal levels, indicating the increased dispersal of the glucose transporter is responsible for the increased glucose transport observed 15 minutes after the initial insulin signal (Stenkula *et al*, 2010).

With the identification of the plasma membrane as the major site of insulin action, in particular a post-docking event, it is now important to pinpoint the proteins present at the plasma membrane which may be targets of insulin, and to study their effect on the rate of GSV fusion with the plasma membrane.

5.2 Aims of this chapter

The aim of this chapter was to purify basal and insulin-stimulated plasma membrane fractions from 3T3-L1 adipocytes and to reconstitute the proteins found in these fractions into liposomes, similar to the *in vitro* fusion assay. Once reconstituted, the liposomes were silver stained and western blotted to identify SNAREs and SNARE-binding proteins, and run in a modified fusion assay to test their fusogenic capabilities, and to assess the site of insulin action at the plasma membrane.

5.3 Results

5.3.1 Purification of Plasma Membrane fractions from 3T3-L1 adipocytes

In order to obtain isolated plasma membrane from 3T3-L1 adipocytes, the cells were cultured and subjected to sub-cellular fractionation by differential centrifugation, as outlined in Section 2.2.4. This method of fractionation has been well

characterised (Piper *et al*, 1991; Thurmond *et al*, 1998) and isolates purified plasma membrane fractions.

Before harvesting, the cells were left untreated (basal) or treated with 100 nM insulin for either 2 or 15 minutes. Usually, ten 10 cm^2 plates of confluent adipocytes were required to obtain sufficient plasma membrane for each condition. A full fractionation, consisting of cytosol, high-density microsome (HDM, containing endoplasmic reticulum), low density microsome (LDM, containing insulin-responsive GSVs) and plasma membrane fractions, was performed to ensure that GLUT4 was trafficked from the LDM to the plasma membrane as expected. Samples were also analysed for t-SNARE content to investigate whether the levels of these proteins in each sub-cellular fraction are altered by insulin stimulation, as shown in Figure 5.1.

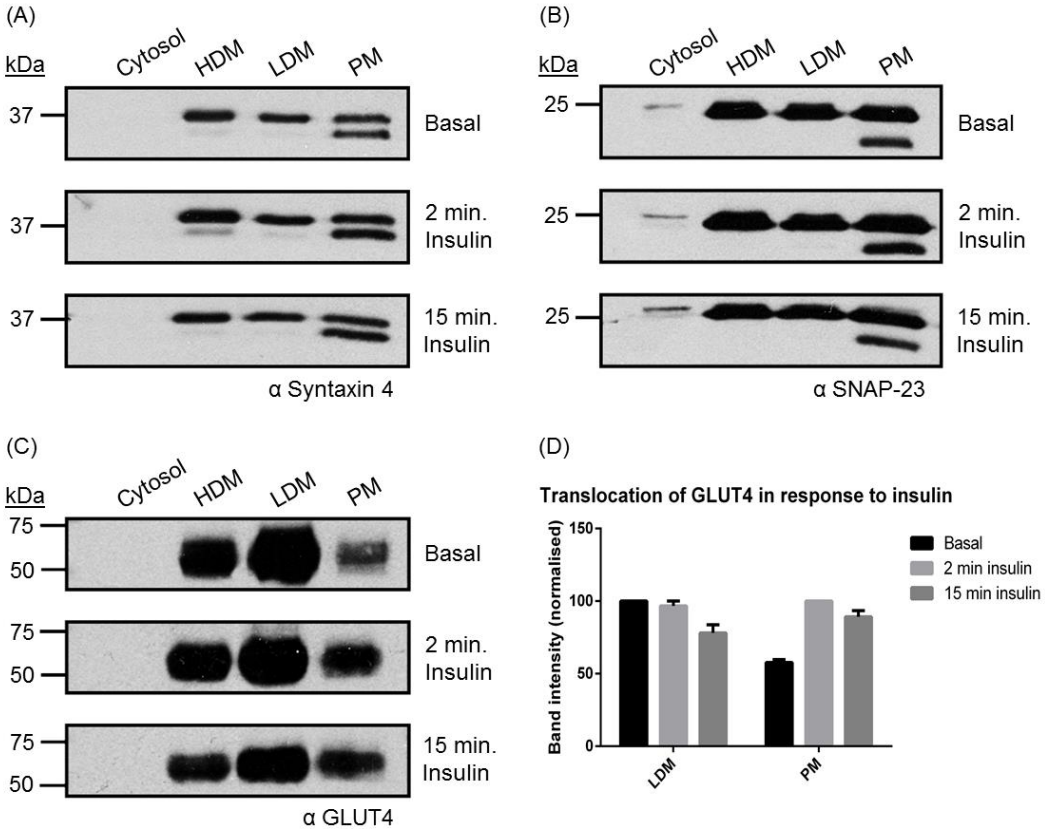

Figure 5.1 Sub-cellular fractionation of 3T3-L1 adipocytes
After sub-cellular fractionation by differential centrifugation, each 3T3-L1 fraction was quantified by Bradford protein assay, and 15 µg of each fraction analysed by SDS PAGE on a 15 % gel. Proteins were transferred onto nitrocellulose, and analysed by western blotting using the antibodies specified. Molecular weight markers are indicated, and these results are representative of at least three independent fractionations. GLUT4 translocation was quantified using ImageJ software (NIH) and plotted as a bar graph showing mean band intensity and standard deviation where n=3.

Upon insulin-stimulation, GLUT4 is trafficked from an intracellular pool (located within the low density microsome (LDM) fraction of 3T3-L1 adipocytes (James *et al*, 1987)) to the plasma membrane. As Figure 5.1D shows, insulin stimulation causes a decrease in the amount of GLUT4 present in the LDM fraction, and an increase in the amount in the plasma membrane fraction, indicating that GLUT4 is being correctly trafficked in response to insulin. Each time a fractionation was performed, a sample was blotted to check for correct GLUT4 trafficking before proceeding with any reconstitution.

The levels of t-SNARE proteins in each sub-cellular fraction were unaffected by insulin stimulation, confirming previous observations (Tellam *et al*, 1997; St-Denis *et al*, 1999), and suggesting that any effect of insulin on the rate of SNARE-mediated membrane fusion is not due to an increase in SNARE protein levels, but could perhaps be attributed to changes in SNARE conformation, repositioning of the SNARE proteins on the plasma membrane or post-translational modifications in order to form functional binary t-SNARE complexes.

5.3.2 Optimisation of plasma membrane reconstitution conditions

In order to examine the effect of insulin on the fusogenic properties of the plasma membrane of 3T3-L1 adipocytes, isolated plasma membrane fractions were reconstituted into liposomes in order to be tested in a modified *in vitro* fusion assay.

The reconstitution method devised for this project was based on the methods outlined in both Weber *et al* (1998) and Koumanov *et al* (2005) which describe the original SNARE liposome reconstitution and fusion experiments, and the reconstitution and fusion of endogenous rat plasma membrane fractions respectively. In standard *in vitro* fusion assays using recombinant protein, 500 µl of ~0.5-1 µg t-SNARE binary complex is reconstituted into the proteoliposomes. Since ~ 1.5 µg plasma membrane is obtained from each fractionation of ten 10 cm^3 plates, it was important to determine how much plasma membrane to reconstitute in order to obtain sufficient fusion.

The protein concentration of each plasma membrane fraction was determined by Bradford assay (Section 2.2.3.4) and three dilutions were prepared, with final total protein concentrations of 0.3 mg/ml, 0.75 mg/ml and 1.5 mg/ml made up to a total volume of 500 µl in HES + PI buffer containing 0.8 % (w/v) n-octyl-β-D-glucopyranoside in order to solubilise the plasma membrane. Similar to the methods outlined for recombinant proteoliposomes (Sections 2.2.5.3 and 3.3.4), plasma membrane acceptor vesicles were prepared using a 15 mM lipid mix containing 85 mol % POPC and 15 mol % DOPS. The lipid film was dried under nitrogen for 15 minutes, and residual chloroform removed by vacuum dessication for 30 minutes. The film was resuspended in the plasma membrane protein solution by vortexing for 5 minutes and the detergent diluted by drop-wise addition of 1 ml Exchange/Reconstitution buffer containing 1 mM DTT. The samples were then dialysed overnight in 4 L Exchange/Reconstitution buffer containing 1 mM DTT at 4°C. The next day, proteoliposomes were recovered by gradient centrifugation (Section 2.2.5.4) and protein content analysed by SDS PAGE and western blotting.

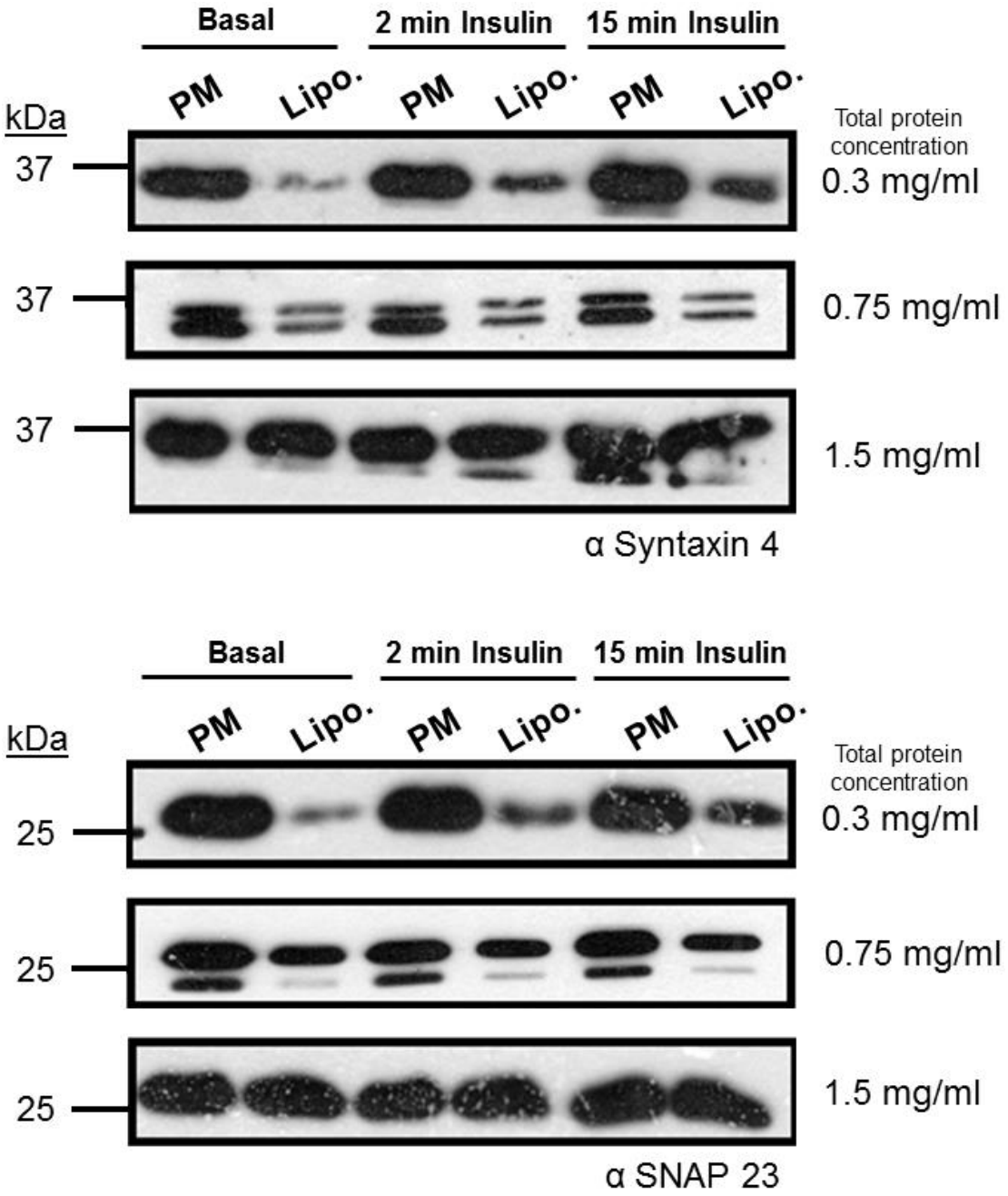

Figure 5.2 Analysis of t-SNARE reconstitution from 3T3-L1 PM fractions
Plasma membrane (PM) samples were made up to the final concentrations indicated in a total volume of 500 µl with HES buffer + PI and reconstituted with 100 µl of acceptor lipid (Section 2.2.5.3). Proteoliposomes (Lipo.) were recovered by gradient centrifugation (Section 2.2.5.4). 10 µg of plasma membrane was run alongside 10 µl of liposome sample for each reconstitution condition on an SDS PAGE gel and analysed for t-SNARE content by western blotting with the specified antibodies. Molecular weight markers are indicated, and results are representative of at least three independent experiments.

The t-SNAREs obtained from each plasma membrane concentration were reconstituted into liposomes, as shown in Figure 5.2. The amount of t-SNARE reconstituted was dependent on the concentration of plasma membrane added,

with higher concentrations of membrane leading to greater amounts of t-SNARE reconstitution. It is also interesting to note that doublet bands appear for some samples, most strikingly in the 0.75 mg/ml samples. Both t-SNAREs are known to be phosphorylated (discussed further in Section 5.3.5), and these bands could indicate the presence of phospho-SNAREs. It is important to note, however, that the doublet bands are not observed in all samples. This could be due to lower protein levels in the 0.3 mg/ml samples, preventing detection of the lower band. Similarly, the high protein levels in the 1.5 mg/ml samples could be preventing clear resolution of the bands.

5.3.3 Optimisation of fusion assay conditions

Unlike our previous *in vitro* fusion assays performed using recombinant SNAREs (Chapters 3 and 4), the proteoliposomes created using 3T3-L1 adipocyte plasma membrane are likely to contain more proteins than simply the t-SNAREs, as it is plausible that any protein with a transmembrane domain can be incorporated into the lipid bilayer. Therefore, we were required to optimise the assay to ensure that the controls and reaction conditions were suitable for this fusion assay.

5.3.3.1 Optimisation of control reaction

Previous investigations into SNARE fusion using a recombinant *in vitro* fusion assay used a v-SNARE control in order to ensure that fusion is due to SNARE-SNARE interactions, and is not spontaneous. This control utilises the cytosolic domain of the v-SNARE VAMP 2. When added to the reaction, the cytosolic v-SNARE binds to the t-SNARE complexes, preventing the v-SNARE in the donor vesicles from interacting with its cognate t-SNAREs, thus acting as a negative control by preventing fusion (Weber *et al*, 1998; Brandie *et al*, 2008; Ji *et al*, 2010).

In order to optimise the control experiment for our fusion assay using proteins isolated from plasma membranes, we performed two controls. The first involved incubating the cytosolic domain of VAMP 2 with the plasma membrane- and v-SNARE containing vesicles overnight. The second control used protein-free donor liposomes in place of the VAMP 2-containing vesicles.

Experiments into the fusion of reconstituted rat adipose plasma membrane with GLUT4 and VAMP 2-containing donor vesicles were performed slightly differently than those using recombinant proteins, as fluorescence was measured for a period of 30 minutes rather than two hours. It appears that this was due to the fact that close to maximal fluorescence was achieved at this time-point, and this matched the time-course for insulin stimulation of glucose transport in intact cells (Koumanov *et al*, 2005; Karnieli *et al*, 1981). As our experiments combined both recombinant and plasma-membrane derived liposomes, we chose to alter our *in vitro* fusion assay protocol in order to account for both systems.

Plasma membrane-derived vesicles were incubated overnight at 4°C with either 5 µl protein-free donor liposomes; 5 µl VAMP 2-containing liposomes plus 5 µl cytosolic VAMP 2; or 5 µl VAMP 2-containing liposomes. The next morning, the plate was warmed to 37 °C in a FLUOstar Optima spectrophotometer for 15 minutes, before fluorescence readings were taken every two minutes for one hour, as this was an intermediate time-point between experiments performed by Koumanov *et al* and the *in vitro* fusion assay. 10 µl of 2.5 % (w/v) n-dodecylmaltoside was then added in order to lyse the vesicles and obtain a maximum NBD fluorescence reading. Data was normalised as described previously and plotted as a percentage of maximum NBD fluorescence.

(A)

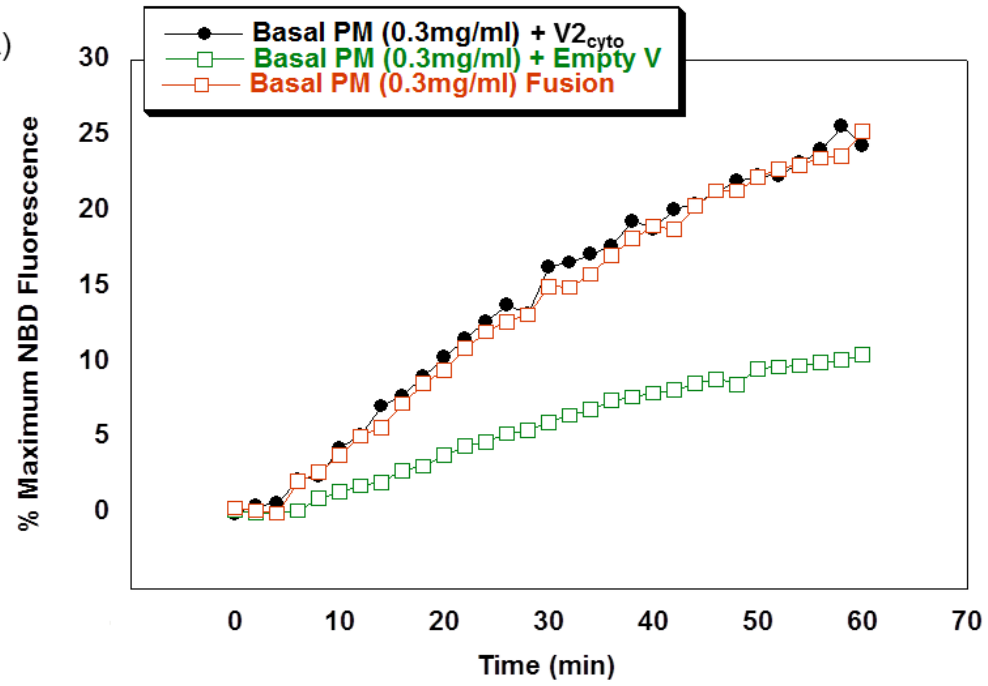
Basal PM (0.3mg/ml) + V2cyto
Basal PM (0.3mg/ml) + Empty V
Basal PM (0.3mg/ml) Fusion
% Maximum NBD Fluorescence
0
5
10
15
20
25
30
0
10
20
30
40
50
60
70
Time (min)

(B)

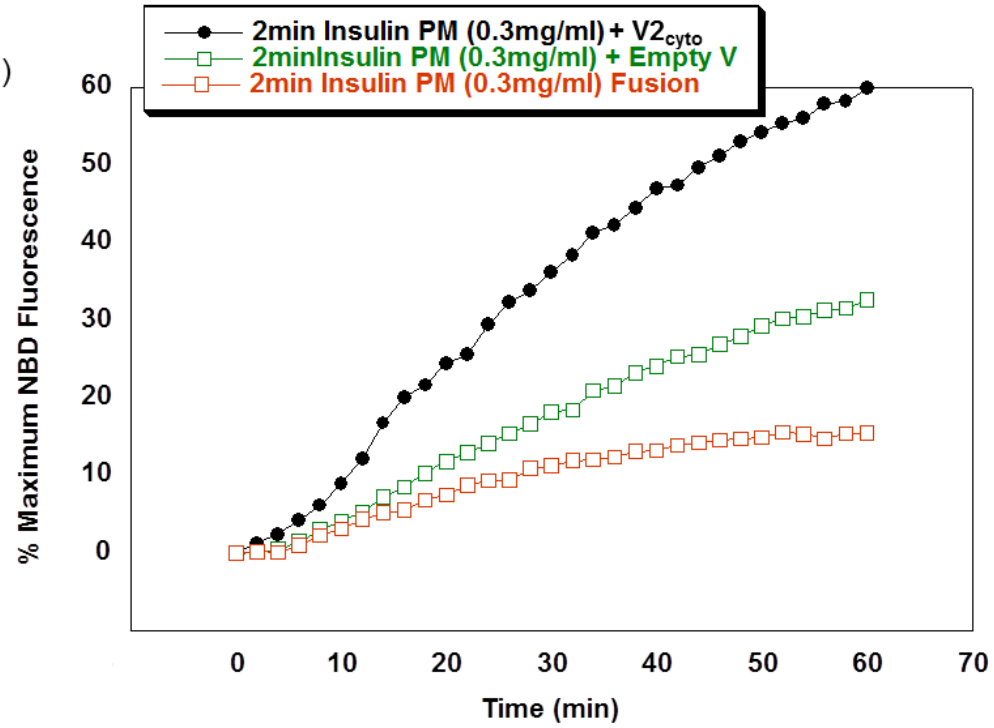
2min Insulin PM (0.3mg/ml) + V2cyto
2minInsulin PM (0.3mg/ml) + Empty V
2min Insulin PM (0.3mg/ml) Fusion
% Maximum NBD Fluorescence
0
10
20
30
40
50
60
0
10
20
30
40
50
60
70
Time (min)

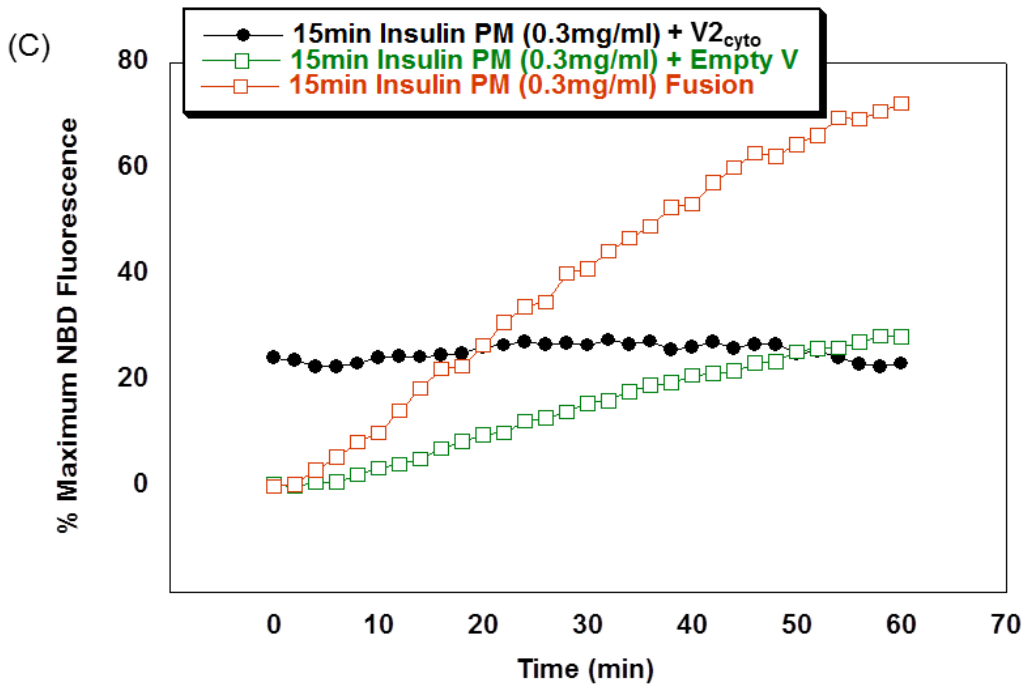

Figure 5.3 Optimisation of plasma membrane fusion assay controls
45 µl acceptor liposomes derived from (A) basal (B) 2 minute insulin-stimulated or (C) 15 minute insulin-stimulated plasma membrane were incubated overnight with either 5 µl protein-free liposomes (red squares), 5 µl VAMP 2 vesicles in the presence of the cytosolic domain of VAMP 2 (black circles) or 5 µl HES + PI buffer (green squares). Fusion was measured for 60 minutes, and maximum NBD fluorescence obtained by lysis of the donor vesicles with detergent. Figure shows representative data from three independent experiments.

These experiments revealed the scope of variability in this approach to studying the effect of insulin on the plasma membrane of 3T3-L1 adipocytes, and highlighted several stages which required further optimisation. Firstly, using the cytosolic domain of VAMP 2 as a control was not sufficient, as it did not appear to inhibit SNARE-mediated fusion: for both the liposomes derived from basal (Figure 5.3A), and 2 minute insulin-stimulated (Figure 5.3B) plasma membrane, the rate of "inhibited" fusion is the same or greater than the uninhibited reaction. For the liposomes derived from 15 minute insulin-stimulated plasma membrane (Figure 5.3C), the cytosolic domain of VAMP 2 appears to inhibit fusion, although the final level of fluorescence is quite high (~20 %).

Compared to the cytosolic VAMP 2 control, the empty liposomes inhibited the rate of fusion to a greater extent. However, it is interesting to note that the rate of fusion for the liposomes derived from 2 minute insulin-stimulated plasma membrane was lower than both controls (Figure 5.3B). We chose to continue on

using protein-free vesicles as a control for the fusion reactions, as the cytosolic VAMP 2 control did not appear to be functioning as expected, and given the complex protein content of the plasma membrane-derived vesicles, protein-free vesicles would allow us to focus solely on the effect of SNARE-mediated membrane fusion.

These experiments were carried out using 0.3 mg/ml plasma membrane liposomes, and due to the varying rates of fusion (for example, the liposomes derived from 2 minute insulin-stimulated plasma membrane have the lowest level of fusion), we were required to further optimise the concentration of plasma membrane required to accurately measure fusion.

5.3.3.2 Optimisation of PM concentrations

As mentioned previously, three concentrations of plasma membrane were reconstituted (final total protein concentrations of 0.3, 0.75 and 1.5 mg/ml in a total volume of 500 µl). In order to determine the optimum concentration of plasma membrane required, fusion assays were performed using liposomes derived from basal and insulin-stimulated plasma membrane at these concentrations.

Fusion assays were set up and run as described previously (Section 5.3.3.1) using empty liposomes as a control, with fluorescence readings recorded every two minutes for one hour. The vesicles were then lysed by addition of 10 µl 2.5 % (w/v) n-dodecylmaltoside in order to obtain a maximum NBD fluorescence reading from the donor vesicles. Normalised data was plotted as a percentage of maximum NBD fluorescence and is shown in Figure 5.4.

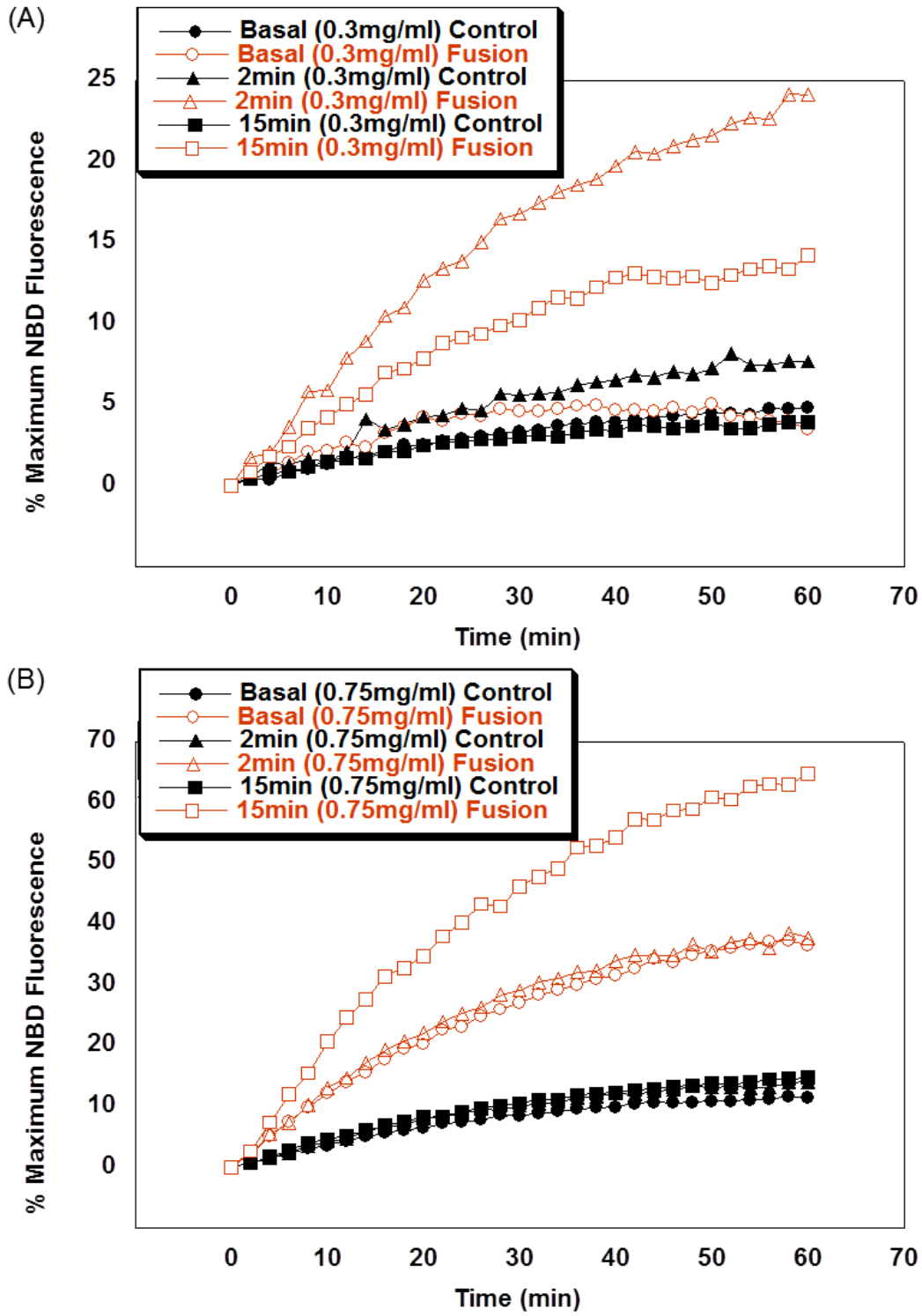

Figure 5.4 Fusion of liposomes containing protein derived from 3T3-L1 plasma membrane
45 µl (A) 0.3 mg/ml or (B) 0.75 mg/ml plasma membrane-containing liposomes were incubated overnight with 5 µl empty (shaded symbols) or VAMP 2-containing (open symbols) liposome. Fusion was measured for 60 minutes, and maximum NBD fluorescence obtained by lysis of the donor vesicles with detergent. Figure shows representative data from three independent experiments.

Both populations of liposomes exhibit varying degrees of fusion, dependent on insulin-stimulation, as shown in Figure 5.4. Using 0.3 mg/ml liposomes, the rate of fusion is lowest at basal insulin, increases after 2 minutes of insulin stimulation, and then decreases after 15 minutes of insulin stimulation; whereas the 0.75 mg/ml liposomes exhibit and increase in fusion only after 15 minutes of insulin stimulation, with no difference between basal and 2 minutes of insulin stimulation.

It is also of interest to note that fusion assays using 0.75 mg/ml plasma membrane show consistent inhibition of fusion using protein-free liposomes, whist there is some variation between the 0.3 mg/ml liposome controls.

No results were obtained from the liposomes created using 1.5 mg/ml plasma membrane. After gradient centrifugation, the recovered liposomes appeared yellow/orange in colour. When added to the *in vitro* fusion assay, these liposomes produced auto-fluorescence, bleaching the reaction and preventing any fluorescence readings from being recorded.

Based on the data from these experiments, we chose to continue our analysis using liposomes created using 0.75 mg/ml plasma membrane. These liposomes closely resembled the rates of fusion we would expect to see *in vivo*, with insulin increasing the rate of SNARE-mediated membrane fusion. Furthermore, these liposomes produced consistent controls, allowing us to confirm that the fusion observed in due to SNARE complex formation. For these reasons, we performed the rest of our analysis using these liposomes.

5.3.4 Silver staining of plasma membrane-derived liposomes

As observed in Section 5.3.3, the rate of fusion observed using plasma membrane-derived liposomes was significantly higher than that observed using liposomes containing recombinant t-SNAREs, as shown in Chapter 3. Due to the abundance of proteins found in the plasma membrane of 3T3-L1 adipocytes, it was important to try to identify any which may have an effect on the rate of SNARE-mediated fusion if reconstituted along with the t-SNAREs. These could include Rab GTPases, kinases, NSF/α-SNAP or Sec1/Munc-18 proteins.

In order to identify potential interacting proteins which may have been reconstituted, samples of plasma membrane and liposome were analysed by SDS PAGE and silver staining (Figure 5.5).

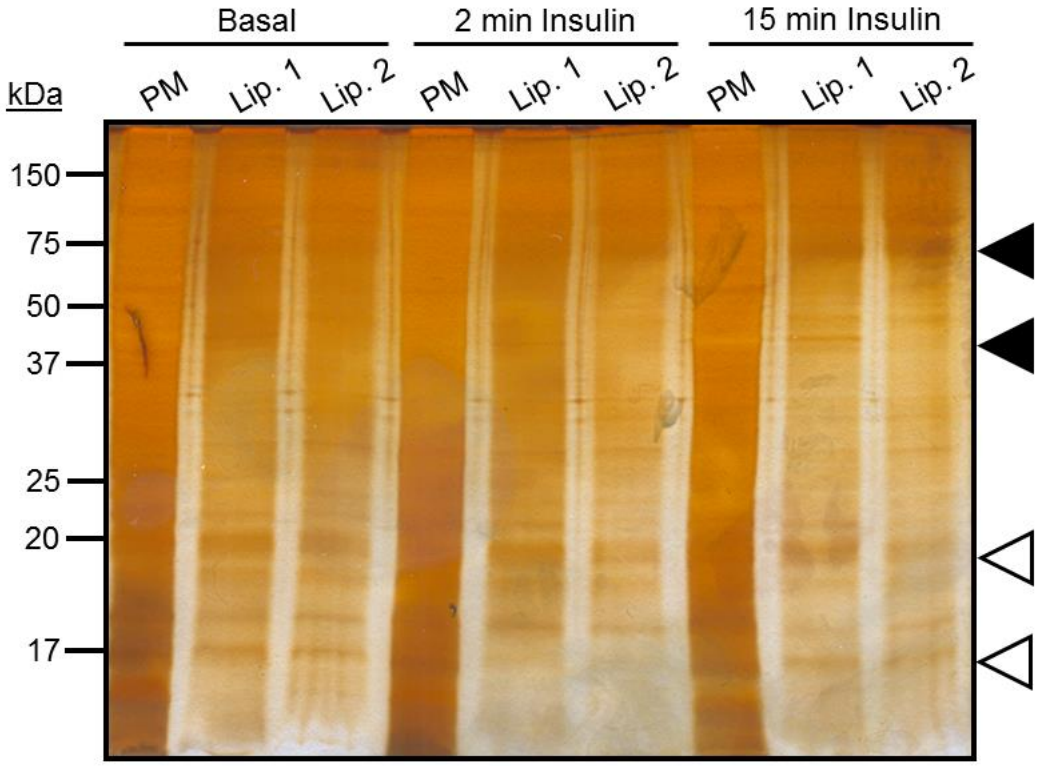

Figure 5.5 Silver staining of plasma membrane and liposome samples
10 µg of 3T3-L1 plasma membrane and 20 µl of liposome sample were run on a 15 % SDS PAGE gel and subjected to silver staining. Bands of interest, where protein amount appears to increase (shaded arrows) or decrease (open arrows) upon insulin stimulation, and molecular weight markers have been indicated. Lanes Lip. 1 and Lip.2 represent two separate plasma membrane purifications and reconstitutions.

Once stained, bands of interest could be identified, including proteins which appeared to change amount depending on insulin stimulation, and those which are present in high abundance (indicated in Figure 5.5). Although we were primarily interested in the SNARE proteins reconstituted into the liposomes, SNAREs are not the only proteins reconstituted, and thus identifying other proteins reconstituted could allow for greater dissection of the effect of insulin at the plasma membrane, and could also allow us to understand the differing rates of fusion observed due to differing lengths of insulin stimulation.

5.3.5 Western blotting for SNARE effectors

As Figure 5.5 shows, many proteins are present in the liposomes reconstituted from plasma membrane samples. To identify a few potential SNARE-effectors which may have been reconstituted, we decided to perform preliminary analysis on the liposome samples by western blotting for proteins known to interact with SNAREs. We chose the three kinases Protein Kinase A (PKA), Protein Kinase B (Akt), Protein Kinase C (PKC), all of which have a possible role in GLUT4 translocation.

Syntaxin 4 has been shown to be a substrate of PKA, and phosphorylated Syntaxin 4 exhibits less binding to SNAP-23, implying a negative role for this kinase in GSV fusion (Foster *et al*, 1998). PKC has also been identified as an important kinase in the regulation of SNARE complex formation. Syntaxin 4, SNAP-23 and VAMP 2 have all been identified as substrates for PKC and, for Syntaxin 4 and SNAP-23, phosphorylation by this kinase leads to a decrease in affinity for their cognate t-SNARE partner (Chung *et al*, 2000; Polgár *et al*, 2003). VAMP 2 has also been identified as a substrate for PKC; however no functional role has been attributed to this phosphorylation (Braiman *et al*, 2001).

The Sec1/Munc-18 protein Munc-18c can be phosphorylated on multiple residues. The insulin receptor, specifically the cytosolic β-subunit of the protein (Aran *et al*, 2011), was found to phosphorylate Munc-18c directly on residues Tyr219 and Tyr521 (Jewell *et al*, 2011). Phosphorylation at Tyr521 has since been found to reduce binding of the SM protein to Syntaxin 4 and VAMP 2 (Aran *et al*, 2011). PKC has also been identified as a kinase for Munc-18c, and phosphorylation leads to a decrease in affinity for Syntaxin 4 (Schraw *et al*, 2003).

Samples of basal and insulin-stimulated whole-cell lysate (WCL), plasma membrane (PM) and liposome were analysed by SDS PAGE and western blotting for the presence of kinases.

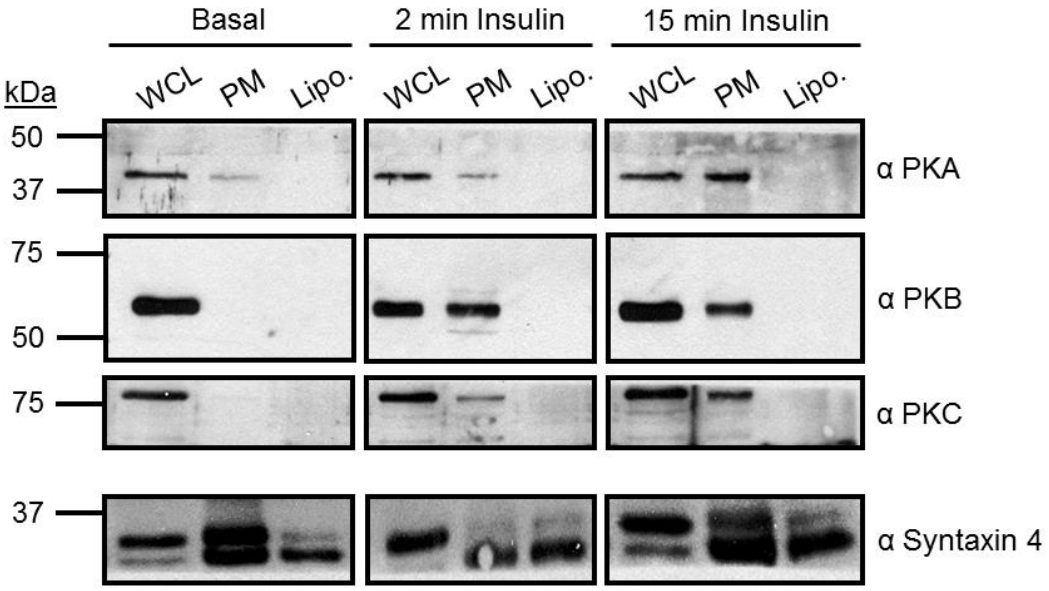

Figure 5.6 Kinases in 3T3-L1 adipocyte lysate, PM and liposomes
15 µg whole-cell lysates (WCL) and plasma membrane (PM), and 20 µl liposome (Lipo.) were analysed on a 12 % SDS PAGE gel. After transfer onto nitrocellulose, the membrane was cut into strips and blotted using the antibodies specified, with Syntaxin 4 acting as a loading control. Molecular weight markers are indicated, and data is representative of three independent experiments.

As Figure 5.6 shows, insulin causes an increase all three kinase levels at the plasma membrane of 3T3-L1 adipocytes, consistent with previous studies (Farese *et al*, 1992; Carvalho *et al*, 2000). However, despite an increase in PKA, –B and –C at the plasma membrane in response to insulin, none of these kinases are reconstituted into the liposomes. Although the kinases are not detectable in the liposomes, their effect on the t-SNAREs and SM protein may still be observed in the fusion assay via phosphorylation of their target proteins. This may be consistent with the presence of doublet bands: the Syntaxin 4 loading control in Figure 5.6 contains a doublet which may be consistent with the presence of phospho-Syntaxin 4, however further robust tests would be required to link these kinases to the rate of plasma membrane fusion.

5.4 Conclusions

This chapter aimed to study the effect of insulin on the plasma membrane of 3T3-L1 adipocytes using a modified version of our previously established *in vitro* fusion assay. Isolated plasma membrane fractions from basal and insulin-stimulated 3T3-

L1 adipocytes were reconstituted into liposomes and the protein content of these vesicles was assessed by silver staining and western blotting. The proteoliposomes were then added to the *in vitro* fusion assay with VAMP 2-containing donor vesicles in order to measure their fusogenic properties.

Previous studies into the effect of insulin on SNARE-mediate fusion of GSVs at the plasma membrane of adipocytes utilised liposomes created using both isolated plasma membrane fractions and GSVs from rat adipocytes: both were reconstituted into separate vesicle populations, and their ability to fuse was analysed (Koumanov *et al*, 2005). Using this method, it was discovered that the fusion of GSVs with the plasma membrane of adipocytes was SNARE and cytosol-dependent; in particular, the presence of PKB in the cytosol was necessary to sustain rapid insulin-stimulated fusion (Koumanov *et al*, 2005). This necessity for PKB is perhaps unsurprising, given that many of the effects of insulin signalling are mediated by PKB (Taniguchi *et al*¸ 2006).

Results from our investigation partially confirm those obtained in the study by Koumanov and colleagues. Insulin-stimulation in our system leads to changes in the plasma membrane which culminate in an increase in the rate of SNARE-mediated fusion (Figure 5.4B). However, unlike the experiments performed by Koumanov and colleague, our experiments did not require addition of cytosol in order to sustain fusion, although it may be interesting to test the effect of cytosol addition to our assay in future experiments. Further to this, direct addition of PKB to our assay was not required in order to sustain fusion; however we did observe an increase in PKB at the plasma membrane of 3T3-L1 adipocytes (Figure 5.6). Although the kinase was not detected in our liposomes, it is possible that it had an effect on plasma membrane-located proteins which are then reconstituted, leading to the observed increase in SNARE-mediated membrane fusion; a hypothesis which would warrant further investigation.

Although our experimental system draws from that outlined by Koumanov and colleagues, one fundamental difference exists that may explain the necessity for cytosol to sustain fusion in their system. As our investigation sought to understand

the effect of insulin solely on the plasma membrane of 3T3-L1 adipocytes, we chose to use VAMP 2-containing vesicles as our donor liposomes. This allowed us to attribute any changes observed in the rate of fusion to changes at the plasma membrane. In contrast, the Koumanov study utilised isolated GSVs as their donor liposomes, adding further variables to the reaction. It is therefore plausible that the addition of cytosol may have an effect on the GSVs, rather than the plasma membrane, leading to their observed increase in fusion. It would be interesting to further utilise our assay to investigate the observations made by Koumanov and colleagues, for example by isolating the plasma membrane fractions from 3T3-L1 adipocytes which have been depleted of cytosolic proteins, for example PKB, and studying the effect of insulin on membrane fusion in these cells. In this way, our assay could be used to further dissect the proteins and interactions involved in SNARE-mediated membrane fusion in 3T3-L1 adipocytes.

Western blot analysis of basal and insulin-stimulated plasma membrane indicated that insulin does not alter the amount of t-SNARE present at the plasma membrane, however insulin signalling does increase the level of GLUT4 (Figure 5.1). This suggests that insulin signalling alters the conformation of the proteins; induces binding or dissociation of effector proteins; or perhaps alters the plasma membrane localisation of the proteins, bringing together binary t-SNARE complexes. This hypothesis was further supported by the increase in PKA, PKB and PKC at the plasma membrane upon insulin stimulation (Figure 5.6), however we could not accurately show the exact effect of these kinases on the rate of fusion due to the high number of proteins present in both the plasma membrane and liposome samples (Figure 5.5).

Optimisation of the fusion assay conditions using liposomes derived from basal and insulin stimulated plasma membrane indicated that, similar to the recombinant *in vitro* fusion assay, protein-free liposomes were an effective control to ensure that the fusion observed was due to SNARE-SNARE interactions. Furthermore, it was also observed that liposomes reconstituted using 0.75 mg/ml plasma membrane showed more consistent controls and fusion than those with lower (0.3 mg/ml) or higher (1.5 mg/ml) protein concentrations.

Silver staining indicated that there were more proteins reconstituted into our liposomes than the t-SNAREs alone (Figure 5.5); however we have as yet been unable to identify any of these proteins. Although preliminary investigation detected an increase in PKA, PKB and PKC at the plasma membrane upon insulin stimulation, the proteins were not reconstituted into the liposomes with the t-SNAREs (Figure 5.6). Although these proteins are not present in the liposomes, it is possible that they are still having an effect on the rate of membrane fusion by phosphorylation of target proteins which are then reconstituted. Although we cannot definitively say that this is the case, the next stage for this project would be to identify the bands present in the liposome samples by mass spectrometry and confirm any findings by western blotting, alongside further robust investigations into the effect of kinases on SNARE-mediated membrane fusion.

6 Discussion

Diabetes UK estimates that around 3 million people in the UK have been diagnosed with diabetes, and that 90 % of these have Type 2 diabetes (Diabetes in the UK, Diabetes UK 2011/2012). With 552 million people worldwide expected to be affected by diabetes by 2030, it is important to understand the molecular mechanisms behind the condition with a view to treating or curing it.

Under normal physiological conditions, after a meal there is an increase in blood-sugar concentration. To counter this, the pancreas produces the hormone insulin, which acts on fat and adipose tissue to translocate the glucose transporter GLUT4 from intracellular stores to the plasma membrane. Once at the plasma membrane, this transporter lowers blood-glucose levels by transporting glucose into muscle and adipose tissues where it is stored as glycogen and triglycerides respectively. Type 2 diabetes is characterised as an impaired glucose uptake in response to insulin signalling due to lower levels of GLUT4 on the cell surface.

The SNARE proteins Syntaxin 4, SNAP-23 and VAMP 2 have been implicated in the fusion of GSVs with the plasma membrane in response to insulin signalling (Cheatham et al, 1996), and thus understanding SNARE complex formation and regulation is key to unravelling the impaired mechanisms which characterise Type 2 diabetes. Sec1/Munc-18 (SM) proteins are a family of proteins implicated in the regulation of SNARE-mediated membrane fusion, with Munc-18c involved in the regulation of GSV fusion at the plasma membrane. This thesis aimed to investigate the interactions between the SNARE and the SM protein Munc-18c, which are involved in GLUT4 translocation in response to insulin.

6.1 Regulation of membrane fusion by SNARE proteins in an *in vitro* system

The original aim of this section of my thesis was to utilise the *in vitro* fusion assay developed previously in our lab (Brandie et al, 2008) to test whether the location of the His6 purification tag on Munc-18c affected the function of the SM protein. However, as outlined in Chapter 3, our initial attempts at utilising the *in vitro* fusion

assay were unsuccessful and, despite using the same construct and purification/reconstitution methods outlined in the paper by Brandie and colleagues, we were unable to replicate the results. Investigation into why this may be the case indicated the t-SNARE proteins were unable to form stable binary complexes (Figure 3.8), hence low levels of t-SNARE complex were reconstituted into liposomes (Figure 3.6), leading to low levels of membrane fusion (Figure 3.7).

The *in vitro* fusion assay has been long established for other SNARE-mediated membrane fusion events; including neurotransmitter release (Weber et al, 1998; Ji et al, 2010) and yeast ER-Golgi transport (Scott et al, 2003). Although in these assays, binary t-SNARE complexes are formed and reconstituted into liposomes, one notable observation is that a higher level of one t-SNARE is purified and reconstituted into the vesicles, for example, in the initial SNARE-mediated fusion assay developed by Weber and colleagues, more Syntaxin 1a is reconstituted relative to SNAP-25; a characteristic which is observed in later studies utilising these SNAREs (Ji et al, 2010). Indeed, in the study by Brandie and colleagues into the Syntaxin 4/SNAP-23/VAMP 2 fusion system, more SNAP-23 appears to be reconstituted into the vesicles in relation to Syntaxin 4. In all cases, the t-SNAREs were co-expressed from separate vectors, one under the control of the T7 promoter and the other under T5, and expressed in BL21 (DE3) E. coli which, as discussed in Chapter 3, is not ideal for the expression of proteins under the control of the T5 promoter as this exhibits high levels of basal expression, and may account for the uneven expression of the t-SNAREs.

As t-SNARE complex formation appeared to be the root of the issues with our *in vitro* fusion assay, we opted to re-establish the assay utilising binary t-SNARE complexes expressed from the vector pETDuet-1 (Novagen), This vector contains two multiple cloning sites, allowing for simultaneous expression of two target genes. Both multiple cloning sites are under the control of the T7 promoter, preventing basal expression and allowing both genes to be expressed at similar rates to one another. After optimisation of the purification conditions, binary t-SNARE complexes were produced from this vector (Figure 3.9) and reconstituted into vesicles (Figure 3.10). Unlike previous studies, the complexes expressed from

pETDuet-1 contained a much more even ratio of Syntaxin:SNAP; and in agreement with the previous study performed in our lab (Brandie et al, 2008), the SNARE complex consisting of Syntaxin 4, SNAP-23 and VAMP 2 was sufficient to drive the fusion of two vesicle populations *in vitro* (Figure 3.11). No published SNARE-mediated *in vitro* fusion assay has utilised t-SNAREs purified in this way, but as binary t-SNARE complexes it crucial to trans-SNARE complex formation, the vector pETDuet-1 may be a useful tool in isolating evenly formed t-SNARE complexes.

It is important to note the presence of contaminant bands in the SNARE preparations, in particular the full-length and cytosolic VAMP 2 (Figure 3.2 and Figure 3.3). With the full-length protein, this contaminant band is removed through the reconstitution process (Figure 3.5B), possibly through the dialysis step. Samples of the cytosolic domain of VAMP 2 were dialysed against Exchange/Reconstitution buffer to remove traces of Imidazole present in the elution buffer, and it is plausible that this too would remove the contaminant band, however as samples of the cytosolic domain of VAMP 2 were generally not run on a gel after concentration. It is interesting to note, as mentioned in Chapter 3, a contaminant band of the same molecular weight (~25 kDa) was observed in the cytosolic v-SNARE purifications by previous students in our lab who studied both mammalian and yeast fusion (Dr Fiona Brandie and Dr Chris MacDonald), suggesting that this contaminant may be an native E. coli protein which binds with affinity to nickel resin, however further study would be required to confirm this, for example, extraction of the band and analysis by mass spectroscopy.

It would also be beneficial to further purify the proteins using techniques such as ion exchange chromatograph, which uses the isoelectric point of proteins to separate them by charge. This technique was being optimised by a fellow student in the lab, Andrew Fuller, who was looking to purify proteins for use in Isothermal Titration Calorimetry (ITC). Unfortunately this process was never fully optimised; however it would certainly be a useful tool to utilise to ensure that all proteins used in the *in vitro* fusion assay are as pure as possible. It may be difficult to use ion exchange chromatography to purify the binary t-SNARE complexes due to their

differing isoelectric points (5.84 for Syntaxin 4, 4.88 for SNAP-23), however this technique has been used in the past to purify SNARE proteins (Fasshauer *et al*, 1998; Domanska *et al*, 2009) and SNARE complexes (Ernst and Brunger, 2002; Strop *et al*, 2007) and, with optimisation, could be used to further purify the t-SNARE complexes to remove the contaminant bands present in the reconstituted samples (Figure 3.10).

Although the liposome fusion assay is a useful tool for measuring the rate of SNARE-mediate membrane fusion *in vitro*, there are questions surrounding how relevant the assay is with relation to fusion evens *in vivo*. Firstly, there is debate as to how the proteoliposomes utilised in these studies should be generated. At present, two methods exist: the "standard" method (utilised in this study), which involves forming the liposomes alongside the SNARE proteins (Weber *et al*, 1998; Schuette *et al*, 2004; Brandie *et al*, 2008); and the "direct" method, in which the SNARE proteins are inserted into pre-formed liposomes (Kweon *et al*, 2003; Rigaud and Levy, 2003; Lu *et al*, 2005). In the "direct" method, unilamellar vesicles are produced with a diameter of 100 nm, whilst the "standard" method produces vesicles of with a broader range of diameter: vesicles with a diameter lower than 20 nm have been shown to have high membrane curvature stress and are more prone to spontaneous fusion (Suurkuusk *et* al, 1976; Chen *et al*, 2006). Our study showed that almost all our vesicles produced by the "standard" method have a diameter of 20-100 nm, which is within the accepted range outlined by Chen and colleagues. Furthermore, as shown in this and other studies, addition of the cytosolic domain of the v-SNARE inhibits fusion, indicating that the rates of fusion observed in the assay are due to SNARE complex formation, rather that spontaneous fusion of small vesicles (Figure 3.11; Weber *et al*, 1998; Hu *et al*, 2002; Brandie *et al*, 2008).

Contention also surrounds whether the concentration of SNAREs found in proteoliposomes is too high to be physiologically relevant. Studies into the neuronal SNARE complex have used v-SNARE vesicles with high protein:lipid concentration (Weber *et al*, 1998; Lu *et al*, 2005), with around 50 times as many v-SNARE proteins reconstituted per vesicle than is observed *in vivo* (Dennison *et al*,

2006). Fusion assays utilising vesicles with a more physiological concentration of v-SNAREs did not exhibit fusion, leading to the hypothesis that SNARE complex formation may not be the minimal machinery for membrane fusion and that other proteins are necessary to regulate SNARE function (Dennison *et al*, 2005). While the concentration of VAMP 2 in GSVs has not been determined, the total SNARE content of 3T3-L1 adipocytes has been established (Hickson *et al*, 2000), and this would allow further development of our *in vitro* fusion system to incorporate physiological amounts of SNARE protein, especially since we are now able to produce and reconstitute even t-SNARE complexes.

A final criticism of the *in vitro* fusion assay is that it does not measure fusion *per se*, rather it measures lipid mixing. Two methods have been developed in order to overcome this issue: the use of sodium dithionite, and the development of a content mixing *in vitro* assay. Sodium dithionite is a chemical which reduces NBD to a non-fluorescent form (McIntyre and Slight, 1991), and was utilised by Weber and colleagues to essentially strip the fluorescence from the outer leaflet of the donor vesicles and measure the rate of fusion of the inner leaflet, showing that both leaflets of the membrane are involved in fusion. The second technique, a content mixing assay, is designed to measure the rate of a reaction, for example FRET, which occurs when the contents of the donor and acceptor liposomes are mixed: a reaction which can only occur through full membrane fusion. This type of assay has been used to show that the yeast SNAREs involved in transport to the plasma membrane are sufficient to drive membrane fusion (Diao *et al*, 2010), however these assay present the same issues as traditional *in vitro* fusion assays with regards to the concentration of SNAREs present in the vesicles.

Whilst our *in vitro* fusion assay shows high levels of lipid mixing, it would be ideal to perform further experiments designed using the above mentioned criticisms in order to develop our knowledge of the SNARE-mediated fusion events which regulate GSV fusion in adipocytes. By designing an assay which utilises SNARE densities resembling those found *in vivo* (Hickson *et al*, 2000), and changing the assay to measure content rather than lipid mixing, we could determine whether the

SNARE complex consisting of Syntaxin 4, SNAP-23 and VAMP 2 can truly be called the "minimal machinery" driving GSV fusion *in vivo*.

6.2 Regulation of Munc-18c/SNARE complex interactions and their effect on SNARE-mediated membrane fusion

The next section of this thesis involved using the *in vitro* fusion assay to assess the effect of the SM protein Munc-18c on the rate of SNARE-mediated membrane fusion (Chapter 4). At present, no unified theory exists for the function of SM proteins in SNARE-mediated membrane fusion, despite the structural conservation which exists between members of the protein family (Gallwitz and Jahn, 2003). Three binding modes have been observed between different SM/SNARE proteins (outlined in Figure 4.1): binding of the SM protein to "closed" Syntaxin (Mode 1); binding of the SM protein to the N-terminus of Syntaxin (Mode 2) and binding of the SM protein to the assembled SNARE complex (Mode 3). It has been hypothesised that these different binding modes result in different function of the SM/SNARE protein complexes, depending on which mode is undertaken. For example, the neuronal SM protein Munc-18a was found to bind to Syntaxin 1a via both Modes 1 and 2, with each binding mode occurring at a different cellular location: Mode 1 binding was found to occur on intracellular membranes, whilst Mode 2 occurs at the plasma membrane (Rickman *et al*, 2007). This chaperone/activation duality has also been shown in both UNC64 in *Caenorhabditis elegans* (Johnson *et al*, 2009) and the yeast SM protein Vps45p (Bryant and James, 2001). Furthermore, Mode 2 binding has been hypothesised to act as an intermediate step between Modes 1 and 3 binding (Khvotchev *et al*, 2007; Hu *et al*, 2011). This suggests that the different binding modes observed between SM and SNARE proteins may be due to the SM protein having multiple functions before (as a chaperone for Syntaxin during transport) and during (mediating the "opening" of Syntaxin) membrane fusion. Conflicting data has been produced on whether some SM proteins are able to perform Mode 3 binding, for example, experiments using the neuronal SM protein Munc-18a have shown that it is able to perform Mode 3 binding (Zilly *et al*, 2006) whilst others have shown that it cannot (Yang *et al*, 2000). In contrast, the yeast SM protein Sec1p has been shown to bind to

assembled SNARE complexes (Togneri *et al*, 2006), where it acts as a stimulator of fusion (Scott *et al*, 2004).

Munc-18c has been shown to exhibit Mode 1 and 2 binding with Syntaxin 4 (D'Andrea-Merrins *et al*, 2007; Aran *et al*, 2009), with Mode 1 being inhibitory to SNARE complex formation and Mode 2, in particular the "opening" of Syntaxin 4, necessary for SNARE complex formation (D'Andrea-Merrins *et al*, 2007). It has been suggested that the SM protein is also able to bind the assembled Syntaxin 4/SNAP-23/VAMP 2 SNARE complex (Latham *et al*, 2006); however no functional significance of this binding mode has been established.

With the *in vitro* fusion assay now re-established, my first priority was to test our previous finding that Munc-18c acts as a negative regulator of SNARE-mediated membrane fusion. Information from a collaborator suggested that the location of the purification tag on the SM protein could affect the function of the protein in the *in vitro* fusion assay. In order to investigate this, recombinant N- and C-terminally tagged wild-type Munc-18c was purified from bacteria (Figure 4.2), and functionally analysed using GST pull-down assays (Figure 4.3), which indicated that both wild-type proteins bound to Syntaxin 4 equally when incubated overnight, suggesting that the purification tag does not affect this interaction. The function of the wild-type proteins was further analysed using the *in vitro* fusion assay. Following the protocol previously designed for this experiment, N- and C-terminally tagged wild-type SM protein was mixed with t- and v-SNARE liposomes, and fusion measured after overnight incubation at 4 °C to induce pre-docking of the vesicles. Using this method, I observed that both N- and C-terminally tagged Munc-18c are negative regulators of SNARE-mediated membrane fusion (Figure 4.4), confirming previous findings (Brandie *et al*, 2008).

In order to study the interactions involved in binding between Munc-18c and the assembled SNARE complex, point mutants were created in the SM protein which were hypothesised to interfere with this binding mode. Based on mutations made in the SM proteins Munc-18a (Déak *et al*, 2009) and unc-18 (Graham *et al*, 2009), residues E63, E70 and D222 were selected for mutagenesis by sequence alignment

and altered in order to disrupt their ability to interact with the SNARE proteins. I was able to purify the mutant SM proteins to similar concentrations as the wild-type proteins (Figure 4.5), and analysed their functionality using both GST pull-down assays and the *in vitro* fusion assay.

Assembled SNARE complexes were formed using bacterial lysates expressing the different SNARE proteins (Figure 4.7A), and were used to study Mode 3 binding between the complex and Munc-18c. Unfortunately, high levels of non-specific binding were observed between the SM protein and the GST-alone control (Figure 4.7B), preventing accurate analysis of Mode 3 binding in this manner. In order to assess the interactions between the SNARE and SM proteins, I chose to simplify the assay and investigate binding between the wild-type and mutant SM proteins and the individual SNAREs: although this would not give definitive answers with regards to Mode 3 binding (as there is no assembled complex) it was hoped that these experiments may highlight some functional significance of the residues selected for analysis in Munc-18c.

Despite multiple optimisation attempts, we were unable to prevent binding of the SM proteins to the GST control during our pulldown assays, with the exception of the D222N mutant, making it difficult to assign an overall pattern or model. The D222N model did not bind the GST control, but was still able to bind all three SNARE proteins studied (Figure 4.8), however as we were unable to fully quantify binding of the wild-type SM protein, it was impossible to determine the significance to these interactions. However, we were able to investigate the effect of the wild-type and mutant SM proteins in the *in vitro* fusion assay. As we were attempting to investigate Mode 3 binding between the SNARE complex and SM protein, I designed an altered form of the *in vitro* fusion assay, in which t- and v-SNARE vesicles were incubated overnight to induce pre-docking of the SNARE complexes, before addition of Munc-18c just before the assay began. Using this assay, the mutant SM proteins were shown to inhibit SNARE-mediated membrane fusion to a greater extent that the wild-type SM protein, with the D222N mutant showing the strongest dominant negative effect (Figure 4.9). These results were unexpected, as experiments in homologous systems have yielded different results:

mutations to residues E63 and E70 in the neuronal SM protein Munc-18a did not affect the rate of vesicle fusion compared to the wild-type SM protein (Déak *et al*, 2009). In order to understand this effect further, I returned to the C-terminally tagged wild-type Munc-18c protein, to test its function in the "Mode 3" fusion assay (where the SM protein is added after overnight incubation of the liposomes). When tested in this manner, the addition of C-terminally tagged Munc-18c caused an increase in the rate of SNARE-mediated membrane fusion (Figure 4.10), in contrast to our previous tests with this protein (Figure 4.4).

It has been previously shown that the location of a GST tag on the N-terminus of Syntaxin 4 leads to a decrease in binding to recombinant Munc-18c (Aran *et al*, 2009). GST is a large (~25 kDa) purification tag, whilst the polyhistidine tag is much smaller (His_6 <1 kDa), nevertheless, the polyhistidine tag appears to have some effect on the functional properties of Munc-18c when added to the *in vitro* fusion assay in this Mode 3 manner. This also calls into question the results from the experiments utilising the mutant Munc-18c proteins as these too contain an N-terminal polyhistidine tag, which may account for the unexpected results observed when using these proteins in the *in vitro* fusion assay.

In a wider context, this observation also throws doubt onto other studies which utilise tagged SM proteins. Both N- (Shen et al, 2006; Brandie et al, 2008) and C-terminally tagged (Smyth et al, 2010; Schollmeier et al, 2011) SM proteins have been used in various studies into the SM protein function. As discussed earlier in this thesis, controversy and contradiction surround the field of SM protein biology, and the discovery that the position of the purification tag on the SM protein only adds to this.

Comparison of the results obtained when the C-terminally tagged Munc-18c is added to the *in vitro* fusion assay yield an interesting hypothesis into the function of Munc-18c in SNARE complex formation: although the results are conflicting, they may suggest that the effect of Munc-18c is dependent on the timing of the interaction, with Munc-18c acting as a negative regulator when bound to the t-SNARE complex, but a positive regulator when interacting with the assembled

SNARE complex, a hypothesis supported by the observation that insulin signalling causes repositioning of Munc-18c on Syntaxin 4 (Smithers et al, 2008). Similar results were observed in a homologous fusion system, with Munc-18a having both inhibitory and stimulatory effects (Schollmeier et al, 2011). In this study, it was shown that not only is Munc-18a able to stabilise the "closed" conformation of Syntaxin 1a, it is also able to inhibit t-SNARE complex formation, indicating that the protein may have more than one inhibitory mechanism.

As previously mentioned in Section 6.1, there are criticisms surrounding the *in vitro* fusion assay, and these stretch to cover the addition of proteins into the assay to study their effect on the rate of SNARE-mediated membrane fusion. Experiments using squid Munc-18a (sMunc-18a) showed that adding the SM protein to the *in vitro* fusion assay led to a dose-dependent increase in apparent liposome fusion, even in the absence of SNARE proteins (Xu et al, 2011). Denaturing of the sMunc-18a also appeared to cause the protein to bridge membranes, forming hemifusion intermediates, although this study was unable to confirm whether this process had any physiological relevance (Xu et al, 2011). It is important to note however, that when Munc-18c was added to our fusion assay, the protein concentration was lower than that observed in this study (usually 0.2-0.3 µM depending on SNARE concentration), and further to this, the squid SM protein was selected for this study as it does not denature at high (20 µM) concentrations as mammalian SM proteins do. Although these observations cast doubt onto the significance of the sMunc-18a study, it is important to recognise that the assay is not without its flaws, and all data must be backed up with complementary analyses, for example, binding studies between the proteins of interest, or imaging of the liposomes using electron microscopy.

6.3 The effect of insulin on the plasma membrane of 3T3-L1 plasma membrane fractions

In the final section of this thesis, I investigated the effect of insulin stimulation on the plasma membrane of 3T3-L1 adipocytes, as outlined in Chapter 5. Whilst binding of insulin to its receptor is known to trigger a signalling cascade which ultimately leads to the translocation of GLUT4 to the cell surface (Cushman et al,

1980; Suzuki and Kono, 1980), the exact effect of insulin on the plasma membrane of adipose cells is less well understood. A previous study identified the plasma membrane of rat adipose cells as being the location of the "key regulated step" in GSV fusion, and identified PKB in the cytosol of adipocytes as being important in the fusion reaction (Koumanov et al, 2005).

Fractionation of 3T3-L1 adipocytes showed that insulin-stimulation did not alter the levels of the t-SNAREs Syntaxin 4 and SNAP-23 at the plasma membrane; however GLUT4 did translocate from an intracellular store to the cell surface (Figure 5.1). Although initially used as a quality control step to ensure that the adipocytes responded to insulin as they should, the unaltered levels of t-SNARE in response to insulin allowed us to hypothesise as to how the hormone may affect these proteins. As Syntaxin 4 is known to undergo conformational changes which affect its function, it is possible that insulin functions, directly or indirectly, by altering the conformation of Syntaxin 4, potentially by recruiting or dissociating regulatory proteins. Syntaxin 4 is has also been shown to form distinct clusters on the plasma membrane (Sieber et al, 2006), thus it is possible that insulin functions by spatially bringing together t-SNARE complexes on the cell surface, aiding SNARE complex formation.

As my aim was to establish a new fusion assay in order to study the protein found at the plasma membrane of 3T3-L1 adipocytes, it was important to optimise the reaction, as more proteins were likely to be involved than the SNAREs alone. Three concentrations of plasma membrane were utilised in this study (0.3, 0.75 and 1.5 mg/ml total protein) in order to determine the optimum concentration to reconstitute in order to observe vesicle fusion. Both Syntaxin 4 and SNAP-23 reconstituted into liposomes at all three total protein concentrations, with higher protein levels reconstituted from higher protein concentrations (Figure 5.2).

The next stage of optimisation concerned the control reaction for these fusion experiments. Addition of the cytosolic domain of VAMP 2 to the plasma membrane-derived liposomes had no effect on the rate of SNARE-mediated membrane fusion (Figure 5.4) and thus was deemed an insufficient control. It is possible that the cytosolic VAMP 2 which was added to the reaction is interacting

with another protein (other than the t-SNAREs) on the plasma membrane of 3T3-L1 adipocytes, meaning that it is not available to bind the t-SNARE complex and inhibit fusion. Identification of this binding partner could further elucidate the interactions involved in SNARE complex regulation and would be of interest for further study. Alternatively, post-translational modifications to the t-SNAREs may prevent the cytosolic domain of VAMP 2 from forming a stable complex, instead only facilitating a transient interaction.

Although protein-free vesicles appeared to function as a good control for SNARE-mediated fusion, further controls could be utilised to ensure that the levels of fusion observed are due to SNARE complex formation. Trypsin digestion of vesicles can be used to cleave SNARE proteins (Graham *et al*, 2004; D'Andrea-Merrins *et al*, 2007), and pre-treatment of the donor vesicles with trypsin (followed by dialysis to remove the protease) could be used to show that cleavage of the v-SNARE prevents SNARE complex formation. Further to this, neurotoxins could be used in a similar fashion to cleave the SNARE proteins in both the PM-derived and v-SNARE donor vesicles; however if these were to be used on the PM-derived vesicles, further investigation would be required into the protein content of these vesicles, in particular the SNARE protein content, as different toxins have been shown to cleave different SNARE proteins (Schiavo *et al*, 1995; Macaulay *et al*, 1997; Binz *et al*, 2010), which may lead to unexpected effects on membrane fusion.

In this study, in order to ensure that the observed rate of fusion was due to SNARE complex formation, we utilised protein-free liposomes as our control (Figure 5.4), which resulted in low levels of fusion compared to the uninhibited reaction, indicating the fusion observed is due to SNARE complex formation and is not spontaneous. It is interesting to note, however, that the levels of fusion observed in these control reactions are higher than those using recombinant SNARE proteins (as seen in Chapter 3), suggesting that the liposomes are able to fuse without SNARE complex formation. As many proteins are present in the liposomes derived from 3T3-L1 plasma membrane, it is possible that we are observing a small amount of spontaneous fusion driven by the presence of one or more of these proteins. This could be a similar observation to that of Xu *et al* (2011), where high concentrations

of denatured SM protein caused hemifusion and vesicle clustering (mentioned above in Section 6.2), and may warrant further investigation.

The final optimisation step involved investigating which liposomes best represented observed *in vivo* GSV fusion. Liposomes derived from both 0.3 and 0.75 mg/ml plasma membranes were able to sustain fusion (Figure 5.4). Liposomes derived from 0.75 mg/ml plasma membrane best resembled fusion observed *in vivo*, with insulin increasing the rate of membrane fusion. Furthermore, these liposomes displayed more consistent controls, allowing us to be certain that our observations were indeed due to SNARE-mediated membrane fusion.

Although silver staining of plasma membrane and liposome samples identified that many proteins were present in the samples (Figure 5.5), we were unable to detect the presence of any proteins of interest in the liposomes by western blotting (Figure 5.5). Although the kinases PKA, –B and –C were not found in the liposomes, levels of all three proteins increased at the plasma membrane in response to insulin, indicating that they may have functioned to phosphorylate proteins on the plasma membrane, despite not being reconstituted themselves. It is important to note that these experiments were performed in the absence of ATP and phosphatase inhibitors; however these experiments were performed late in this study, and were designed as a preliminary investigation into kinase location, not a conclusive study into their function in this assay.

Previous study indicated that SNARE-mediated membrane fusion is dependent on the presence of PKB (Koumanov *et al*, 2005). It is important to note, however, that this previous study utilised both plasma membrane and GSVs from rat adipose tissue, and attempted to fuse both in a modified *in vitro* fusion assay. Although our results do suggest that PKB may have a function at the plasma membrane of 3T3-L1 adipocytes, direct addition of the kinase was not necessary to sustain fusion in this assay. This is likely due to the fact that we did not use GSVs as our "donor" liposomes; rather we used VAMP 2-containing vesicles. Therefore, it is plausible that the addition of PKB to the assay relieves inhibition on the GSVs, not the plasma membrane. Indeed, it has previously been shown that PKB is targeted to (or

near) GSVs upon insulin stimulation (Calera *et al*, 1998; Kupriyanova and Kandror, 1999) where it has a positive effect on GSV translocation (Ducluzeau *et al*, 2002).

6.4 Future Work

Several interesting observations have arisen from this work, each of which warrants further study. Firstly, the discovery that the location of the polyhistidine tag affects the function of the protein deserves further investigation as it impacts not only this, but other studies which have utilised tagged SM proteins. Ideally, all experiments involving Munc-18c (both wild-type and mutant) should be repeated using untagged SM protein in addition to N- and C-terminally tagged protein in order to ascertain what the true function of Munc-18c is, and to give insight into why the purification tag causes such an effect. In conjunction with this, it would be interesting to conduct structural studies using tagged and untagged SM protein to investigate why such a small tag has such a profound effect. Nuclear Magnetic Resonance (NMR) spectroscopy would be useful in this endeavour, as it utilises protein in solution, which may allow us to study the SM protein in complex with the assembled SNARE complex as well as individual SNAREs.

To complement this, binding studies would also be useful, for example, Surface Plasmon Resonance (SPR) or Isothermal Titration Calorimetry (ITC), both of which have been previously used to study binding between SNARE and SM proteins (Burkhardt *et al*, 2008; Aran *et al*, 2009). These techniques would allow calculation of the dissociation (K_d) and binding constants (K_D) which would give an insight into the strength of the complexes investigated, allowing us to ascertain how physiologically relevant any observed interactions may be. Again, these experiments should be performed utilising both tagged and untagged SM protein to observe any differences between the proteins.

I would also like to deconstruct the *in vitro* liposome fusion assay and utilise the method outlined in Schollmeier *et al* (2011). In this paper, monomeric Syntaxin 1a is reconstituted into the "acceptor" liposomes, and soluble SNAP-25 is added to form binary t-SNARE complexes. Using this method, they were able to investigate the role of the SM protein on t-SNARE complex formation, as well as SNARE complex

formation. This method would be useful alongside some of the binding assays mentioned previously (SPR, ITC etc.) to help dissect the interactions involved in SNARE complex regulation. It is important to note, however, that both Syntaxin 4 and SNAP-23 may have to be cloned into new expression vectors, as this assay is dependent on the formation of binary t-SNARE complexes, something we were unable to achieve with our previous constructs (Figure 3.8). It would also be interesting to develop this assay to utilise content mixing (as discussed in Section 6.1) to ensure that full membrane fusion is being observed.

I would also like to further utilise my plasma membrane fusion assay to study the proteins involved in fusion of GSVs with the plasma membrane of 3T3-L1 adipocytes. Now that the assay has been established, it would be interesting to knockdown (or knockout) proteins known to play a role in SNARE-mediated membrane fusion, for example, the SNARE proteins themselves, PKB or Munc-18c, and to assess what effect this has on membrane fusion in response to insulin. It would also be interesting to analyse the protein content of the liposomes derived from plasma membrane fractions by mass spectrometry in order to identify if any known SNARE-interacting proteins, such as Munc-18c, Synip (Min *et al*, 1999) or Rab 4 (Li *et al*, 2001). This would allow for a greater library of proteins to knockdown in 3T3-L1 adipocytes to assess their effect on membrane fusion.

Bibliography

ALEDO JC, LAVOIE L, VOLCHUK A, KELLER SR, KLIP A, HUNDAL HS. (1997) Identification and characterization of two distinct intracellular GLUT4 pools in rat skeletal muscle: evidence for an endosomal and an insulin-sensitive GLUT4 compartment. *Biochem J*. **325**: 727-732.

ARAN V, BRANDIE FM, BOYD AR, KANTIDAKIS T, RIDEOUT EJ, KELLY SM, GOULD GW, BRYANT NJ. (2009) Characterization of two distinct binding modes between Syntaxin 4 and Munc18c. *Biochem J*. **419**: 655-660.

ARAN V, BRYANT NJ, GOULD GW. (2011) Tyrosine phosphorylation of Munc18c on residue 521 abrogates binding to Syntaxin 4. *BMC Biochem.* **12**: 19.

BAI L, WANG Y, FAN J, CHEN Y, JI W, QU A, XU P, JAMES DE, XU T. (2007) Dissecting multiple steps of GLUT4 trafficking and identifying the sites of insulin action. *Cell Metab*. **5**: 47-57.

BAUMERT M, TAKEI K, HARTINGER J, BURGER PM, FISCHER VON MOLLARD G, MAYCOX PR, DE CAMILLI P, JAHN R. (1990) P29: a novel tyrosine-phosphorylated membrane protein present in small clear vesicles of neurons and endocrine cells. *J Cell Biol*. **110**: 1285-1294.

BELL GI, KAYANO T, BUSE JB, BURANT CF, TAKEDA J, LIN D, FUKUMOTO H, SEINO S. (1990) Molecular-biology of mammalian glucose transporters. *Diabetes Care* **13**: 198-208.

BENNETT MK, CALAKOS N, SCHELLER RH. (1992) Syntaxin - a synaptic protein implicated in docking of synaptic vesicles at presynaptic active zones. *Science* **257**: 255-259.

BENNETT MK, GARCÍA-ARRARÁS JE, ELFERINK LA, PETERSON K, FLEMING AM, HAZUKA CD, SCHELLER RH. (1993) The Syntaxin family of vesicular transport receptors. *Cell* **74**: 863-873.

BINZ T, SIKORRA S, MAHRHOLD S. (2010) Clostridial neurotoxins: mechanism of SNARE cleavage and outlook on potential substrate specificity reengineering. *Toxins* **2**: 665-682.

BLOCK MR, GLICK BS, WILCOX CA, WIELAND FT, ROTHMAN JE. (1988) Purification of an N-ethylmaleimide-sensitive protein catalyzing vesicular transport. *Proc Natl Acad Sci USA* **85**: 7852-7856.

BOLIVAR F, RODRIGUEZ RL, GREENE PJ, BETLACH MC, HEYNEKER HL, BOYER HW, CROSA JH, FALKOW S. (1977) Construction and characterization of new cloning vehicles. II. A multipurpose cloning system. *Gene* **2**: 95-113.

BOSTRÖM P, ANDERSSON L, RUTBERG M, PERMAN J, LIDBERG U, JOHANSSON BR, FERNANDEZ-RODRIGUEZ J, ERICSON J, NILSSON T, BORÉN J, OLOFSSON, SO. (2007) SNARE proteins mediate fusion between cytosolic lipid droplets and are implicated in insulin sensitivity. *Nat Cell Biol.* **9**: 1286-1293.

BOSTRÖM P, ANDERSSON L, VIND B, HÅVERSEN L, RUTBERG M, WICKSTRÖM Y, LARSSON E, JANSSON PA, SVENSSON MK, BRÅNEMARK R, LING C, BECK-NIELSEN H, BORÉN J, HØJLUND K, OLOFSSON SO. (2010) The SNARE protein SNAP23 and the SNARE-interacting protein Munc18c in human skeletal muscle are implicated in insulin resistance/type 2 diabetes. *Diabetes* **59**: 1870-1878.

BRACHER A, WEISSENHORN W. (2002) Structural basis for the Golgi membrane recruitment of Sly1p by Sed5p. *Embo J.* **21**: 6114-6124.

BRAIMAN L, ALT A, KUROKI T, OHBA M, BAK A, TENNENBAUM T, SAMPSON SR. (2001) Activation of protein kinase C zeta induces serine phosphorylation of VAMP2 in the GLUT4 compartment and increases glucose transport in skeletal muscle. *Mol Cell Biol.* **21**: 7852-7861.

BRANDIE FM, ARAN V, VERMA A, MCNEW JA, BRYANT NJ, GOULD GW. (2008) Negative regulation of Syntaxin4/SNAP-23/VAMP2-mediated membrane fusion by Munc18c *in vitro*. *PLoS ONE* **3**: e4074.

BRENNER S. (1974) The genetics of *Caenorhabditis elegans*. *Genetics* **77**: 71-94.

BRYANT NJ, GOULD GW. (2011) SNARE proteins underpin insulin-regulated GLUT4 traffic. *Traffic* **12**: 657-664.

BRYANT NJ, GOVERS R, JAMES DE. (2002) Regulated transport of the glucose transporter GLUT4. *Nat Rev Mol Cell Biol.* **3**: 267-277.

BRYANT NJ, JAMES DE. (2001) Vps45p stabilizes the Syntaxin homologue Tlg2p and positively regulates SNARE complex formation. *EMBO J.* **20**: 3380-3388.

BURGOYNE RD, MORGAN A. (2007) Membrane trafficking: Three steps to fusion. *Curr Biol*. **17**: R255-R258.

CAIN CC, TRIMBLE WS, LIENHARD GE. (1992) Members of the VAMP family of synaptic vesicle proteins are components of glucose transporter-containing vesicles from rat adipocytes. *J Biol Chem.* **267**: 11681-11684.

CALERA MR, MARTINEZ C, LIU H, JACK AK, BIRNBAUM MJ, PILCH PF. (1998) Insulin increases the association of Akt-2 with GLUT4-containing vesicles. *J Biol Chem*. **273**: 7201-7204.

CARPP LN, CIUFO LF, SHANKS SG, BOYD A, BRYANT NJ. (2006) The Sec1p/Munc18 protein Vps45p binds its cognate SNARE proteins via two distinct modes. *J Cell Biol*. **173**: 927-936.

CARR CM, GROTE E, MUNSON M, HUGHSON FM, NOVICK PJ. (1999) Sec1p binds to SNARE complexes and concentrates at sites of secretion. *J Cell Biol*. **146**: 333-344.

CARVALHO E, ELIASSON B, WESSLAU C, SMITH U. (2000) Impaired phosphorylation and insulin-stimulated translocation to the plasma membrane of protein kinase B/Akt in adipocytes from Type II diabetic subjects. *Diabetologia* **43**: 1107-1115.

CHAPMAN ER, AN S, BARTON N, JAHN R. (1994) SNAP-25, a t-SNARE which binds to both Syntaxin and Synaptobrevin via domains that may form coiled coils. *J Biol Chem*. **269**: 27427-27432.

CHEATHAM B, VOLCHUK A, KAHN CR, WANG L, RHODES CJ, KLIP A. (1996) Insulin-stimulated translocation of GLUT4 glucose transporters requires SNARE-complex proteins. *Proc Natl Acad Sci USA* **93**: 15169-15173.

CHEN F, FORAN P, SHONE CC, FOSTER KA, MELLING J, DOLLY JO. (1997) Botulinum neurotoxin B inhibits insulin-stimulated glucose uptake into 3T3-L1 adipocytes and cleaves cellubrevin unlike type A toxin which failed to proteolyze the SNAP-23 present. *Biochem*. **36**: 5719-5128.

CHEN X, ARAÇ D, WANG TM, GILPIN CJ, ZIMMERBERG J, RIZO J. (2006) SNARE-mediated lipid mixing depends on the physical state of the vesicles. *Biophys J*. **90**: 2062-74.

CHEN YA, SCHELLER RH. (2001) SNARE-mediated membrane fusion. *Nat Rev Mol Cell Biol*. **2**: 98-106.

CHERNOMORDIK LV, MELIKOV K. (2006) Are there too many or too few SNAREs in proteoliposomes? *Biophys J*. **90**: 2657-2868.

CHRISTIE MP, WHITTEN AE, KING GJ, HU SH, JARROTT RJ, CHEN KE, DUFF AP, CALLOW P, COLLINS BM, JAMES DE, MARTIN JL. (2012) Low-resolution solution structures of Munc18:Syntaxin protein complexes indicate an open binding mode driven by the Syntaxin N-peptide. *Proc Natl Acad Sci USA* **109**: 9816-9821.

CHUNG SH, POLGAR J, REED GL. (2000) Protein kinase C phosphorylation of Syntaxin 4 in thrombin-activated human platelets. *J Biol Chem*. **275**: 25286-25291.

CLARY DO, GRIFF IC, ROTHMAN JE. (1990) SNAPs, a family of NSF attachment proteins involved in intracellular membrane fusion in animals and yeast. *Cell* **61**: 709-721.

COSTER AC, GOVERS R, JAMES DE. (2004) Insulin stimulates the entry of GLUT4 into the endosomal recycling pathway by a quantal mechanism. *Traffic* **5**: 763-771.

CUSHMAN SW, WARDZALA LJ. (1980) Potential mechanism of insulin action on glucose-transport in the isolated rat adipose cell - apparent translocation of intracellular-transport systems to the plasma-membrane. *J Biol Chem.* **255**: 4758-4762.

D'ANDREA-MERRINS M, CHANG L, LAM AD, ERNST SA, STUENKEL EL. (2007) Munc18c interaction with Syntaxin 4 monomers and SNARE complex intermediates in GLUT4 vesicle trafficking. *J Biol Chem*. **282**: 16553-16566.

DEÁK F, XU Y, CHANG WP, DULUBOVA I, KHVOTCHEV M, LIU X, SÜDHOF TC, RIZO J. (2009) Munc18-1 binding to the neuronal SNARE complex controls synaptic vesicle priming. *J Cell Biol.* **184**: 751-764.

DIAO J, SU Z, ISHITSUKA Y, LU B, LEE KS, LAI Y, SHIN YK, HA T. (2010) A single-vesicle content mixing assay for SNARE-mediated membrane fusion. *Nat Commun*. **1**:54.

DOMANSKA MK, KIESSLING V, STEIN A, FASSHAUER D, TAMM LK. (2009) Single vesicle millisecond fusion kinetics reveals number of SNARE complexes optimal for fast SNARE-mediated membrane fusion. *J Biol Chem.* **284**: 32158-32166.

DUCLUZEAU PH, FLETCHER LM, WELSH GI, TAVARÉ JM. (2002) Functional consequence of targeting protein kinase B/Akt to GLUT4 vesicles. *J Cell Sci.* **115**: 2857-2866.

DULUBOVA I, KHVOTCHEV M, LIU S, HURYEVA I, SÜDHOF TC, RIZO J. (2007) Munc18-1 binds directly to the neuronal SNARE complex. *Proc Natl Acad Sci USA* **104**: 2697-2702.

DULUBOVA I, SUGITA S, HILL S, HOSAKA M, FERNANDEZ I, SÜDHOF TC, RIZO J. (1999) A conformational switch in Syntaxin during exocytosis: role of Munc18. *Embo J.* **18**: 4372-4382.

DULUBOVA I, YAMAGUCHI T, ARAC D, LI H, HURYEVA I, MIN SW, RIZO J, SÜDHOF TC. (2003) Convergence and divergence in the mechanism of SNARE binding by Sec1/Munc18-like proteins. *Proc Natl Acad Sci USA* **100**: 32-37.

ERNST JA, BRUNGER AT. (2003) High resolution structure, stability, and Synaptotagmin binding of a truncated neuronal SNARE complex. *J Biol Chem*. **278**: 8630-8636.

FARESE RV, STANDAERT ML, FRANCOIS AJ, WAYS K, ARNOLD TP, HERNANDEZ H, COOPER DR. (1992) Effects of insulin and phorbol esters on subcellular distribution of protein kinase C isoforms in rat adipocytes. *Biochem J.* **288**: 319-323.

FASSHAUER D, SUTTON RB, BRUNGER AT, JAHN R. (1998) Conserved structural features of the synaptic fusion complex: SNARE proteins reclassified as Q- and R-SNAREs. *Proc Nat Acad Sci USA* **95**: 15781-15786.

FERNANDEZ I, UBACH J, DULUBOVA I, ZHANG XY, SÜDHOF TC, RIZO J. (1998) Three-dimensional structure of an evolutionarily conserved N-terminal domain of Syntaxin 1A. *Cell* **94**: 841-849.

FLETCHER LM, WELSH GI, OATEY PB, TAVARÉ JM. (2000) Role for the microtubule cytoskeleton in GLUT4 vesicle trafficking and in the regulation of insulin-stimulated glucose uptake. *Biochem J.* **352**: 267-276.

FOSTER LJ, YEUNG B, MOHTASHAMI M, ROSS K, TRIMBLE WS, KLIP A. (1998) Binary interactions of the SNARE proteins Syntaxin-4, SNAP23, and VAMP-2 and their regulation by phosphorylation. *Biochem.* **37**: 11089-11096.

FÖRSTER T. (1948) Zwischenmolekulare Energiewanderung und Fluoreszenz *Annal Phy.* **437**: 55-75.

GALLWITZ D, JAHN R. (2003) The riddle of the Sec1/Munc-18 proteins - new twists added to their interactions with SNAREs. *Trends Biochem Sci.* **28**: 113-116.

GENGYO-ANDO K, KAMIYA Y, YAMAKAWA A, KODAIRA K, NISHIWAKI K, MIWA J, HORI I, HOSONO R. (1993) The *C. elegans* unc-18 gene encodes a protein expressed in motor neurons. *Neuron* **11**: 703-711.

GLICK BS, ROTHMAN JE. (1987) Possible role for fatty acyl-coenzyme-a in intracellular protein-transport. *Nature* **326**: 309-312.

GOVERS R, COSTER AC, JAMES DE. (2004) Insulin increases cell surface GLUT4 levels by dose dependently discharging GLUT4 into a cell surface recycling pathway. *Mol Cell Biol.* **24**: 6456-6466.

GRAHAM ME, BARCLAY JW, BURGOYNE RD. (2004) Syntaxin/Munc18 interactions in the late events during vesicle fusion and release in exocytosis. *J Biol Chem.* **279**: 32751-32760.

GRAHAM ME, EDWARDS MR, HOLDEN-DYE L, MORGAN A, BURGOYNE RD, BARCLAY JW. (2009) UNC-18 modulates ethanol sensitivity in *Caenorhabditis elegans*. *Mol Biol Cell.* **20**: 43-55.

GUIDOTTI G. (1972) Membrane proteins. *Ann Rev Biochem.* 41: 731-752.

HATA Y, SLAUGHTER CA, SÜDHOF TC. (1993) Synaptic vesicle fusion complex contains UNC-18 homolog bound to Syntaxin. *Nature* **366**: 347-351.

HAYASHI T, MCMAHON H, YAMASAKI S, BINZ T, HATA Y, SÜDHOF TC, NIEMANN H. (1994) Synaptic vesicle membrane fusion complex: action of clostridial neurotoxins on assembly. *EMBO J*. 13: 5051-5061.

HAYASHI T, YAMASAKI S, NAUENBURG S, BINZ T, NIEMANN H. (1995) Disassembly of the reconstituted synaptic vesicle membrane fusion complex *in vitro*. *EMBO J*. **14**: 2317-2325.

HESS DT, SLATER TM, WILSON MC, SKENE JHP. (1992) The 25 kDa synaptosomal-associated protein SNAP-25 is the major methionine-rich polypeptide in rapid axonal-transport and a major substrate for palmitoylation in adult CNS. *J Neurosci*. **12**: 4634-4641.

HICKSON GR, CHAMBERLAIN LH, MAIER VH, GOULD GW. (2000) Quantification of SNARE protein levels in 3T3-L1 adipocytes: implications for insulin-stimulated glucose transport. *Biochem Biophys Res Commun*. **270**: 841-845.

HIMSWORTH HP. (1936) Diabetes mellitus: its differentiation into insulin-sensitive and insulin-insensitive types. *Lancet* **227**: 127-130.

HODGKINSON CP, MANDER A, SALE GJ. (2005) Protein kinase-zeta interacts with Munc18c: role in GLUT4 trafficking. *Diabetologia* **48**: 1627-1636.

HOHL TM, PARLATI F, WIMMER C, ROTHMAN JE, SÖLLNER TH, ENGELHARDT H. (1998) Arrangement of subunits in 20 S particles consisting of NSF, SNAPs, and SNARE complexes. *Mol Cell* **2**: 539-548.

HOLMAN GD, KASUGA M. (1997) From receptor to transporter: insulin signalling to glucose transport. *Diabetologia* **40**: 991-1003.

HOLMAN GD, LO LEGGIO L, CUSHMAN SW. (1994) Insulin-stimulated GLUT4 glucose transporter recycling. A problem in membrane protein subcellular trafficking through multiple pools. *J Biol Chem*. **269**: 17516-17524.

HOLT M, VAROQUEAUX F, WIEDERHOLD K, TAKAMORI S, URLAUB H, FASSHAUER D, JAHN R. (2006) Identification of SNAP-47, a novel Qbc-SNARE with ubiquitous expression. *J Biol Chem*. **281**: 17076-17083.

HU K, CARROLL J, FEDOROVICH S, RICKMAN C, SUKHODUB A, DAVLETOV B. (2002) Vesicular restriction of Synaptobrevin suggests a role for calcium in membrane fusion. *Nature* **415**: 646-650.

HU S-H, LATHAM CF, GEE CL, JAMES DE, MARTIN JL. (2007) Structure of the Munc18c/Syntaxin4 N-peptide complex defines universal features of the N-peptide binding mode of Sec1/Munc18 proteins. *Proc Nat Acad Sci USA* **104**: 8773-8778.

HU SH, CHRISTIE MP, SAEZ NJ, LATHAM CF, JARROTT R, LUA LH, COLLINS BM, MARTIN JL. (2011) Possible roles for Munc18-1 domain 3a and Syntaxin1 N-peptide and C-terminal anchor in SNARE complex formation. *Proc Natl Acad Sci USA* **108**: 1040-1045.

HU SH, GEE CL, LATHAM CF, ROWLINSON SW, ROVA U, JONES A, HALLIDAY JA, BRYANT NJ, JAMES DE, MARTIN JL. (2003) Recombinant expression of Munc18c in a baculovirus system and interaction with Syntaxin4. *Prot Exp Purif.* **31**: 305-310.

INOUE A, OBATA K, AKAGAWA K. (1992) Cloning and sequence-analysis of cDNA for a neuronal cell-membrane antigen, HPC-1. *J Biol Chem.* **267**: 10613-10619.

INOUE M, CHANG L, HWANG J, CHIANG SH, SALTIEL AR. (2003) The exocyst complex is required for targeting of GLUT4 to the plasma membrane by insulin. *Natu*re **422**: 629-633.

INOUE M, CHIANG SH, CHANG L, CHEN XW, SALTIEL AR. (2006) Compartmentalization of the exocyst complex in lipid rafts controls GLUT4 vesicle tethering. *Mol Biol Cell* **17**: 2303-2311.

JAHN R, LANG T, SÜDHOF TC. (2003) Membrane fusion. *Cell* **112**: 519-533.

JAMES DE, BROWN R, NAVARRO J, PILCH PF. 1988. Insulin-regulatable tissues express a unique insulin-sensitive glucose-transport protein. *Nature* **333**: 183-185.

JAMES DE, LEDERMAN L, PILCH PF. (1987) Purification of insulin-dependent exocytic vesicles containing the glucose transporter. *J Biol Chem.* **262**: 11817-11824.

JAMES DJ, KOWALCHYK J, DAILY N, PETRIE M, MARTIN TF. (2009) CAPS drives *trans*-SNARE complex formation and membrane fusion through Syntaxin interactions. *Proc Natl Acad Sci USA* **106**: 17308-17313.

JANZ R, SÜDHOF TC. (1998) Cellugyrin, a novel ubiquitous form of Synaptogyrin that is phosphorylated by pp60c-src. *J Biol Chem.* **273**: 2851-2857.

JANZ R, SÜDHOF TC, HAMMER RE, UNNI V, SIEGELBAUM SA, BOLSHAKOV VY. (1999) Essential roles in synaptic plasticity for Synaptogyrin I and Synaptophysin I. *Neuron* **24**: 687-700.

JEWELL JL, OH E, RAMALINGAM L, KALWAT MA, TAGLIABRACCI VS, TACKETT L, ELMENDORF JS, THURMOND DC. (2011) Munc18c phosphorylation by the insulin receptor links cell signalling directly to SNARE exocytosis. *J Cell Biol*. **193**: 185-199.

JI H, COLEMAN J, YANG R, MELIA TJ, ROTHMAN JE, TARESTE D. (2010) Protein Determinants of SNARE-Mediated Lipid Mixing. *Biophys J*. **99**: 553-560.

JIANG ZY, ZHOU QL, COLEMAN KA, CHOUINARD M, BOESE Q, CZECH MP. (2003) Insulin signaling through Akt/protein kinase B analyzed by small interfering RNA-mediated gene silencing. *Proc Natl Acad Sci USA* **100**: 7569-7574.

JOHNSON JR, FERDEK P, LIAN LY, BARCLAY JW, BURGOYNE RD, MORGAN A. (2009) Binding of UNC-18 to the N-terminus of syntaxin is essential for neurotransmission in *Caenorhabditis elegans*. *Biochem J*. **418**: 73-80.

JOOST HG, THORENS B. (2001) The extended GLUT-family of sugar/polyol transport facilitators: nomenclature, sequence characteristics, and potential function of its novel members. *Mol Mem Biol*. **18**: 247-256.

KARNIELI E, ZARNOWSKI MJ, HISSIN PJ, SIMPSON IA, SALANS LB, CUSHMAN SW. (1981) Insulin-stimulated translocation of glucose transport systems in the isolated rat adipose cell. Time course, reversal, insulin concentration dependency, and relationship to glucose transport activity. *J Biol Chem*. **256**: 4772-4777.

KARYLOWSKI O, ZEIGERER A, COHEN A, MCGRAW TE. (2004) GLUT4 is retained by an intracellular cycle of vesicle formation and fusion with endosomes. *Mol Biol Cell* **15**: 870-882.

KAWAGUCHI T, TAMORI Y, KANDA H, YOSHIKAWA M, TATEYA S, NISHINO N, KASUGA M. (2010) The t-SNAREs Syntaxin4 and SNAP23 but not v-SNARE VAMP2 are indispensable to tether GLUT4 vesicles at the plasma membrane in adipocyte. *Biochem Biophys Res Commun.* **391**:1336-1341.

KAWANISHI M, TAMORI Y, OKAZAWA H, ARAKI S, SHINODA H, KASUGA M. (2000) Role of SNAP23 in insulin-induced translocation of GLUT4 in 3T3-L1 adipocytes. Mediation of complex formation between Syntaxin4 and VAMP2. *J Biol Chem.* **275**: 8240-8247.

KEMBLE GW, DANIELI T, WHITE JM. (1994) Lipid-anchored influenza hemagglutinin promotes hemifusion, not complete fusion. *Cell* **76**: 383-391.

KHVOTCHEV M, DULUBOVA I, SUN J, DAI H, RIZO J, SÜDHOF TC. (2007) Dual modes of Munc18-1/SNARE interactions are coupled by functionally critical binding to syntaxin-1 N terminus. *J Neurosci*. **27**: 12147-12155.

KOUMANOV F, JIN B, YANG J, HOLMAN GD. (2005) Insulin signaling meets vesicle traffic of GLUT4 at a plasma-membrane-activated fusion step. *Cell Metab*. **2**: 179-189.

KUPRIYANOVA TA, KANDROR KV. (1999) Akt-2 binds to Glut4-containing vesicles and phosphorylates their component proteins in response to insulin. *J Biol Chem*. **274**: 1458-1464.

KUPRIYANOVA TA, KANDROR KV. (2000) Cellugyrin is a marker for a distinct population of intracellular Glut4-containing vesicles. *J Biol Chem.* **275**: 36263-36268.

KUPRIYANOVA TA, KANDROR V, KANDROR KV. (2002) Isolation and characterization of the two major intracellular GLUT4 storage compartments. *J Biol Chem.* **277**: 9133-9138.

KWEON DH, KIM CS, SHIN YK. (2003) Regulation of neuronal SNARE assembly by the membrane. *Nat Struct Biol*. **10**: 440-447.

LAMB CA, MCCANN RK, STÖCKLI J, JAMES DE, BRYANT NJ. (2010) Insulin-regulated trafficking of GLUT4 requires ubiquitination. *Traffic* 11: 1445-14454.

LATHAM CF, LOPEZ JA, HU SHH, GEE CL, WESTBURY E, BLAIR DH, ARMISHAW CJ, ALEWOOD PF, BRYANT NJ, JAMES DE, MARTIN JL. (2006) Molecular dissection of the Munc18c/Syntaxin4 interaction: Implications for regulation of membrane trafficking. *Traffic* **7**: 1408-1419.

LI G, ALEXANDER EA, SCHWARTZ JH. 2003. Syntaxin isoform specificity in the regulation of renal H+-ATPase exocytosis. *J Biol Chem*. **278**: 19791-19797.

LI L, OMATA W, KOJIMA I, SHIBATA H. (2001) Direct interaction of Rab4 with Syntaxin 4. *J Biol Chem*. **276**: 5265-5273.

LIN RC, SCHELLER RH. (1997) Structural organization of the synaptic exocytosis core complex. *Neuron* **19**: 1087-1094.

LIVINGSTONE C, JAMES DE, RICE JE, HANPETER D, GOULD GW. (1996) Compartment ablation analysis of the insulin-responsive glucose transporter (GLUT4) in 3T3-L1 adipocytes. *Biochem J*. **315**: 487-495.

LIZUNOV VA, MATSUMOTO H, ZIMMERBERG J, CUSHMAN SW, FROLOV VA. (2005) Insulin stimulates the halting, tethering, and fusion of mobile GLUT4 vesicles in rat adipose cells. *J Cell Biol*. **169**: 481-489.

LU X, ZHANG F, MCNEW JA, SHIN YK. (2005) Membrane fusion induced by neuronal SNAREs transits through hemifusion. *J Biol Chem*. **280**: 30538-30541.

MACAULAY SL, REA S, GOUGH KH, WARD CW, JAMES DE. (1997) Botulinum E toxin light chain does not cleave SNAP-23 and only partially impairs insulin stimulation of GLUT4 translocation in 3T3-L1 cells. *Biochem Biophys Res Commun*. **237**: 388-393.

MALHOTRA V, ORCI L, GLICK BS, BLOCK MR, ROTHMAN JE. (1988) Role of an N-ethylmaleimide-sensitive transport component in promoting fusion of transport vesicles with cisternae of the Golgi stack. *Cell* **54**: 221-227.

MALIDE D, RAMM G, CUSHMAN SW, SLOT JW. (2000) Immunoelectron microscopic evidence that GLUT4 translocation explains the stimulation of glucose transport in isolated rat white adipose cells. *J Cell Sci*. **113**: 4203-4210.

MARTIN LB, SHEWAN A, MILLAR CA, GOULD GW, JAMES DE. (1998) Vesicle-associated membrane protein 2 plays a specific role in the insulin-dependent trafficking of the facilitative glucose transporter GLUT4 in 3T3-L1 adipocytes. *J Biol Chem*. **273**: 1444-1452.

MARTIN S, TELLAM J, LIVINGSTONE C, SLOT JW, GOULD GW, JAMES DE. (1996) The glucose transporter (GLUT-4) and vesicle-associated membrane protein-2 (VAMP-2) are segregated from recycling endosomes in insulin-sensitive cells. *J Cell Biol*. **134**: 625-635.

MCINTYRE JC, SLEIGHT RG. (1991) Fluorescence assay for phospholipid membrane asymmetry. *Biochem*. **30**: 11819-11827.

MILLAR CA, SHEWAN A, HICKSON GR, JAMES DE, GOULD GW. (1999) Differential regulation of secretory compartments containing the insulin-responsive glucose transporter 4 in 3T3-L1 adipocytes. *Mol Biol Cell* **10**: 3675-3688.

MIMA J, HICKEY CM, XU H, JUN Y, WICKNER W. (2008) Reconstituted membrane fusion requires regulatory lipids, SNAREs and synergistic SNARE chaperones. *EMBO J*. **27**: 2031-2042.

MIN J, OKADA S, KANZAKI M, ELMENDORF JS, COKER KJ, CERESA BP, SYU LJ, NODA Y, SALTIEL AR, PESSIN JE. (1999) Synip: a novel insulin-regulated Syntaxin 4-binding protein mediating GLUT4 translocation in adipocytes. *Mol Cell* **3:** 751-760.

MISURA KMS, SCHELLER RH, WEIS WI. (2000) Three-dimensional structure of the neuronal-Sec1-Syntaxin 1a complex. *Nature* **404**: 355-362.

MOLLINEDO F, LAZO PA. (1997) Identification of two isoforms of the vesicle-membrane fusion protein SNAP-23 in human neutrophils and HL-60 cells. *Biochem Biophys Res Commun*. **231**: 808-812.

MUNSON M, BRYANT NJ. (2009) A role for the Syntaxin N-terminus. *Biochem J*. **418**: e1-3.

NOVICK P, FIELD C, SCHEKMAN R. (1980) Identification of 23 complementation groups required for post-translational events in the yeast secretory pathway. *Cell* **21**: 205-215.

NOVICK P, SCHEKMAN R. (1979) Secretion and cell-surface growth are blocked in a temperature-sensitive mutant of *Saccharomyces cerevisiae*. *Proc Nat Acad Sci USA* **76**: 1858-1862.

OH E, SPURLIN BA, PESSIN JE, THURMOND DC. (2005) Munc18c heterozygous knockout mice display increased susceptibility for severe glucose intolerance. *Diabetes* **54**: 638-647.

OH E, THURMOND DC. (2006) The stimulus-induced tyrosine phosphorylation of Munc18c facilitates vesicle exocytosis. *J Biol Chem*. **281**: 17624-17634.

OH E, THURMOND DC. (2009) Munc18c depletion selectively impairs the sustained phase of insulin release. *Diabetes* **58**: 1165-1174.

OYLER GA, HIGGINS GA, HART RA, BATTENBERG E, BILLINGSLEY M, BLOOM FE, WILSON MC. (1989) The identification of a novel synaptosomal-associated protein, SNAP-25, differentially expressed by neuronal subpopulations. *J Cell Biol*. **109**: 3039-3052.

PALADE G. (1975) Intracellular aspects of process of protein-synthesis. *Science* **189**: 347-358.

PENG RW, GALLWITZ D. (2004) Multiple SNARE interactions of an SM protein: Sed5p/Sly1p binding is dispensable for transport. *Embo J*. **23**: 3939-3949.

PEVSNER J, HSU SC, SCHELLER RH. (1994) N-sec1 - a neural-specific Syntaxin-binding protein. *Proc Nat Acad Sci USA* **91**: 1445-1449.

PIPER RC, HESS LJ, JAMES DE. (1991) Differential sorting of two glucose transporters expressed in insulin-sensitive cells. *Am J Physiol*. **260**: C570-580.

POLGÁR J, LANE WS, CHUNG SH, HOUNG AK, REED GL. (2003) Phosphorylation of SNAP-23 in activated human platelets. *J Biol Chem*. **278**: 44369-44376.

PORTIS A, NEWTON C, PANGBORN W, PAPAHADJOPOULOS D. (1979) Studies on the mechanism of membrane fusion: evidence for an intermembrane Ca2+-phospholipid complex, synergism with Mg^{2+}, and inhibition by Spectrin. *Biochem*. **18**: 780-790.

RAMM G, SLOT JW, JAMES DE, STOORVOGEL W. (2000) Insulin recruits GLUT4 from specialized VAMP2-carrying vesicles as well as from the dynamic endosomal/trans-Golgi network in rat adipocytes. *Mol Biol Cell* **11**: 4079-4091.

RAND RP. (1981) Interacting phospholipid-bilayers - measured forces and induced structural-changes. *Ann Rev Biophys Bioeng*. **10**: 277-314.

RANDHAWA VK, BILAN PJ, KHAYAT ZA, DANEMAN N, LIU Z, RAMLAL T, VOLCHUK A, PENG XR, COPPOLA T, REGAZZI R, TRIMBLE WS, KLIP A. (2000) VAMP2, but not VAMP3/Cellubrevin, mediates insulin-dependent incorporation of GLUT4 into the plasma membrane of L6 myoblasts. *Mol Biol Cell* **11**: 2403-2417.

RAVICHANDRAN V, CHAWLA A, ROCHE PA. (1996) Identification of a novel syntaxin- and synaptobrevin/VAMP-binding protein, SNAP-23, expressed in non-neuronal tissues. *J Biol Chem.* **271**: 13300-13303.

REA S, MARTIN LB, MCINTOSH S, MACAULAY SL, RAMSDALE T, BALDINI G, JAMES DE. (1998) Syndet, an adipocyte target SNARE involved in the insulin-induced translocation of GLUT4 to the cell surface. *J Biol Chem.* **273**: 18784-18792.

RICKMAN C, MEDINE CN, BERGMANN A, DUNCAN RR. (2007) Functionally and spatially distinct modes of Munc18-Syntaxin 1 interaction. *J Biol Chem.* **282**: 12097-12103.

RIGAUD JL, LÉVY D. (2003) Reconstitution of membrane proteins into liposomes. *Methods Enzymol*. **372**: 65-86.

RODKEY TL, LIU S, BARRY M, MCNEW JA. (2008) Munc18a scaffolds SNARE assembly to promote membrane fusion. *Mol Biol Cell* **19**: 5422-5434.

ROSSI G, SALMINEN A, RICE LM, BRÜNGER AT, BRENNWALD P. (1997) Analysis of a yeast SNARE complex reveals remarkable similarity to the neuronal SNARE complex and a novel function for the C-terminus of the SNAP-25 homolog, Sec9. *J Biol Chem.* **272**: 16610-16617.

SALZBERG A, COHEN N, HALACHMI N, KIMCHIE Z, LEV Z. (1993) The drosophila-Ras2 and Rop gene pair - a dual homology with a yeast Ras-like gene and a suppressor of its loss-of-function phenotype. *Development* **117**: 1309-1319.

SCHIAVO G, SHONE CC, BENNETT MK, SCHELLER RH, MONTECUCCO C. (1995) Botulinum neurotoxin type C cleaves a single Lys-Ala bond within the carboxyl-terminal region of Syntaxins. *J Biol Chem.* **270**: 10566-10570.

SCHOLLMEIER Y, KRAUSE JM, KREYE S, MALSAM J, SÖLLNER TH. (2011) Resolving the function of distinct Munc18-1/SNARE protein interaction modes in a reconstituted membrane fusion assay. *J Biol Chem*. **286**: 30582-30590.

SCHRAW TD, LEMONS PP, DEAN WL, WHITEHEART SW. (2003) A role for Sec1/Munc18 proteins in platelet exocytosis. *Biochem J*. **374**: 207-217.

SCHUETTE CG, HATSUZAWA K, MARGITTAI M, STEIN A, RIEDEL D, KÜSTER P, KÖNIG M, SEIDEL C, JAHN R. (2004) Determinants of liposome fusion mediated by synaptic SNARE proteins. *Proc Natl Acad Sci USA* **101**: 2858-2863.

SCOTT BL, VAN KOMEN J, LIU S, WEBER T, MELIA TJ, MCNEW JA. (2003) Liposome fusion assay to monitor intracellular membrane fusion machines. *Liposomes* **372**: 274-300.

SCOTT BL, VAN KOMEN JS, IRSHAD H, LIU S, WILSON KA, MCNEW JA. (2004) Sec1p directly stimulates SNARE-mediated membrane fusion *in vitro*. *J Cell Biol*. **167**: 75-85.

SHEN J, TARESTE DC, PAUMET F, ROTHMAN JE, MELIA TJ. (2007) Selective activation of cognate SNAREpins by Sec1/Munc18 proteins. *Cell* **128**: 183-195.

SHEWAN AM, VAN DAM EM, MARTIN S, LUEN TB, HONG W, BRYANT NJ, JAMES DE. (2003) GLUT4 recycles via a *trans*-Golgi network (TGN) subdomain enriched in Syntaxins 6 and 16 but not TGN38: involvement of an acidic targeting motif. *Mol Biol Cell* **14**: 973-986.

SIEBER JJ, WILLIG KI, HEINTZMANN R, HELL SW, LANG T. (2006) The SNARE motif is essential for the formation of Syntaxin clusters in the plasma membrane. *Biophys J*. **90**: 2843-2851.

SIMONSEN A, BREMNES B, RONNING E, AASLAND R, STENMARK H. (1998) Syntaxin-16, a putative Golgi t-SNARE. *Euro J Cell Biol*. **75**: 223-231.

SLOT JW, GEUZE HJ, GIGENGACK S, LIENHARD GE, JAMES DE. (1991) Immuno-localization of the insulin regulatable glucose transporter in brown adipose tissue of the rat. *J Cell Biol*. **113**: 123-135.

SMITHERS NP, HODGKINSON CP, CUTTLE M, SALE GJ. (2008) Insulin-triggered repositioning of Muncl8c on Syntaxin-4 in GLUT4 signalling. *Biochem J*. **410**: 255-260.

SMYTH AM, RICKMAN C, DUNCAN RR. (2010) Vesicle fusion probability is determined by the specific interactions of munc18. *J Biol Chem*. **285**: 38141-38148.

SÖLLNER T, WHITEHART SW, BRUNNER M, ERDJUMENTBROMAGE H, GEROMANOS S, TEMPST P, ROTHMAN JE. (1993) SNAP receptors implicated in vesicle targeting and fusion. *Nature* **362**: 318-324.

SÖLLNER T, BENNETT MK, WHITEHEART SW, SCHELLER RH, ROTHMAN JE. (1993b) A protein assembly-disassembly pathway *in vitro* that may correspond to sequential steps of synaptic vesicle docking, activation, and fusion. *Cell* **75**: 409-418.

ST-DENIS JF, CABANIOLS JP, CUSHMAN SW, ROCHE PA. (1999) SNAP-23 participates in SNARE complex assembly in rat adipose cells. *Biochem J.* **338**: 709-715.

STEEGMAIER M, YANG B, YOO JS, HUANG B, SHEN M, YU S, LUO Y, SCHELLER RH. (1998) Three novel proteins of the Syntaxin/SNAP-25 family. *J Biol Chem*. **273**: 34171-34179.

STEIN A, WEBER G, WAHL MC, JAHN R. (2009) Helical extension of the neuronal SNARE complex into the membrane. *Nature* **460**: 525-528.

STENKULA KG, LIZUNOV VA, CUSHMAN SW, ZIMMERBERG J. (2010) Insulin controls the spatial distribution of GLUT4 on the cell surface through regulation of its postfusion dispersal. *Cell Metab*. **12**: 250-259.

STORLIEN LH, PAN DA, KRIKETOS AD, O'CONNOR J, CATERSON ID, COONEY GJ, JENKINS AB, BAUR LA. (1996) Skeletal muscle membrane lipids and insulin resistance. *Lipids* **31**: S261-265.

STROP P, KAISER SE, VRLJIC M, BRUNGER AT. (2008) The structure of the yeast plasma membrane SNARE complex reveals destabilizing water-filled cavities. *J Biol Chem*. **283**: 1113-1119.

STRUCK DK, HOEKSTRA D, PAGANO RE. (1981) Use of resonance energy-transfer to monitor membrane-fusion. *Biochem*. **20**: 4093-4099.

STRYER L. (1978) Fluorescence energy transfer as a spectroscopic ruler. *Annu Rev Biochem.* **47**: 819-846.

SÜDHOF TC. (1995) The synaptic vesicle cycle - a cascade of protein-protein interactions. *Nature* **375**: 645-653.

SUGITA S, JANZ R, SÜDHOF TC. (1999) Synaptogyrins regulate Ca^{2+}-dependent exocytosis in PC12 cells. *J Biol Chem*. **274**: 18893-18901.

SUMITANI S, RAMLAL T, LIU Z, KLIP A. (1995) Expression of Syntaxin 4 in rat skeletal muscle and rat skeletal muscle cells in culture. *Biochem Biophys Res Commun*. **213**: 462-468.

SUTTON RB, FASSHAUER D, JAHN R, BRUNGER AT. (1998) Crystal structure of a SNARE complex involved in synaptic exocytosis at 2.4 angstrom resolution. *Nature* **395**: 347-353.

SUURKUUSK J, LENTZ BR, BARENHOLZ Y, BILTONEN RL, THOMPSON TE. (1976) A calorimetric and fluorescent probe study of the gel-liquid crystalline phase transition in small, single-lamellar dipalmitoylphosphatidylcholine vesicles. *Biochem*. **15**: 1393-1401.

SUZUKI K, KONO T. (1980) Evidence that insulin causes translocation of glucose-transport activity to the plasma-membrane from an intracellular storage site. *Proc Nat Acad Sci USA* **77**: 2542-2545.

TANIGUCHI CM, EMANUELLI B, KAHN CR. (2006) Critical nodes in signalling pathways: insights into insulin action. *Nat Rev Mol Cell Biol*. **7**: 85-96.

TELLAM JT, MACAULAY SL, MCINTOSH S, HEWISH DR, WARD CW, JAMES DE. (1997) Characterization of Munc-18c and Syntaxin-4 in 3T3-L1 adipocytes - Putative role in insulin-dependent movement of GLUT-4. *J Biol Chem*. **272**: 6179-6186.

TELLAM JT, MCINTOSH S, JAMES DE. (1995) Molecular-identification of 2 novel Munc-18 isoforms expressed in nonneuronal tissues. *J Biol Chem*. **270**: 5857-5863.

TENG FYH, WANG Y, TANG BL. (2001) The Syntaxins. *Genome Biol*. **2**: 7.

THURMOND DC, CERESA BP, OKADA S, ELMENDORF JS, COKER K, PESSIN JE. (1998) Regulation of insulin-stimulated GLUT4 translocation by Munc18c in 3T3L1 adipocytes. *J Biol Chem*. **273**: 33876-33883.

THURMOND DC, KANZAKI M, KHAN AH, PESSIN JE. (2000) Munc18c function is required for insulin-stimulated plasma membrane fusion of GLUT4 and insulin-responsive amino peptidase storage vesicles. *Mol Cell Biol*. **20**: 379-388.

TOGNERI J, CHENG YS, MUNSON M, HUGHSON FM, CARR CM. (2006) Specific SNARE complex binding mode of the Sec1/Munc-18 protein, Sec1p. *Proc Natl Acad Sci USA* 103: 17730-17735.

UMAHARA M, OKADA S, YAMADA E, SAITO T, OHSHIMA K, HASHIMOTO K, YAMADA M, SHIMIZU H, PESSIN JE, MORI M. (2008) Tyrosine phosphorylation of Munc18c regulates platelet-derived growth factor-stimulated glucose transporter 4 translocation in 3T3L1 adipocytes. *Endocr*. **149**: 40-49.

VERHAGE M, MAIA AS, PLOMP JJ, BRUSSAARD AB, HEEROMA JH, VERMEER H, TOONEN RF, HAMMER RE, VAN DEN BERG TK, MISSLER M, GEUZE HJ, SÜDHOF TC. (2000) Synaptic assembly of the brain in the absence of neurotransmitter secretion. *Science* **287**: 864-869.

VESSBY B. (2000) Dietary fat and insulin action in humans. *Br J Nutr*. **83**: S91-96.

VICOGNE J, PESSIN JE. (2008) SNARE-mediated fusion of liposomes. *Methods Mol Biol*. **457**: 241-251.

VOLCHUK A, WANG Q, EWART HS, LIU Z, HE L, BENNETT MK, KLIP A. (1996) Syntaxin 4 in 3T3-L1 adipocytes: regulation by insulin and participation in insulin-dependent glucose transport. *Mol Biol Cell* **7**: 1075-1082.

WATSON RT, PESSIN JE. (2000) Functional cooperation of two independent targeting domains in syntaxin 6 is required for its efficient localization in the *trans*-Golgi network of 3T3L1 adipocytes. *J Biol Chem*. **275**: 1261-1268.

WEBER T, ZEMELMAN BV, MCNEW JA, WESTERMANN B, GMACHL M, PARLATI F, SÖLLNER TH, ROTHMAN JE. (1998) SNAREpins: Minimal machinery for membrane fusion. *Cell* **92**: 759-772.

WEIDMAN PJ, MELANÇON P, BLOCK MR, ROTHMAN JE. (1989) Binding of an N-ethylmaleimide-sensitive fusion protein to Golgi membranes requires both a soluble protein(s) and an integral membrane receptor. *J Cell Biol.* **108**: 1589-1596.

WILLIAMS D, PESSIN JE. (2008) Mapping of R-SNARE function at distinct intracellular GLUT4 trafficking steps in adipocytes. *J Cell Biol*. **180**: 375-387.

WILSON DW, WILCOX CA, FLYNN GC, CHEN E, KUANG WJ, HENZEL WJ, BLOCK MR, ULLRICH A, ROTHMAN JE. (1989) A fusion protein required for vesicle-mediated transport in both mammalian cells and yeast. *Nature* **339**: 355-259.

WIMMER C, HOHL TM, HUGHES CA, MÜLLER SA, SÖLLNER TH, ENGEL A, ROTHMAN JE. (2001) Molecular mass, stoichiometry, and assembly of 20S particles. *J Biol Chem*. **276**: 29091-29097.

WOLF DE, WINISKI AP, TING AE, BOCIAN KM, PAGANO RE. (1992) Determination of the transbilayer distribution of fluorescent lipid analogues by nonradiative fluorescence resonance energy transfer. *Biochem*. **31**: 2865-2873.

XU Y, SEVEN AB, SU L, JIANG QX, RIZO J. (2011) Membrane bridging and hemifusion by denaturated Munc18. *PLoS One* **6**: e22012.

YANG B, STEEGMAIER M, GONZALEZ LC, SCHELLER RH. (2000) nSec1 binds a closed conformation of syntaxin1A. *J Cell Biol*. **148**: 247-252.

YANG C, COKER KJ, KIM JK, MORA S, THURMOND DC, DAVIS AC, YANG B, WILLIAMSON RA, SHULMAN GI, PESSIN JE. (2001) Syntaxin 4 heterozygous knockout mice develop muscle insulin resistance. *J Clin Invest*. **107**: 1311-1318.

YANG Y, XIA Z, LIU Y. (2000) SNAP-25 functional domains in SNARE core complex assembly and glutamate release of cerebellar granule cells. *J Biol Chem*. **275**: 29482-29487.

YASSINE W, MILOCHAU A, BUCHOUX S, LANG J, DESBAT B, ODA R. (2010) Effect of monolayer lipid charges on the structure and orientation of protein VAMP 1 at the air-water interface. *Biochim Biophys Acta* **1798**: 928-937.

ZHAO P, YANG L, LOPEZ JA, FAN J, BURCHFIELD JG, BAI L, HONG W, XU T, JAMES DE. (2009) Variations in the requirement for v-SNAREs in GLUT4 trafficking in adipocytes. *J Cell Sci*. **122**: 3472-3480.

ZILLY FE, SORENSEN JB, JAHN R, LANG T. (2006) Munc18-bound syntaxin readily forms SNARE complexes with synaptobrevin in native plasma membranes. *Plos Biol.* **4**: 1789-1797.

ZIMMERBERG J, VOGEL SS, CHERNOMORDIK LV. (1993) Mechanisms of membrane-fusion. *Ann Rev Biophys Biomol Struct*. **22**: 433-466.

7 Appendices

7.1 Oligonuleotides used in this study

Oligo name	Sequence (5'→ 3')
NheINHisM18c	GCTAGCCGCCGCCGGTATCGGAGC
XhoISTOPNHisM18c	CTCGAGTTACTCATCCTTAAAGGAAACTTTATCCTTTG
NcoICHisM18c	CCATGGCGCCGCCGGTATCGGAGC
XhoICHisM18c	CTCGAGCTCATCCTTAAAGGAAACTTTATCCTTTG
E63KM18c_F	CTAGAGGAGGCCATAACTGTTATAAAGAATATTTATAAGAATCGTGAACCTGTC
E63KM18c_R	GACAGGTTCACGATTCTTATAAATATTCTTTATAACAGTTATGCCCTCCTCTAG
E70AM18c_F	GTTATAGAGAATATTTATAAGAATCGTGCACCTGTCAGACAAATGAAAGCTCTT
E70AM18c_R	AAGAGCTTTCATTTGTCTGACAGGTGCACGATTCTTATAAATATTCTCTATAAC
D222NM18c_F	CTTGAAGACTACTACAAAATTAATGAAAAAGGCCTAATAAAGGGT
D222NM18c_R	ACCCTTTATTAGGCCTTTTTCATTAATTTTGTAGTAGTCTTCAAG

7.2 Raw Fluorescence for *in vitro* fusion assay

7.2.1 Supplementary figures for Chapter 3

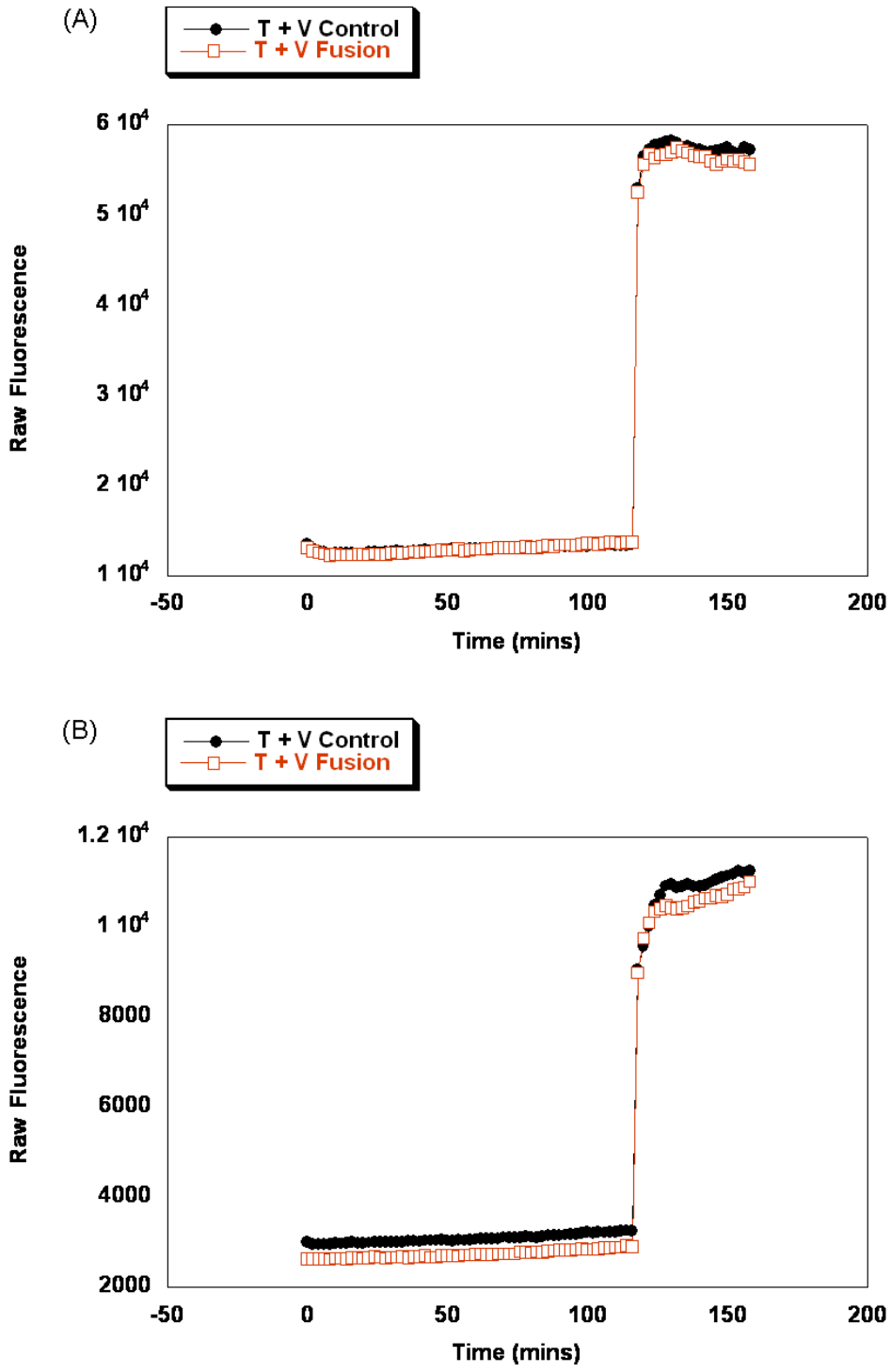

Figure I Raw fluorescence for Figure 3.7
45 µl t-SNARE and 5 µl v-SNARE liposomes were incubated overnight at 4 °C in the presence (black circles) or absence (red squares) of the cytosolic domain of VAMP 2, before analysis of fusion. Raw fluorescence data was exported from Microsoft Excel and imported to KaleidaGraph software (Synergy systems) for analysis. Raw fluorescence readings are presented here: data is shown before normalisation or adjustment to 100 % detergent signal.

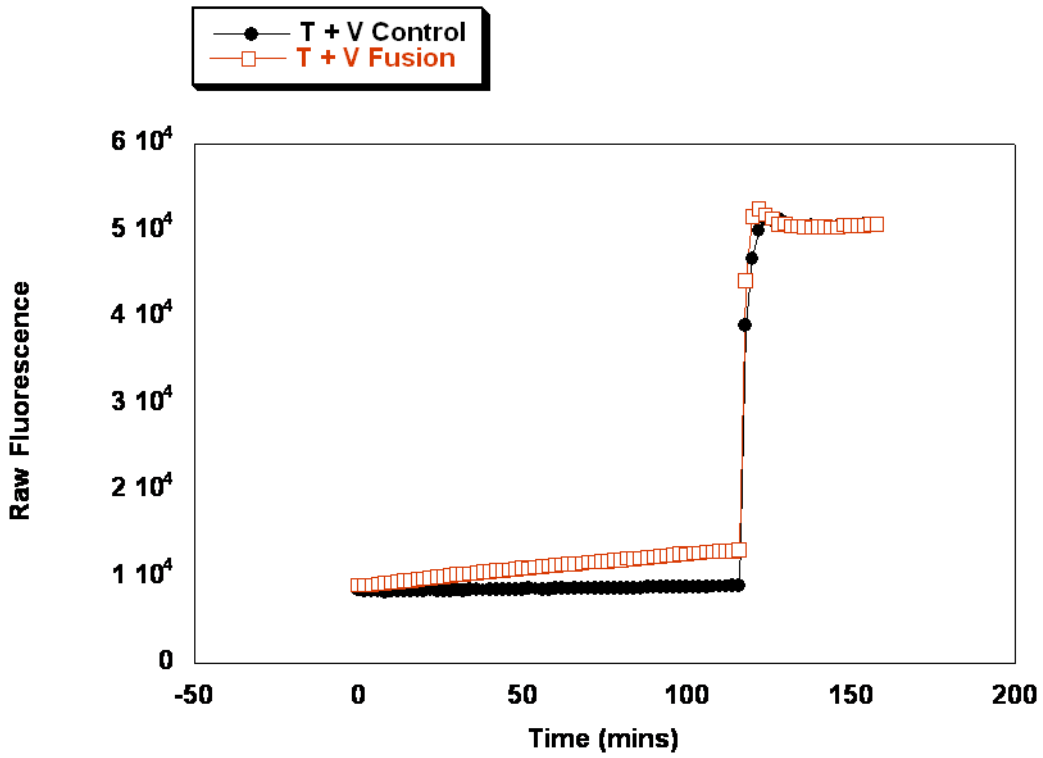

Figure II Raw fluorescence for Figure 3.12
45 µl t-SNARE and 5 µl v-SNARE liposomes were incubated overnight at 4 °C in the presence (black circles) or absence (red squares) of the cytosolic domain of VAMP 2, before analysis of fusion. Raw fluorescence data was exported from Microsoft Excel and imported to KaleidaGraph software (Synergy systems) for analysis. Raw fluorescence readings are presented here: data is shown before normalisation or adjustment to 100 % detergent signal.

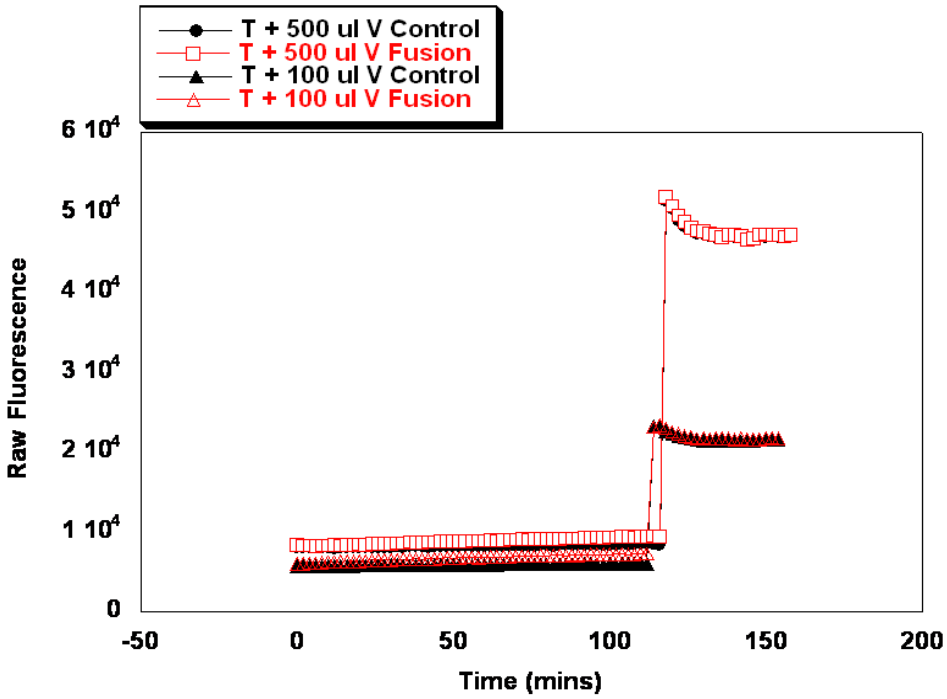

Figure III Raw fluorescence for Figure 3.13(B)
45 µl t-SNARE and 5 µl v-SNARE liposomes were incubated overnight at 4 °C in the presence (black circles) or absence (red squares) of the cytosolic domain of VAMP 2, before analysis of fusion. Raw fluorescence data was exported from Microsoft Excel and imported to KaleidaGraph software (Synergy systems) for analysis. Raw fluorescence readings are presented here: data is shown before normalisation or adjustment to 100 % detergent signal.

7.2.2 Supplementary figures for Chapter 4

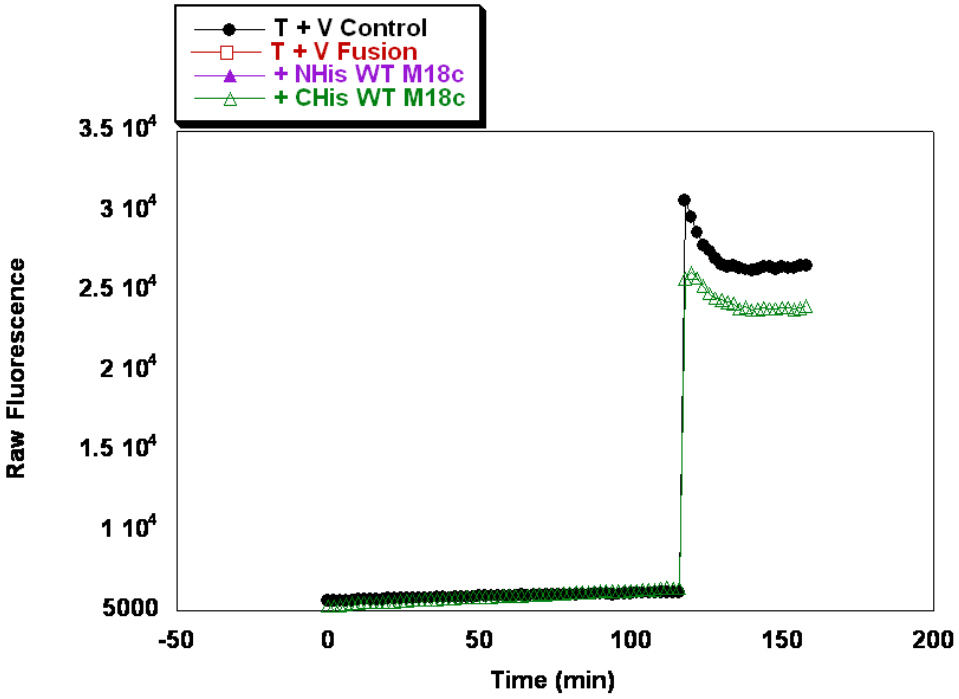

Figure IV Raw fluorescence for Figure 4.4
45 µl t-SNARE and 5 µl either protein-free (black circles) or v-SNARE liposomes (triangles/squares) were incubated overnight at 4 °C in the presence of wild-type $NHis_6$ (purple triangles) or $CHis_6$ (green triangles) Munc-18c before analysis of fusion. Raw fluorescence data was exported from Microsoft Excel and imported to KaleidaGraph software (Synergy systems) for analysis. Raw fluorescence readings are presented here: data is shown before normalisation or adjustment to 100 % detergent signal.

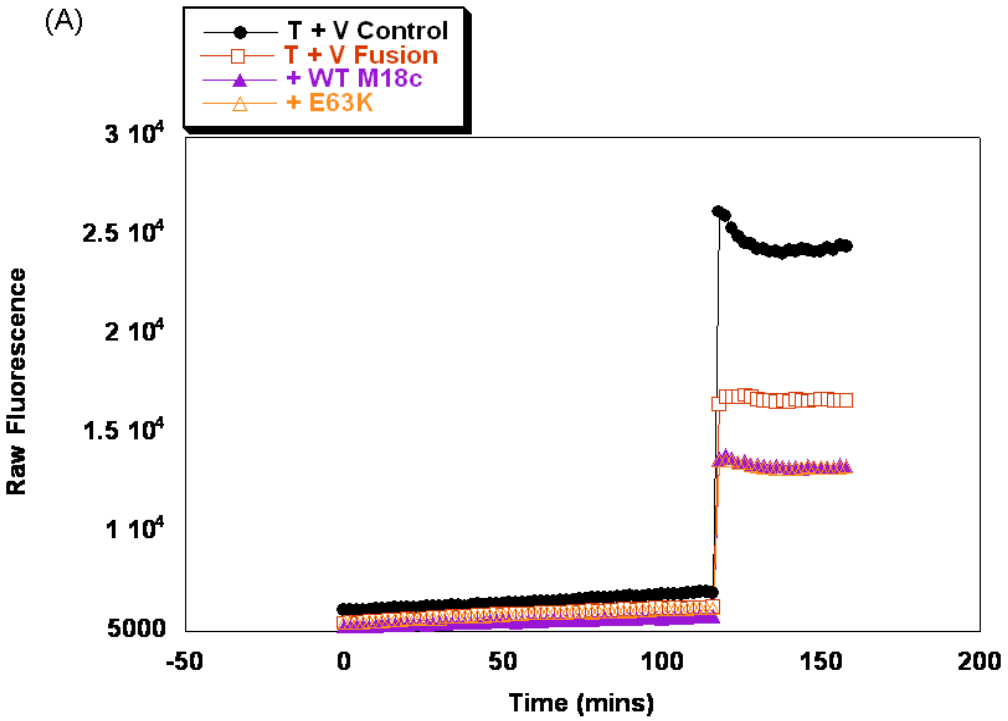
(A)
T + V Control
T + V Fusion
+ WT M18c
+ E63K
Raw Fluorescence
3 10^4
2.5 10^4
2 10^4
1.5 10^4
1 10^4
5000
-50
0
50
100
150
200
Time (mins)

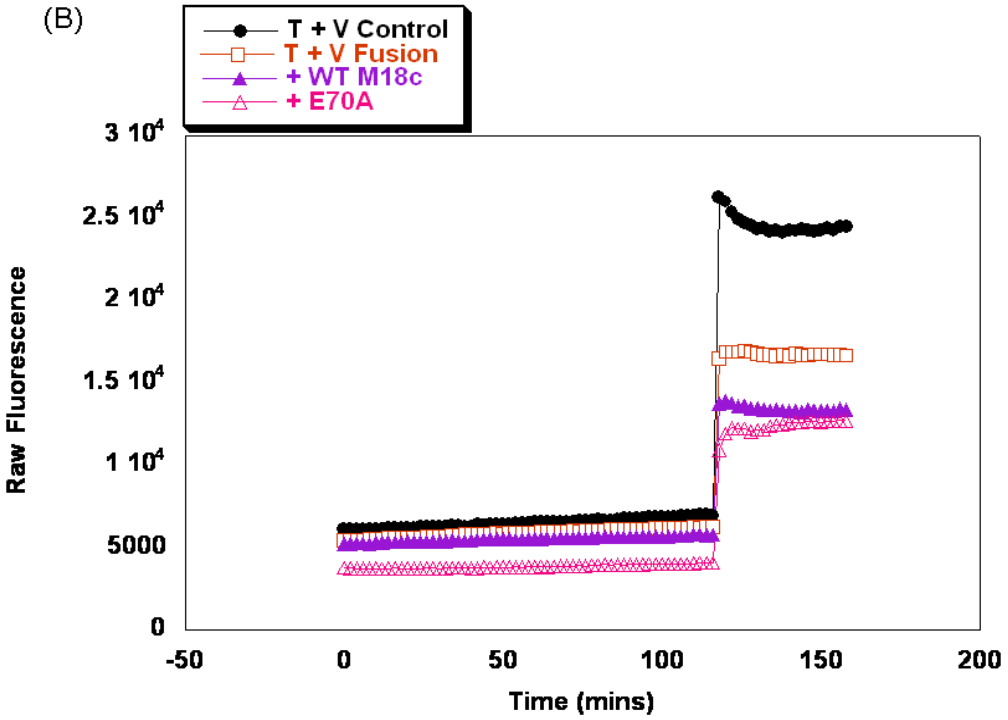
(B)
T + V Control
T + V Fusion
+ WT M18c
+ E70A
Raw Fluorescence
3 10^4
2.5 10^4
2 10^4
1.5 10^4
1 10^4
5000
0
-50
0
50
100
150
200
Time (mins)

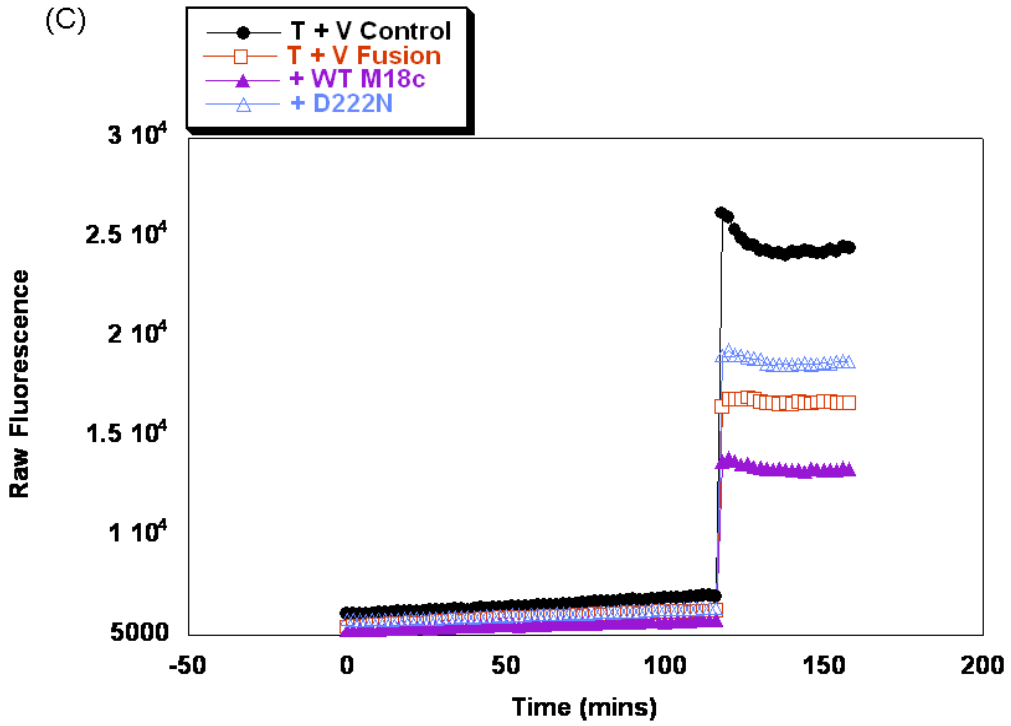

Figure V Raw fluorescence for Figure 4.8
45 µl t-SNARE and 5 µl either protein-free (black circles) or v-SNARE liposomes (triangles/squares) were incubated overnight at 4 °C. (A) E63K (B) E70A or (C) D222N Munc-18c was added to wells before analysis of fusion. Raw fluorescence data was exported from Microsoft Excel and imported to KaleidaGraph software (Synergy systems) for analysis. Raw fluorescence readings are presented here: data is shown before normalisation or adjustment to 100 % detergent signal.

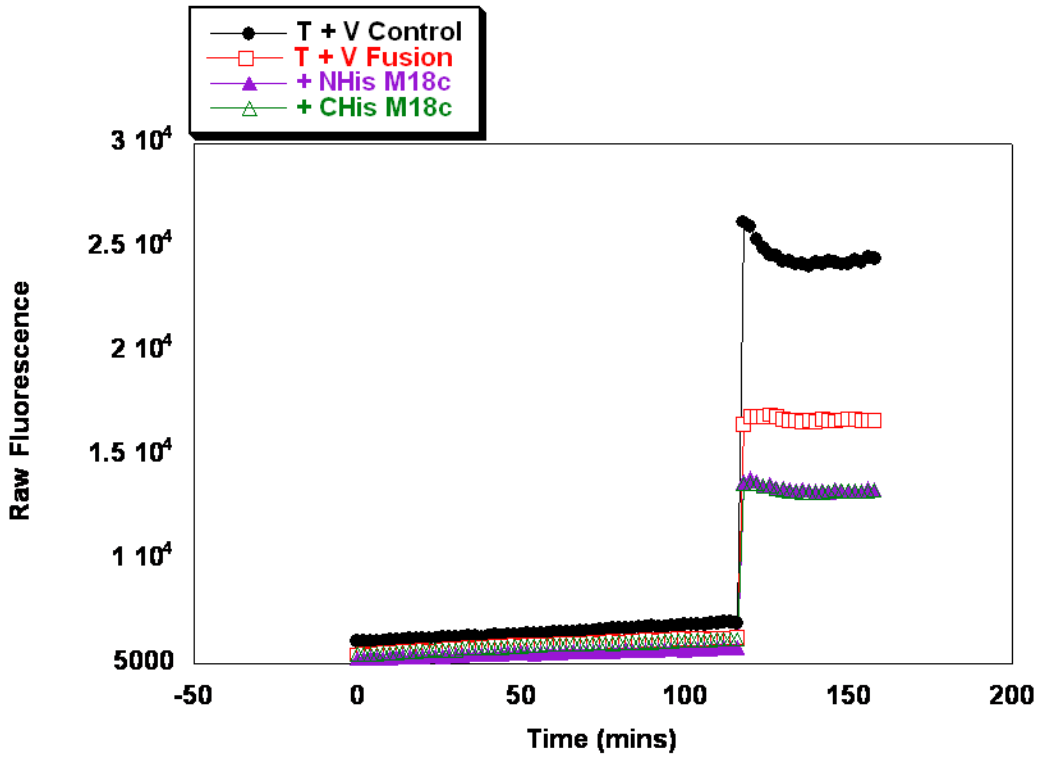

Figure 7.1 Raw Fluorescence for Figure 4.10
45 µl t-SNARE and either 5µl protein-free (black circles) or v-SNARE liposomes (triangles/squares) were incubated together overnight at 4°C. N- (purple triangles) or C-terminally (green triangles) tagged wild-type Munc-18c was added to separate experimental wells before analysis of fusion. Raw fluorescence data was exported from Microsoft Excel and imported to KaleidaGraph software (Synergy systems) for analysis. Raw fluorescence readings are presented here: data is shown before normalisation or adjustment to 100 % detergent signal.

7.2.3 Supplementary figures for Chapter 5

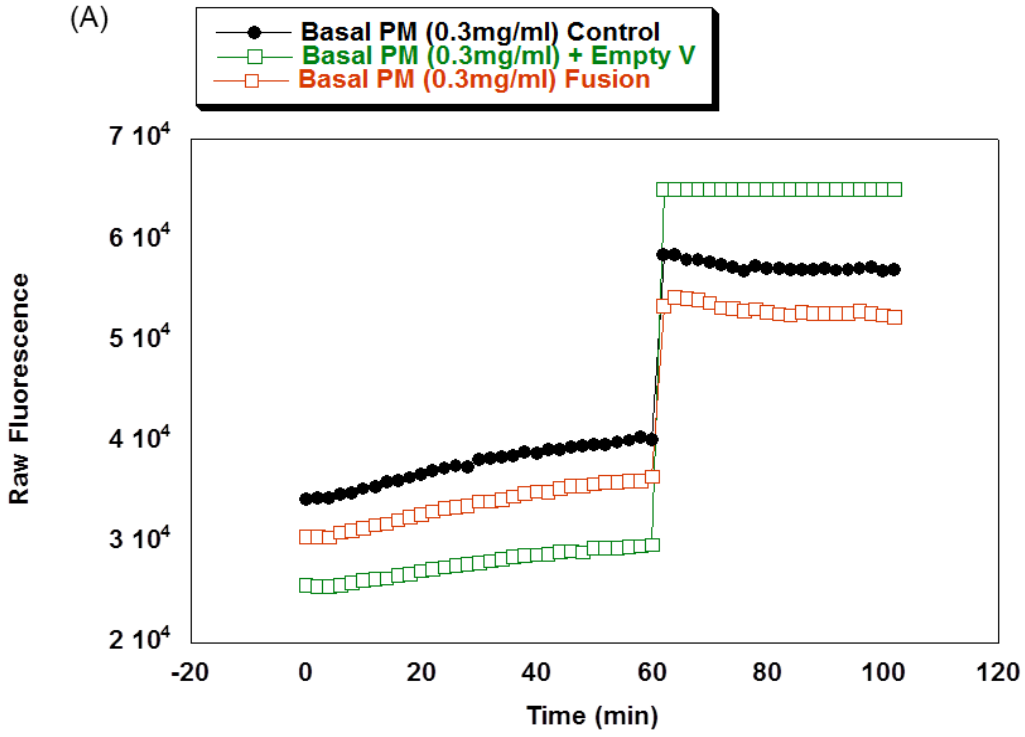

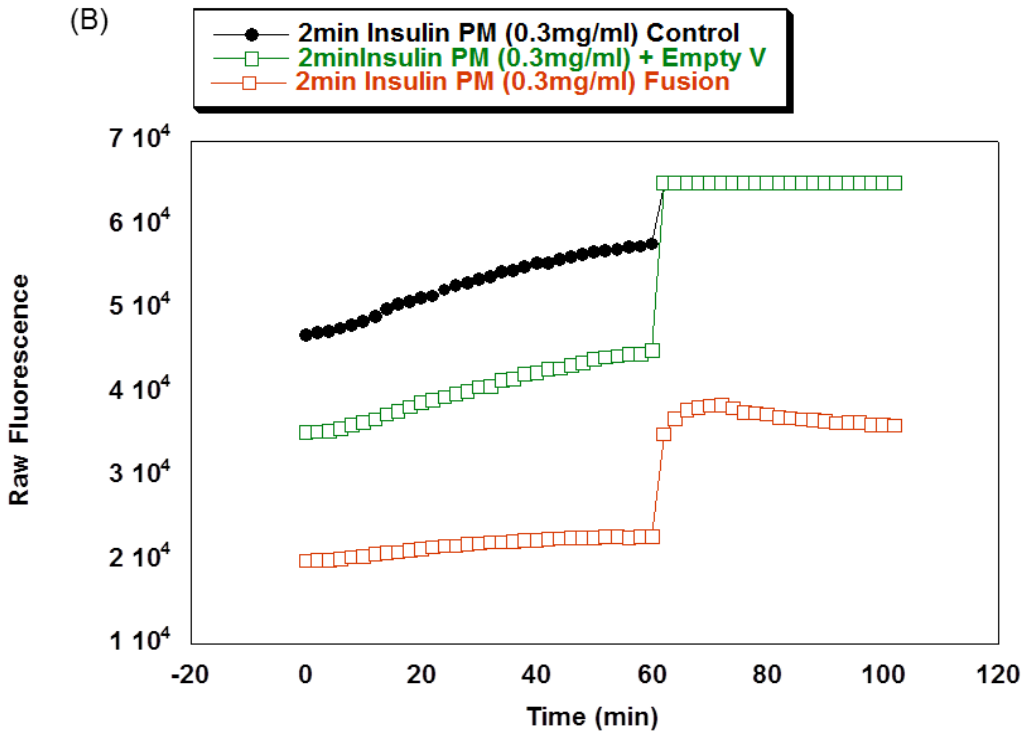

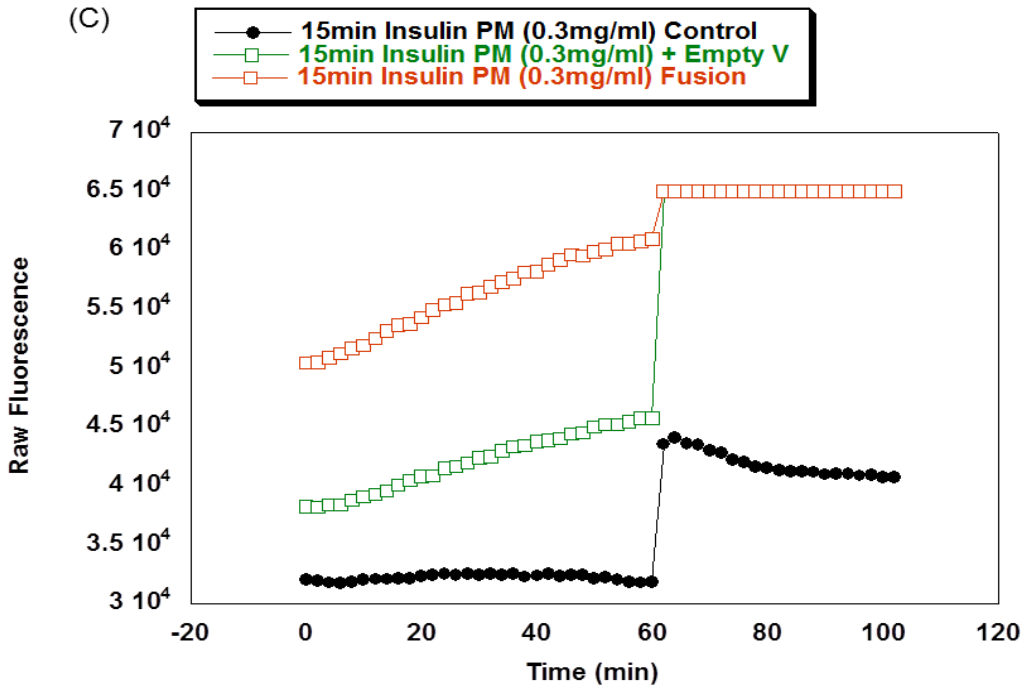

Figure VII Raw Fluorescence for Figure 5.3

Basal or insulin-stimulated plasma membrane was isolated from 3T3-L1 adipocytes, and reconstituted into liposomes. 45 µl of each liposome population was incubated overnight with 5 µl protein-free liposomes (black circles), or with 5 µl v-SNARE liposomes in the presence (green squares) or absence (red squares) of cytosolic VAMP 2. The next day, the plate was warmed to reaction temperature and the fusogenic ability of (A) basal (B) 2 minute insulin-stimulated or (C) 15 minute insulin-stimulated plasma membrane was assessed. Raw fluorescence data was exported from Microsoft Excel and imported to KaleidaGraph software (Synergy systems) for analysis. Raw fluorescence readings are presented here: data is shown before normalisation or adjustment to 100 % detergent signal.

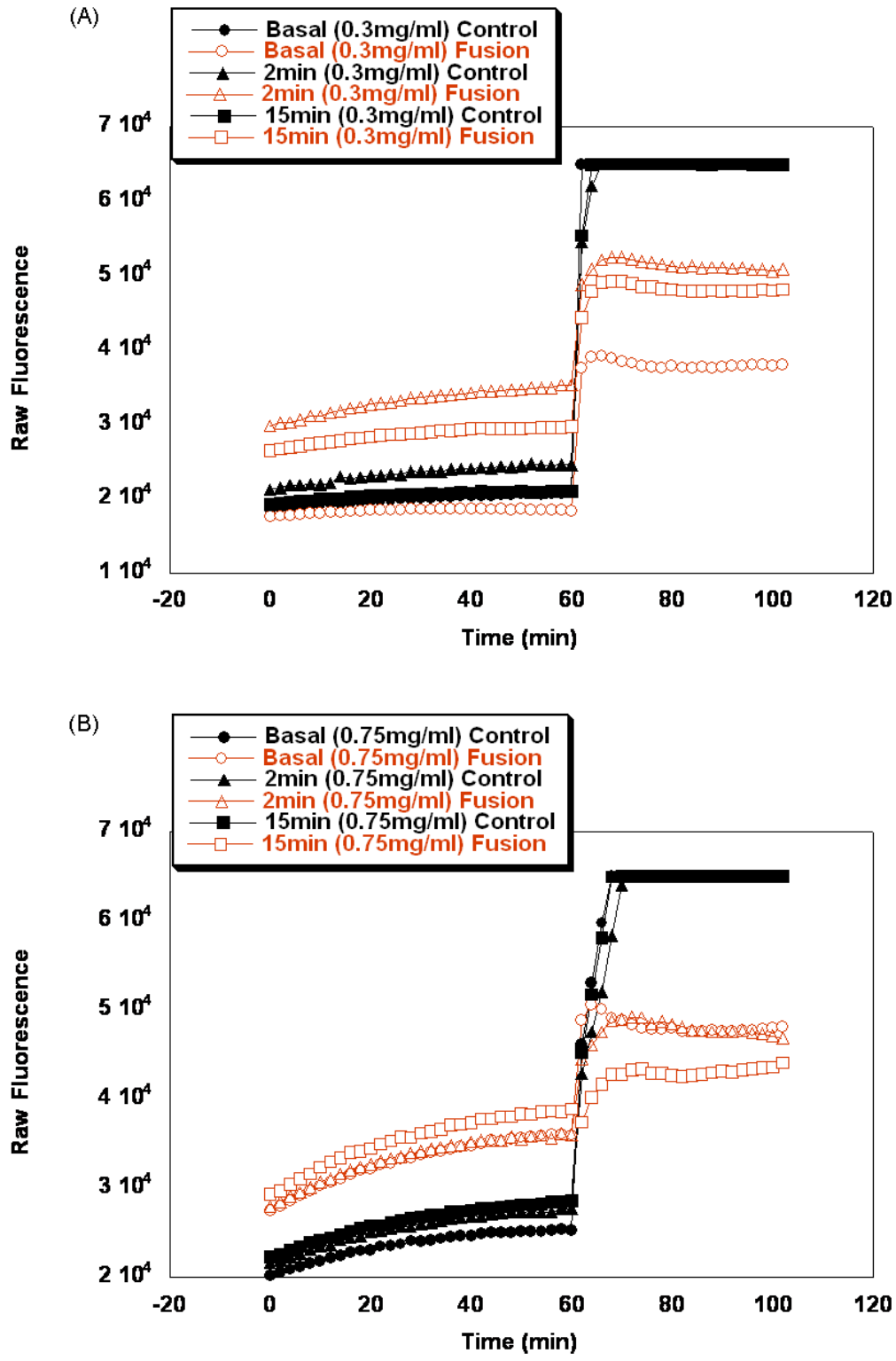

Figure 7.2 Raw Fluorescence for Figure 5.4
45 µl liposome derived from basal and insulin-stimulated (A) 0.3 mg/ml or (B) 0.75 mg/ml plasma membrane were incubated overnight with either protein-free (black symbols) or VAMP 2 vesicles (red symbols). After warming to reaction temperature, the fusogenic ability of the basal and insulin-stimulated plasma membrane was assessed. Raw fluorescence data was exported from Microsoft Excel and imported to KaleidaGraph software (Synergy systems) for analysis. Raw fluorescence readings are presented here: data is shown before normalisation or adjustment to 100 % detergent signal.